

## THE DISK POPULATION OF THE CHAMAELEON I STAR-FORMING REGION<sup>1</sup>

K. L. LUHMAN<sup>2</sup>, L. E. ALLEN<sup>3</sup>, P. R. ALLEN<sup>2</sup>, R. A. GUTERMUTH<sup>3</sup>, L. HARTMANN<sup>4</sup>, E. E. MAMAJEK<sup>3</sup>, S. T. MEGEATH<sup>5</sup>,  
P. C. MYERS<sup>3</sup>, AND G. G. FAZIO<sup>3</sup>

*Draft version December 3, 2018*

### ABSTRACT

We present a census of circumstellar disks in the Chamaeleon I star-forming region. Using the Infrared Array Camera and the Multiband Imaging Photometer onboard the *Spitzer Space Telescope*, we have obtained images of Chamaeleon I at 3.6, 4.5, 5.8, 8.0, and 24  $\mu\text{m}$ . To search for new disk-bearing members of the cluster, we have performed spectroscopy on objects that have red colors in these data. Through this work, we have discovered four new members of Chamaeleon I with spectral types of M4, M6, M7.5, and L0. The first three objects are highly embedded ( $A_J \sim 5$ ) and reside near known protostars, indicating that they may be among the youngest low-mass sources in the cluster ( $\tau < 1$  Myr). The L0 source is the coolest known member of Chamaeleon I. Its luminosity implies a mass of 0.004-0.01  $M_\odot$ , making it the least massive brown dwarf for which a circumstellar disk has been reliably detected. To characterize the disk population in Chamaeleon I, we have classified the infrared spectral energy distributions of the 203 known members that are encompassed by the *Spitzer* images. Through these classifications, we find that the disk fraction in Chamaeleon I is roughly constant at  $\sim 50\%$  from 0.01 to 0.3  $M_\odot$ . These data are similar to the disk fraction of IC 348, which is a denser cluster at the same age as Chamaeleon I. However, the disk fraction at  $M \gtrsim 1 M_\odot$  is significantly higher in Chamaeleon I than in IC 348 (65% vs. 20%), indicating longer disk lifetimes in Chamaeleon I for this mass range. Thus, low-density star-forming regions like Chamaeleon I may offer more time for planet formation around solar-type stars than denser clusters.

*Subject headings:* accretion disks – planetary systems: protoplanetary disks – stars: formation — stars: low-mass, brown dwarfs — stars: pre-main sequence

### 1. INTRODUCTION

Low-mass stars and brown dwarfs are important sites for studies of planet formation because most stars in the galaxy are low-mass stars while brown dwarfs offer an opportunity to explore planet formation in an extreme environment. Planet formation around low-mass stars and brown dwarfs can be investigated through observations of their primordial circumstellar disks. These observations are most easily performed at mid-infrared (IR) wavelengths ( $\lambda \sim 5\text{-}20 \mu\text{m}$ ) because this wavelength range provides the best combination of contrast of the disk relative to stellar photosphere, disk brightness, and sensitivity of available telescopes.

Molecular clouds that contain ongoing star formation

( $\tau \lesssim 5$  Myr) are the natural laboratories for observations of circumstellar disks. Among these regions, Chamaeleon I is arguably the best site for studying disks around low-mass stars and brown dwarfs. It is one of the nearest star-forming regions to the Sun ( $d = 160\text{-}170$  pc, Whittet et al. 1997; Wichmann et al. 1998; Bertout et al. 1999), making its low-mass members relatively bright. The cluster is young enough that it retains a significant population of primordial disks, but it is old enough that most of its members are no longer highly obscured by dust ( $A_V \lesssim 5$ ). Because of the relatively low extinction, optical wavelengths are accessible for the spectral classification of the stellar population (Comerón et al. 2004; Luhman 2004a, references therein) and for measuring diagnostics of accretion (Mohanty et al. 2005; Muzerolle et al. 2005). Optical and near-IR imaging and spectroscopic surveys of Chamaeleon I have produced an extensive census of the stellar and substellar cluster members (Luhman 2007). In particular, this census is unbiased in terms of disks, which is essential for measuring the prevalence of disks. With  $\sim 200$  known members at masses of 0.01-1  $M_\odot$ , Chamaeleon I is sufficiently rich for a statistical analysis of disks around low-mass stars and brown dwarfs. This region is also well-suited for observations of disks at mid-IR wavelengths. The stellar population is sparse enough that current mid-IR telescopes can resolve individual members, while compact enough for deep imaging of a large fraction of the cluster in a reasonable amount of time. In addition, the cloud exhibits relatively little nebulosity and extended emission at mid-IR wavelengths, which enables accurate photometry of the faint, low-mass members.

<sup>1</sup> Based on observations performed with the Magellan Telescopes at Las Campanas Observatory, Gemini Observatory, and the *Spitzer Space Telescope*. Gemini Observatory is operated by AURA under a cooperative agreement with the NSF on behalf of the Gemini partnership: the NSF (United States), the Particle Physics and Astronomy Research Council (United Kingdom), the National Research Council (Canada), CONICYT (Chile), the Australian Research Council (Australia), CNPq (Brazil) and CONICET (Argentina). *Spitzer* is operated by the Jet Propulsion Laboratory (JPL), California Institute of Technology under NASA contract 1407. Support for this work was provided by NASA through contract 1256790 issued by JPL. Support for the IRAC instrument was provided by NASA through contract 960541 issued by JPL.

<sup>2</sup> Department of Astronomy and Astrophysics, The Pennsylvania State University, University Park, PA 16802; kluhman@astro.psu.edu.

<sup>3</sup> Harvard-Smithsonian Center for Astrophysics, Cambridge, MA 02138.

<sup>4</sup> Department of Astronomy, The University of Michigan, Ann Arbor, MI 48109.

<sup>5</sup> Department of Physics and Astronomy, The University of Toledo, Toledo, OH 43606.

Several studies have searched for evidence of disks in Chamaeleon I through near- and mid-IR photometry. During pointed observations of known members, Glass (1979) and Jayawardhana et al. (2003) obtained photometry in the *JHKL* bands (1.2, 1.6, 2.2, 3.4  $\mu\text{m}$ ) for 17 and 15 members with spectral types as late as M4 and M8, respectively. Using a similar set of filters, Gómez & Kenyon (2001) and Kenyon & Gómez (2001) performed wide-field imaging of a 0.5 deg<sup>2</sup> field that encompassed a large fraction of the Chamaeleon I cloud. Photometry at wavelengths longward of the *L*-band offers more reliable detections of disks because of the better contrast of cool circumstellar dust relative to warmer stellar photospheres. To obtain data of this kind for known young stars in Chamaeleon I and to search for new disk-bearing members of the cluster, Baud et al. (1984) observed Chamaeleon I with the *Infrared Astronomical Satellite* (*IRAS*) at 12, 25, 60, and 100  $\mu\text{m}$ . They detected 70 sources, half of which are cluster members. A mid-IR survey with better sensitivity and spatial resolution was later conducted with the *Infrared Space Observatory* (*ISO*, Nordh et al. 1996; Persi et al. 2000), which provided photometry for 99 known members, including a brown dwarf with a spectral type near M8 (Natta & Testi 2001; Apai et al. 2002). Mid-IR imaging also has been performed toward smaller areas surrounding the three most prominent reflection nebulae in the Chamaeleon I cloud using *IRAS* (Assendorp et al. 1990; Prusti et al. 1991) and *ISO* (Lehtinen et al. 2001).

The *Spitzer Space Telescope* (Werner et al. 2004) is currently the most advanced telescope operating at mid-IR wavelengths. Because of its high spatial resolution, excellent sensitivity, and large field of view, *Spitzer* is proficient at identifying disk-bearing members of young clusters (Allen et al. 2004; Gutermuth et al. 2004; Megeath et al. 2004; Muzerolle et al. 2004). This capability has been widely utilized through *Spitzer* surveys of nearby star-forming regions and young associations ( $\tau \lesssim 10$  Myr), including Taurus (Hartmann et al. 2005; Luhman et al. 2006; Guieu et al. 2007), Perseus (Luhman et al. 2005b; Lada et al. 2006; Jørgensen et al. 2006; Muench et al. 2007; Rebull et al. 2007; Gutermuth et al. 2007), Lupus (Allen et al. 2007), Serpens (Harvey et al. 2006, 2007; Winston et al. 2007),  $\sigma$  Ori (Hernández et al. 2007; Caballero et al. 2007; Zapatero Osorio et al. 2007; Scholz & Jayawardhana 2007),  $\lambda$  Ori (Barrado y Navascués et al. 2007), Orion OB1b (Hernández et al. 2006),  $\eta$  Cha (Megeath et al. 2005), Chamaeleon II (Young et al. 2005; Allers et al. 2006; Porras et al. 2007), NGC 2362 (Dahm & Hillenbrand 2007), Upper Sco (Carpenter et al. 2006; Scholz et al. 2007), Tr 37, and NGC 7160 (Sicilia-Aguilar et al. 2006). Extensive *Spitzer* imaging has been performed in Chamaeleon I as well. Some of these data have been used to examine the properties of the disk population of Chamaeleon I (Luhman et al. 2005b; Damjanov et al. 2007), identify low-mass brown dwarfs with disks (Luhman et al. 2005a,c), and search for outflows (Bally et al. 2006). In this paper, we present a comprehensive census of disks in Chamaeleon I using most of the *Spitzer* images between 3.6 and 24  $\mu\text{m}$  that have been obtained in this region. We begin by describing the collection and

analysis of the *Spitzer* images (§ 2) and the identification of new disk-bearing members of the cluster with these data (§ 3). We then use the *Spitzer* photometry of the known members of the cluster to investigate the global properties of the disk population of Chamaeleon I (§ 4).

## 2. INFRARED IMAGES

### 2.1. Observations

For our census of the disk population in Chamaeleon I, we use images at 3.6, 4.5, 5.8, and 8.0  $\mu\text{m}$  obtained with *Spitzer*'s Infrared Array Camera (IRAC; Fazio et al. 2004a) and images at 24  $\mu\text{m}$  obtained with the Multi-band Imaging Photometer for *Spitzer* (MIPS; Rieke et al. 2004). The fields of view are  $5.2' \times 5.2'$  and  $5.4' \times 5.4'$  for IRAC and the 24  $\mu\text{m}$  channel of MIPS, respectively. The cameras produce images with FWHM=1.6-1.9'' from 3.6 to 8.0  $\mu\text{m}$  and FWHM=5.9'' at 24  $\mu\text{m}$ .

In this paper, we consider all IRAC and MIPS 24  $\mu\text{m}$  observations that have been performed within a radius of 3° from  $\alpha = 11^{\text{h}}07^{\text{m}}00^{\text{s}}$ ,  $\delta = -77^{\circ}10'00''$  (J2000) with the exception of the recently executed Legacy program of L. Allen, which has a program identification (PID) of 30574. These data were obtained through IRAC Guaranteed Time Observations (GTO) for PID=6, 36, and 37 (G. Fazio), IRAC and IRS GTO for PID=30540 (G. Fazio, J. Houck), IRS GTO for PID=40302 (J. Houck), Director's Discretionary Time for PID=248 (S. Mohanty), and Legacy programs for PID=139, 173 (N. Evans), and 148 (M. Meyer). The characteristics of the IRAC and MIPS images are summarized in Tables 1 and 2, respectively. The boundaries of these images are indicated in the maps of Chamaeleon I in Figure 1.

### 2.2. Data Reduction

Initial processing of the IRAC images was performed with the *Spitzer* Science Center (SSC) S14.0.0 pipeline. The resulting Basic Calibrated Data (BCD) images were automatically treated for bright source artifacts (jailbar, pulldown, muxbleed, and banding) with customized versions of IDL routines developed by the IRAC instrument team (Hora et al. 2004; Pipher et al. 2004). Mosaicking of the treated BCDs was performed using R. Gutermuth's WCSmosaic IDL package, which includes the following features: a redundancy-based cosmic ray detection and rejection algorithm; frame-by-frame distortion correction, derotation, and subpixel offsetting in a single transformation (to minimize data smoothing); and on-the-fly background matching. WCSmosaic was built with heavy dependence on the FITS and WCS access and manipulation procedures provided by the IDL Astronomy Users Library (Landsman et al. 1993). We selected a plate scale of 0.86'' pixel<sup>-1</sup> for the reduced IRAC mosaics, which is the native scale divided by  $\sqrt{2}$ .

For the processing of the MIPS data, the SSC pipeline versions were S16.0.1 for Astronomical Observation Request (AOR) identifications of 5687040, 5688064, 5688320, and 5688576 and S16.1.0 for all other AORs. The resulting 24  $\mu\text{m}$  images were reduced further with the MOPEX software from the SSC. The plate scale of the final images was 2.45'' pixel<sup>-1</sup>.

We used the IRAF task STARFIND to identify all point sources in the reduced IRAC and MIPS images. From the initial list of 3.6  $\mu\text{m}$  detections from

STARFIND, we rejected sources that were not detected in the  $4.5\ \mu\text{m}$  image for areas that were imaged by both channels. Similarly, we rejected STARFIND detections at  $4.5\ \mu\text{m}$  that did not have a corresponding detection at  $3.6\ \mu\text{m}$ . For the data at  $5.8$  and  $8.0\ \mu\text{m}$ , we retained only the sources that were detected in the  $3.6$  and  $4.5\ \mu\text{m}$  images, respectively. We marked the sources produced by these criteria on the images and removed remaining spurious detections through visual inspection.

We measured aperture photometry for the IRAC and MIPS sources using the IRAF task PHOT. We adopted zero point magnitudes ( $ZP$ ) of 19.670, 18.921, 16.855, 17.394, and 15.119 in the  $3.6$ ,  $4.5$ ,  $5.8$ ,  $8.0$ , and  $24\ \mu\text{m}$  bands, where  $M = -2.5 \log(DN/sec) + ZP$  (Reach et al. 2005; Engelbracht et al. 2007). For IRAC, we used an aperture radius of 4 pixels and inner and outer radii of 4 and 5 pixels, respectively, for the sky annulus. For MIPS, we adopted radii of 3, 3, and 4 pixels for the aperture and the inner and outer boundaries of the sky annulus, respectively. Using bright, isolated stars in the IRAC and MIPS images, we measured aperture corrections between our adopted apertures and the larger ones employed by Reach et al. (2005) and Engelbracht et al. (2007). For the MIPS data, we combined our aperture correction with the one estimated by Engelbracht et al. (2007) between their aperture and an infinite one. The total aperture corrections applied to our measurements are 0.18, 0.17, 0.23, 0.48, and 0.8 mag for  $3.6$ ,  $4.5$ ,  $5.8$ ,  $8.0$ , and  $24\ \mu\text{m}$ , respectively. Smaller apertures (and the appropriate aperture corrections) were used for sources that were near other stars, including the known members Hn 21W and E, the new member 2MASS J11062942–7724586 and its candidate companion Cha J11062788–7724543, and the new member 2MASS J11084296–7743500, which is close to the protostar IRN. Our quoted photometric errors include the Poisson errors in the source and background emission and the 2% and 4% uncertainties in the calibrations of IRAC and MIPS, respectively (Reach et al. 2005; Engelbracht et al. 2007). The errors do not include an additional error of  $\pm 0.05$  mag due to location-dependent variations in the IRAC calibration.

To illustrate the detection and completeness limits of the IRAC data, we consider the two shallow maps (AOR=3960320, 3651328) and two of the three deep maps (AOR=3955968, 12620032) that are centered on the northern and southern subclusters. The total exposure times at a given position in these maps are 20.8 and 968 s, respectively. For each exposure time and filter, we estimate the completeness limit by measuring the magnitude at which the logarithm of the number of sources as a function of magnitude departs from a linear slope and begins to turn over. Based on the distributions of IRAC magnitudes, which are shown in Figure 2, we arrive at completeness limits of 16.25, 16.25, 14.25, and 13.5 for the short exposures and 17.0, 16.75, 16.0, and 15.25 for the long exposures at  $3.6$ ,  $4.5$ ,  $5.8$ , and  $8.0\ \mu\text{m}$ , respectively. The estimates for the short exposures are confirmed by the comparisons of the histograms for the short and long exposures in Figure 2. The improvement in the completeness limits from the short exposures to the long ones is smaller at  $3.6$  and  $4.5\ \mu\text{m}$  than at  $5.8$  and  $8.0\ \mu\text{m}$  because the short exposures at  $3.6$  and  $4.5\ \mu\text{m}$  are already near the depth at which source confusion begins to reduce

completeness (Fazio et al. 2004b). Thus, the completeness limits of the longer exposures at  $3.6$  and  $4.5\ \mu\text{m}$  do not scale with  $\sqrt{\tau}$  and instead are limited by confusion. Our limits at  $3.6$  and  $4.5\ \mu\text{m}$  are similar to those measured by Fazio et al. (2004b) for deeper images of extragalactic fields. The short exposures at  $8.0\ \mu\text{m}$  exhibit the brightest completeness limit in our data, corresponding to a mass of  $\sim 0.015 M_{\odot}$  and a spectral type of  $\sim M9$  for an age of 2 Myr and the distance of Chamaeleon I according to evolutionary models (Chabrier et al. 2000). The fainter completeness limits of the other filters and exposure times are equivalent to masses of  $\sim 0.003$ – $0.01 M_{\odot}$  for members of Chamaeleon I.

### 3. NEW MEMBERS OF CHAMAELEON I

#### 3.1. Selection of Candidate Members

As shown in the maps of Chamaeleon I in Figure 1, most of the star-forming region has been imaged by IRAC and MIPS. Thus, we can use these data to search for new disk-bearing members of the cluster through the presence of mid-IR emission in excess above that expected from stellar photospheres. A color-color diagram constructed from IRAC measurements is an efficient tool for identifying sources of this kind (Allen et al. 2004; Megeath et al. 2004). Because our images encompass a large fraction of the known stellar population of Chamaeleon I, we can use our photometry for these sources to delineate the typical IRAC colors of young stars with disks. In Figure 3, we plot a diagram of  $[3.6] - [4.5]$  versus  $[5.8] - [8.0]$  for all known members that are not saturated and that have photometric uncertainties less than 0.1 mag in all of the IRAC bands, which consists of 153 sources. If an object has multiple measurements available in a given band, we have adopted the average of those measurements. As in other star-forming regions (Hartmann et al. 2005), the known members of Chamaeleon I form two distinct populations in Figure 3, stars clustering tightly near the origin and stars with much redder colors. The former are consistent with stellar photospheres while the latter indicate the presence of hot, optically-thick dust. In surveys for new members of Taurus and Lupus, Luhman et al. (2006) and Allen et al. (2007) used color criteria of  $[3.6] - [4.5] > 0.15$  and  $[5.8] - [8.0] > 0.3$  for selecting stars that might have disks. These colors bound the disk population in Chamaeleon I as well. Thus, we have applied these criteria to all sources in our photometric catalog for Chamaeleon I that have errors less than 0.1 mag in all four bands, which are shown in Figure 3. Stars classified as nonmembers in previous studies have been omitted (Luhman 2004a, 2007). This process produced 350 candidate disk-bearing sources. Although its photometric errors are larger than 0.1 mag, we have also identified 2MASS J11084296–7743500 as a promising candidate because of its red IRAC colors and its close proximity to the protostar IRN.

We selected 17 candidates for spectroscopy to assess their membership, focusing on sources that are within the two main subclusters of Chamaeleon I and that are bright enough for optical or near-IR spectroscopy. The spectroscopic observations of eight of these candidates were described by Luhman (2007) while the data for the remaining nine candidates are presented in § 3.2. Using these

spectra, we classify four candidates as new members and 13 candidates as nonmembers. One of the nonmembers, 2MASS J11081204–7622124, falls outside of the boundaries of the color-color diagram in Figure 3. Three of the nonmembers, 2MASS J11085651–7645154, 2MASS J11105185–7642259, and 2MASS J11105353–7726389, were identified as candidates because they exhibited excesses in preliminary photometric measurements that were used for selecting candidates for spectroscopy. However, upon further data analysis, we found that those apparent excesses were caused by contamination from cosmic rays, and that the sources do not exhibit excesses in our final photometry. For this reason, these three objects are excluded from Figure 3.

### 3.2. Spectroscopy of Candidates

#### 3.2.1. Observations

We performed optical and near-IR spectroscopy on nine of the candidate members of Chamaeleon I that were selected in § 3.1 using the Low Dispersion Survey Spectrograph (LDSS-3) on the Magellan II Telescope and the Gemini Near-Infrared Spectrograph (GNIRS) at Gemini South Observatory. The GNIRS observations were conducted through program GS-2005A-C-13. Table 3 summarizes the observing runs and instrument configurations for the spectra. In Table 4, we indicate the night on which each new member was observed. We also observed known late-type members of Chamaeleon I for comparison to the candidates, obtaining LDSS-3 spectra of OTS 44 and Cha J11091363–7734446 and GNIRS spectra of T50, Hn 12W, Cha H $\alpha$  11, and CHSM 17173. The procedures for the collection and reduction of the LDSS-3 and GNIRS spectra were similar to those described by Luhman (2004c) and Luhman et al. (2004), respectively.

#### 3.2.2. Nonmembers

Our spectroscopic targets are fainter than most of the known members of Chamaeleon I in the IRAC bands, which indicates that they should be low-mass stars or brown dwarfs if they are members of the cluster. Among the 17 candidates observed spectroscopically by Luhman (2007) and in this work, 13 sources do not exhibit the molecular absorption bands that characterize cool, low-mass objects. They also lack the hydrogen emission lines that are often seen in young stars with disks. Therefore, we classify these candidates as nonmembers. The spectral classifications of eight of these nonmembers were presented by Luhman (2004a). The remaining five sources (Cha J11081724–7631107, Cha J11083029–7733067, Cha J11084006–7627085, Cha J11090876–7626234, Cha J11120546–7631376) are classified as <M0 based on the absence of molecular absorption bands.

#### 3.2.3. New Member in Optical Sample

The remaining four candidates do show late-type spectral features and evidence of membership in Chamaeleon I. One of these candidates is in the LDSS-3 sample and the other three objects are in the GNIRS sample. We first discuss the source observed by LDSS-3, Cha J11070768–7626326 (hereafter Cha 1107–7626).

The optical spectrum of this candidate is shown in Figure 4. The most obvious feature of this spectrum is the strong H $\alpha$  emission line. The equivalent width of the line is uncertain because the surrounding continuum is weak and poorly measured, but it appears to have a value of several hundred angstroms. The line is clearly stronger than the emission observed in active late-type field dwarfs (Gizis et al. 2002) and indicates the presence of accretion. The H $\alpha$  emission and the mid-IR excess emission together demonstrate the youth of Cha 1107–7626, and thus we conclude that it is a member of Chamaeleon I.

To measure its spectral type, we have compared Cha 1107–7626 to optically-classified late-type members of Chamaeleon I and other star-forming regions (Luhman 2004a, 2007) as well as standard field dwarfs (Kirkpatrick et al. 1999). The results of our classification are illustrated in Figure 4, where we compare Cha 1107–7626 to the young late-type objects KPNO 4, OTS 44, and Cha J11091363–7734446 and the L0 field dwarf 2MASS J03454316+2540233 (Kirkpatrick et al. 1999). KPNO 4 and OTS 44 have optical spectral types of M9.5 (Briceño et al. 2002; Luhman 2007) and Cha J11091363–7734446 was classified as  $\geq$ M9 with IR spectra (Luhman 2007). We now classify the latter as M9.5 $\pm$ 0.5 based on the similarity to KPNO 4 and OTS 44 in the optical data in Figure 4. Compared to the three young M9.5 objects, Cha 1107–7626 exhibits weaker TiO and VO absorption, which suggests a later spectral type. Indeed, its spectrum agrees better with the L0 field dwarf, as shown in Figure 4. Because the transition from M to L types is defined by the disappearance of TiO absorption at 7000–7200 Å (Kirkpatrick et al. 1999), we need a spectrum with a higher signal-to-noise ratio at those wavelengths to definitively classify Cha 1107–7626 as L-type. However, given that its spectrum agrees significantly better with L0 than M9.5, we tentatively classify it as L0.

The comparison of Cha 1107–7626 to the field dwarf in Figure 4 indicates that it has negligible extinction ( $A_J \lesssim 0.3$ ). By combining its  $J$ -band magnitude with a bolometric correction for L0 (Dahn et al. 2002) and a distance modulus of 6.05 (Luhman 2008), we estimate a bolometric luminosity of  $3.3 \times 10^{-4} L_{\odot}$ . At this luminosity, Cha 1107–7626 is tied with Cha J11083040–7731387 (Luhman 2007) as the least luminous known member of Chamaeleon I.

To estimate the mass of Cha 1107–7626, we begin by examining its position on the Hertzsprung-Russell (H-R) diagram. To do this, we must convert the spectral type of Cha 1107–7626 to an effective temperature. In our previous studies of young late-type objects, we have performed conversions of this kind with the temperature scales from Luhman (1999) and Luhman et al. (2003), which spanned M1 to M9. The former scale was designed to produce coequality for the components of the young quadruple system GG Tau (K7-M7.5) on the model isochrones from Baraffe et al. (1998). Luhman et al. (2003) adjusted that scale at M8 and M9 to improve the coequality between the coolest members of Taurus and IC 348 and the members at earlier types. The resulting scale was then extrapolated to M9.25 and M9.5 as cooler objects were discovered in Taurus and Chamaeleon I

(Briceño et al. 2002; Luhman et al. 2004; Luhman 2007). For the purposes of this study, we continue this extrapolation to L0 for Cha 1107–7626, arriving at a value of 2200 K. Using this temperature and our luminosity estimate, we have placed Cha 1107–7626 on the H-R diagram in Figure 5. We have included all other known low-mass members of Chamaeleon I (Luhman 2007) as well as the three new members that we have found with GNIRS (§ 3.2.4). Four of the previously known members have formal spectral types of  $\geq M9$  because they were classified through H<sub>2</sub>O absorption bands, and the variation of these bands with optical spectral type is unknown for young objects later than M9.5. However, the strengths of the H<sub>2</sub>O bands in these objects do agree with those of OTS 44 and KPNO 4, which have optical types of M9.5. Thus, it is likely that they have spectral types near M9.5.

The cluster sequence for Chamaeleon I in Figure 5 is parallel to the model isochrones for members earlier than M8, which is expected since the adopted temperature scale was designed to produce coevality for the GG Tau system. However, the sequence does not remain parallel to the isochrones at later types. Most members earlier than M8 appear between the isochrones for 1 and 10 Myr, while the coolest brown dwarfs, including Cha 1107–7626, are bracketed by 10 and 100 Myr. It is unlikely that these old ages are valid. For instance, the lifetimes of molecular clouds are too short ( $\tau < 10$  Myr, Hartmann, Ballesteros-Paredes, & Bergin 2001) for the Chamaeleon I clouds to have undergone star formation across such an extended period of time. In addition, objects with ages of 10–100 Myr would have dispersed from the cloud long ago. Instead, the old isochronal ages are probably a reflection of errors in the adopted temperature scale and/or the evolutionary models. If the models are valid, then the temperature scale for young objects at M9–L0 must be much cooler than the adopted one, which is already cooler than the scale measured for field dwarfs (Kirkpatrick 2005). Significant errors are probably present in both the temperature scale, which is unconstrained at the latest types, and the predicted effective temperatures, which are sensitive to various details of the models, such as the treatment of convection (Baraffe et al. 2002). Compared to effective temperature, bolometric luminosity appears to be less sensitive to model uncertainties, at least for ages of  $\tau \gtrsim 1$  Myr (Baraffe et al. 2002), and is easier to measure. Therefore, we have chosen to estimate the mass of Cha 1107–7626 from its luminosity. If we assume that it has an age in the range of values exhibited by the stellar members of Chamaeleon I ( $\tau = 1\text{--}6$  Myr, Luhman 2007), then we arrive at a mass of 0.004–0.01  $M_{\odot}$  for Cha 1107–7626 based on the luminosities predicted by Burrows et al. (1997) and Chabrier et al. (2000). Zapatero Osorio et al. (2007) and Scholz & Jayawardhana (2007) have reported detections of disks for brown dwarfs at comparable masses in the  $\sigma$  Ori cluster using IRAC data. However, because of the very large uncertainties in the 5.8 and 8.0  $\mu\text{m}$  photometry in those studies (0.3–0.5 mag), their detections of excess emission have low significance. Thus, Cha 1107–7626 is the least massive brown dwarf that has definitive evidence for a circumstellar disk.

### 3.2.4. New Members in Infrared Sample

In the GNIRS sample, the three candidates that show evidence of membership in Chamaeleon I are 2MASS J11084296–7743500, 2MASS J11062942–7724586, and 2MASS J11070369–7724307 (hereafter 2M 1108–7743, 2M 1106–7724, 2M 1107–7724). The near-IR spectra of these objects exhibit strong H<sub>2</sub>O absorption bands, which indicates that they are low-mass stars or brown dwarfs rather than galaxies. High levels of reddening in their spectra demonstrate that they are not field stars in the foreground of the cluster and they are too bright to be background field dwarfs. We also detect emission in H<sub>2</sub> 1–0 S(1) at 2.12  $\mu\text{m}$  in 2M 1108–7743, which is a signature of very young stars. Finally, the spectral features that are sensitive to surface gravity in our data, such as the shape of the *H*- and *K*-band continua (Lucas et al. 2001; Luhman et al. 2004; Kirkpatrick et al. 2006), are inconsistent with field dwarfs and giants. Instead, the spectra of 2M 1108–7743, 2M 1106–7724, and 2M 1107–7724 agree well with known cluster members observed with GNIRS in terms of the gravity-sensitive features. Based on these properties and the presence of mid-IR excess emission, we classify these sources as members of Chamaeleon I.

To measure the spectral types of 2M 1108–7743, 2M 1106–7724, and 2M 1107–7724, we have compared their H<sub>2</sub>O and atomic absorption features to those of the optically-classified members of Chamaeleon I that we observed with GNIRS. To facilitate this comparison, we dereddened the spectra of the new members to give them the same slopes as the known members. We also smoothed the spectra to a low resolution when comparing the broad H<sub>2</sub>O absorption bands. The dereddened, smoothed versions of the spectra are shown in Figure 6. Each object is compared to the young standards that provide the closest match to the strength of the H<sub>2</sub>O absorption. Through this comparison and a similar analysis of the atomic absorption lines, we classify 2M 1108–7743, 2M 1106–7724, and 2M 1107–7724 as M4 $\pm$ 1, M6 $\pm$ 1, and M7.5 $\pm$ 1, respectively. These spectral types correspond to masses of  $\sim 0.3$ , 0.1, and 0.04  $M_{\odot}$ , respectively, according to the theoretical evolution models of Baraffe et al. (1998) and Chabrier et al. (2000) and the temperature scale of Luhman et al. (2003) for ages of a few Myr.

The process of dereddening the near-IR spectra of 2M 1108–7743, 2M 1106–7724, and 2M 1107–7724 to match the young standards, which have little if any extinction (Luhman 2007), produces extinction estimates of  $A_J = 5.6$ , 5.6, and 4.7, respectively. It is not surprising that these objects are highly obscured given their locations. 2M 1108–7743 is only 14'' from the protostar IRN while the other two sources are within the group of embedded stars near Cederblad 110. *Spitzer* and 2MASS images of 2M 1106–7724, 2M 1107–7724, and the protostars in Cederblad 110 are shown in Figure 7. Based on their high levels of extinction and their close proximity to known protostars, 2M 1108–7743, 2M 1106–7724, and 2M 1107–7724 may be the youngest known low-mass members of the cluster. By combining our extinction estimates for these sources with their *H* and *K<sub>s</sub>* magnitudes, the appropriate bolometric corrections, and the distance of Chamaeleon I, we arrive at luminosities of

0.053, 0.035, and 0.020  $L_{\odot}$ , respectively. Because the  $H$ - and  $K$ -band spectra for these sources do not show any evidence of continuum veiling, these luminosity estimates should be uncontaminated by disk emission.

The spectral types, extinctions, luminosities, membership evidence, and near-IR photometry for the four new members of Chamaeleon I are provided in Table 4. The IRAC and MIPS photometry for these sources are presented in the tabulation of *Spitzer* data for all known members of the cluster in § 4.1. The IRAC and MIPS measurements for the 13 nonmembers are listed in Table 5.

### 3.3. Remaining Candidates

In the previous section, we obtained spectra for a small sample of the candidate disk-bearing members of Chamaeleon I that were identified in § 3.1 with Figure 3. To investigate the nature of the remaining candidates, we compare them to the known cluster members in *Spitzer* color-magnitude and color-color diagrams in Figure 8. Many of the candidates are as red as the reddest known members, indicating that they are protostellar if they are members. In addition, bona fide members are likely to be brown dwarfs given that nearly all of the candidates are fainter than the stellar members of the cluster, although stars with edge-on disks can also appear very faint. For instance, Cha J11081938–7731522 has a stellar mass according to its spectral type, but it is the faintest and reddest known member in  $[3.6]$  and  $[3.6] - [24]$ , respectively, which is explained by the presence of an edge-on disk (Luhman 2007). However, rather than brown dwarfs or stars with edge-on disks, the vast majority of the candidates are probably galaxies.

We can refine our sample of candidate members and remove some of the galaxy contaminants by applying additional criteria. The initial sample of candidates was defined by colors of  $[3.6] - [4.5] > 0.15$  and  $[5.8] - [8.0] > 0.3$ . However, the sources with  $[3.6] - [4.5] \lesssim 0.7$  and  $[5.8] - [8.0] \gtrsim 1.2$  within that sample have colors that differ significantly from those of all known members of Chamaeleon I, as shown in Figure 3. These objects can be rejected as likely galaxies. Because galaxy contamination increases with fainter magnitudes, brighter candidates are less likely to be galaxies. The probability of membership is also higher for candidates that are close to known members of Chamaeleon I. By applying these criteria, we have identified the most promising candidate disk-bearing members, which are listed in Table 6. The brightest candidate, 2MASS J11085367–7521359, is probably a solar-mass star if it is associated with Chamaeleon I. The magnitudes of the remaining candidates are indicative of brown dwarfs. As noted in Table 6, some of the candidates may be class I sources or companions to known members. The new member 2M 1106–7724 and the candidate Cha J11062788–7724543 could comprise the youngest low-mass binary system discovered to date.

In addition to revealing new candidate members of Chamaeleon I, our mid-IR measurements provide constraints on the membership of sources that have been previously cited as possible members. In a census of Chamaeleon I, Luhman (2004a) assigned membership to a few objects that lacked spectroscopic classification but that exhibited mid-IR excess emission. One of

these objects is ISO 13 (Nordh et al. 1996; Persi et al. 2000). The near-IR counterpart for ISO 13 was not positively identified in previous studies because of uncertainties in the coordinates measured with *ISO*. Based on a comparison of the photometry from *ISO* to measurements from IRAC for sources in the vicinity of the *ISO* coordinates, we conclude that ISO 13 corresponds to 2MASS J11025579–7724304. For this source, we measure magnitudes of 13.87, 13.68, 12.68, 9.87, and 6.54 at 3.6, 4.5, 5.8, 8.0, and 24  $\mu\text{m}$ , respectively. When we combine these data with photometry from the Two-Micron All-Sky Survey (2MASS, Skrutskie et al. 2006), we find that the colors of ISO 13 are relatively blue at 1–5  $\mu\text{m}$  but become very red at 8 and 24  $\mu\text{m}$ . These colors are inconsistent with those of known members of Chamaeleon I, as illustrated by the position of ISO 13 in the IRAC color-color diagram in Figure 3. Therefore, we remove ISO 13 from our list of members of Chamaeleon I because it is probably a galaxy. Luhman (2004a) included ISO 206 in a list of candidate members based on an apparent excess at 6.7  $\mu\text{m}$  in photometry from *ISO*. However, mid-IR excess emission is not present in the IRAC data for this source. As a result, there is no longer any reason to consider ISO 206 as a possible member. Finally, Persi et al. (2001) identified three candidate class I brown dwarfs in the vicinity of Cederblad 110 through the presence of near-IR excess emission. In our IRAC data, we find that one of these candidates, NIR72, is a patch of nebulosity rather than a stellar source while the other two objects, NIR84 and NIR89, do not exhibit excess emission, and thus are not class I sources.

### 3.4. Completeness for Members with Disks

We now use our mid-IR data to examine the completeness of the current census of disk-bearing members of Chamaeleon I. We consider only the areas that have been imaged in all four bands of IRAC, which encompass 170 of the 229 known members of the cluster. Within these areas, 156 members have photometric errors less than 0.1 mag in all IRAC bands, while the remaining 14 known members lack accurate photometry in at least one band because they are saturated, extended, too close to a brighter star, or below the detection limit of all four bands (Cha-MMS1). Thus, the photometric criteria that we used for selecting candidate members with disks in § 3.1 recover all known members with disks in the areas with 4-band coverage with the exception of the brightest stars, faint companions, and the youngest protostars. As a result, our sample of candidates should be complete for disk-bearing members in the same range of magnitudes and extinctions exhibited by the known stellar population. To quantify the completeness limits of this candidate sample, we have plotted the photometric completeness limits at 8  $\mu\text{m}$  for the shortest and longest exposures in the color-magnitude diagram in Figure 8 (§ 2.2). Meanwhile, to evaluate the completeness of the current census of confirmed members with disks, we consider the remaining candidates that lack spectroscopy. As shown in Figure 8, only one candidate is present in the magnitude range of young stars in Chamaeleon I ( $[3.6] \lesssim 12$ ), which is in Table 6. Thus, the current census is nearly complete for stars with disks in the fields imaged by all four bands of IRAC, which encompass most of the Chamaeleon I cloud (Figure 1). Our survey is not com-

plete for brown dwarfs with disks, as indicated by the large number of candidates lacking spectroscopy in Figure 8. However, based on optical and near-IR surveys, the census of substellar cluster members (both with and without disks) is complete for specific fields and ranges of mass and extinction that are described by Luhman (2007).

#### 4. GLOBAL PROPERTIES OF DISK POPULATION

##### 4.1. *Spitzer* Photometry for Known Members

We wish to use our mid-IR photometry from *Spitzer* to investigate the properties of the disk population in Chamaeleon I. To do this, we begin by presenting a tabulation of these measurements for all known members of the cluster. The latest census of Chamaeleon I from Luhman (2007) contained 226 sources. ISO 13 was considered a cluster member in that study, but we now classify it as a probable galaxy (§ 3.3). The census from Luhman (2007) did not include protostellar sources that have been detected only at far-IR wavelengths and longward, such as Cha-MMS1 (Reipurth et al. 1996). Because this source is detected in our 24  $\mu\text{m}$  data (see Figure 7)<sup>6</sup>, we include it in the list of members considered in this work. Eight young stars from Covino et al. (1997) are within the area in which we have reduced nearly all available IRAC and MIPS data, which has a radius of 3° centered at  $\alpha = 11^{\text{h}}07^{\text{m}}00^{\text{s}}$ ,  $\delta = -77^{\circ}10'00''$  (J2000). Three of these stars, RX J1108.8–7519A and B and RX J1129.2–7546, have proper motions that are similar to those of known members of Chamaeleon I, while the other five stars are probably members of the  $\epsilon$  Cha association according to their proper motions (see Appendix). We also find that four of the young stars from Luhman (2007) have proper motions that favor membership in  $\epsilon$  Cha rather than Chamaeleon I. Therefore, we deduct ISO 13 and these four stars from the census of Luhman (2007) and add Cha-MMS1, RX J1108.8–7519A and B, and RX J1129.2–7546. When we include the four new members that we have discovered (§ 3), we arrive at census of Chamaeleon I that contains 229 sources.

The IRAC images encompass 198 of the 229 known members, all of which are detected in at least one IRAC band, except for the protostar Cha-MMS1 and six objects that are unresolved from brighter stars (ESO H $\alpha$  281, 2MASS J11011926–7732383B, 2MASS J11072022–7738111, CHXR 73B, T39B, T33B). The MIPS 24  $\mu\text{m}$  images contain 199 members, 152 of which are detected. Among the MIPS detections, seven stars are saturated and one source, T41, is not measured because it is extended. Thus, we have measured IRAC and MIPS photometry for 191 and 144 known members, respectively. These data are presented in Table 7. Nondetections at 24  $\mu\text{m}$  are indicated for members with IRAC measurements. Sources that lack measurements in both IRAC and MIPS are not included in Table 7, which consist of six unresolved companions (2MASS J11011926–7732383B, 2MASS J11072022–7738111, CHXR 73B, T39B, T33B, CHXR 68B), one member not detected by MIPS and outside of IRAC (2MASS J11155827–7729046), and 19

members outside of both the IRAC and MIPS images. ESO H $\alpha$  281 is unresolved from a brighter background star in 2MASS (Luhman 2007) but is comparable to the latter at 8  $\mu\text{m}$  and is the dominant source at 24  $\mu\text{m}$ . Thus, we were able to measure photometry for ESO H $\alpha$  281 at 24  $\mu\text{m}$  but not in the IRAC bands.

As mentioned in § 1, previous studies have measured photometry for members of Chamaeleon I from the *Spitzer* images considered in this work. Luhman et al. (2005a,b,c) reported IRAC photometry for known members with spectral types later than M6. Those measurements are now superseded by the ones in Table 7, which were performed with newer versions of the image processing software described in § 2.2. More recently, Damjanov et al. (2007) measured IRAC photometry for 81 members from the images for AORs 3960320 and 3651328 and MIPS 24  $\mu\text{m}$  photometry for 59 members from the images for AORs 3661312 and 3962112. To compare the IRAC photometry from Damjanov et al. (2007) to our measurements from the same images, we plot the differences of the IRAC magnitudes from the two studies as a function of magnitude in Figure 9. The two sets of photometry differ by more than 0.1 mag in many cases, particularly at fainter levels and at 5.8  $\mu\text{m}$ . Most of these differences are within the errors quoted by Damjanov et al. (2007), but those errors are much larger than the ones that we estimate for our photometry. We find errors of only a few percent for all of our measurements in Figure 9, while the errors from Damjanov et al. (2007) are as large as  $\sim 50\%$ . To illustrate the relative accuracies of these measurements without making use of the quoted errors, we compare the IRAC color-color diagrams that are produced by the two studies in Figure 10. Our colors form two distinct groups, a tight cluster near the origin and a broader distribution of significantly redder colors, which are indicative of stellar photospheres and stars with disks, respectively. In comparison, the colors from Damjanov et al. (2007) exhibit a much larger scatter and extend to significantly negative colors, which are unphysical for the spectral types in question. Thus, according to both this comparison and the formal error estimates, our measurements have significantly higher accuracies than those from Damjanov et al. (2007).

##### 4.2. SED Classifications

To classify the IR spectral energy distributions (SEDs) of the members of Chamaeleon I, we use the spectral slope defined as  $\alpha = d \log(\lambda F_\lambda) / d \log(\lambda)$  (Lada & Wilking 1984; Adams et al. 1987). This slope is normally measured between  $\lambda \sim 2$   $\mu\text{m}$  and 10–20  $\mu\text{m}$ . We have measured photometry at 8 and 24  $\mu\text{m}$  for 182 and 144 members, respectively. At least one of these bands is available for 197 members. At short wavelengths, data at 3.6  $\mu\text{m}$  are available for 164 members. Slopes from 3.6  $\mu\text{m}$  to 8 or 24  $\mu\text{m}$  can be computed for 160 members. Photometry at  $K_s$  (2.2  $\mu\text{m}$ ) is also useful as a short-wavelength band for spectral slopes since it has been measured for all known members (2MASS; Luhman 2007). Therefore, to provide a spectral slope for as many members as possible, we have computed slopes between four pairs of bands, 2.2–8, 2.2–24, 3.6–8, and 3.6–24  $\mu\text{m}$ . We have dereddened these slopes using the extinctions from Luhman (2007) and the reddening law from Flaherty et al. (2007), except for 10 members

<sup>6</sup> The detection of Cha-MMS1 in the 24  $\mu\text{m}$  data was previously reported by Belloche et al. (2006).

that lack spectral types and extinction estimates. As in § 3.1, we have adopted the average measurement in a given band if an object has been observed at multiple epochs. The resulting values of  $\alpha_{2-8}$ ,  $\alpha_{2-24}$ ,  $\alpha_{3.6-8}$ , and  $\alpha_{3.6-24}$  are listed in Table 8 for the 196 known members of Chamaeleon I that have photometry at 8 or 24  $\mu\text{m}$  and at shorter wavelengths (i.e., excluding Cha-MMS1).

The distributions of spectral slopes from Table 8 are shown in Figure 11. Like the colors in Figure 3, the slopes form two distinct populations that are well-separated from each other. The narrow group of bluer objects corresponds to stellar photospheres while the broader distribution of redder sources represents stars with disks. We investigate these data in greater detail by plotting the slopes as a function of spectral type in Figure 12. The widths of the photospheric sequences for  $\alpha_{2-24}$  and  $\alpha_{3.6-24}$  increase at later spectral types because of the larger photometric errors at 24  $\mu\text{m}$  for cooler, fainter objects. Most photospheres later than M6 are below the detection limit at 24  $\mu\text{m}$ . Because of the close proximity and low background of Chamaeleon I, this detection limit of M6 for stellar photospheres is significantly cooler than the limits typically achieved in MIPS 24  $\mu\text{m}$  surveys of other star-forming regions. In the two slopes based on 8  $\mu\text{m}$ , the separations between the two populations are smaller than in  $\alpha_{2-24}$  and  $\alpha_{3.6-24}$ , but the photospheric sequences are also tighter because of the higher photometric accuracies at 8  $\mu\text{m}$  relative to 24  $\mu\text{m}$ . The distributions of dereddened slopes in Figure 12 are nearly identical to the distributions of observed values except that the sequences of stellar photospheres are slightly tighter after dereddening.

In Figure 12,  $\alpha_{2-8}$  and  $\alpha_{3.6-8}$  are approximately constant for stellar photospheres with types of B through K, but they change noticeably at later spectral types. As a result, we should not use fixed thresholds in  $\alpha_{2-8}$  and  $\alpha_{3.6-8}$  for identifying stars with disks. Instead, our adopted thresholds are fits to the photospheric sequences that have been offset by 0.3 so that they are significantly greater than the scatter in each sequence. A constant threshold of  $-2.2$  is sufficient for identifying stars with disks for both  $\alpha_{2-24}$  and  $\alpha_{3.6-24}$ , as shown in Figure 12. Following the standard classification scheme for SEDs of young stars (Lada 1987; Greene et al. 1994), we classify stars with slopes below the thresholds in Figure 12 as class III while redder stars with  $\alpha < -0.3$ ,  $-0.3 \leq \alpha \leq 0.3$ , and  $\alpha > 0.3$  are designated as class II, flat-spectrum, and class I, respectively. We cannot classify Cha-MMS1 with our data because it is not detected at wavelengths shorter than 24  $\mu\text{m}$ , but it is probably in the class 0 stage or an earlier, prestellar phase (Reipurth et al. 1996; Lehtinen et al. 2001; Belloche et al. 2006).

The SED classifications produced by  $\alpha_{2-8}$ ,  $\alpha_{2-24}$ ,  $\alpha_{3.6-8}$ , and  $\alpha_{3.6-24}$  disagree for a small number of sources. The classes from three of the four slopes agree for T14A, C1-2, Ced 110-IRS4, ISO 97, ISO 217, ISO 237, Hn10E, C1-25, and Cha H $\alpha$  1. For each of these stars, we assign the classification from the three slopes that agree. ISO 86 and Ced 110-IRS6 are class I by  $\alpha_{2-8}$  and  $\alpha_{2-24}$  and are class II by  $\alpha_{3.6-8}$  and  $\alpha_{3.6-24}$ . We adopt the latter classification for these stars because of the possibility of variability during the time between the  $K_s$  and *Spitzer* observations. For the same reason, we adopt the classification from  $\alpha_{3.6-8}$  over the one from

$\alpha_{2-8}$  for T29. Because the 8  $\mu\text{m}$  slopes of CHSM 15991 indicate a flat-spectrum class while the 24  $\mu\text{m}$  slopes are only slightly below the flat/II threshold, we adopt the former classification for this star. The SEDs of T11, CHXR 22E, and CHXR 71 are consistent with stellar photospheres at  $\lambda \leq 8 \mu\text{m}$  but are much redder at 24  $\mu\text{m}$ . SEDs of this kind are indicative of disks with inner holes, which are also known as transitional disks (Calvet et al. 2002, 2005; D’Alessio et al. 2005; Espaillat et al. 2007a,b; Furlan et al. 2007). CHXR 76 may have a transitional disk as well, although the size of the 24  $\mu\text{m}$  excess is small and the star is slightly below the adopted II/III thresholds for  $\alpha_{2-24}$  and  $\alpha_{3.6-24}$ . We classify these four stars as class II rather than class III since they exhibit disk emission at 24  $\mu\text{m}$ . The SEDs of Cha J11081938–7731522 and ESO H $\alpha$  569 also become more steeply rising at longer wavelengths. For these stars, the data at 8 and 24  $\mu\text{m}$  indicate classes II and I, respectively. Both Cha J11081938–7731522 and ESO H $\alpha$  569 show evidence of edge-on disks (Luhman 2007), which is consistent with the distinctive shapes of their SEDs. Thus, we conclude that they are probably edge-on class II systems. Hn 21E and the new member near IRN, 2M J1108–7743, have different classifications according to  $\alpha_{2-8}$  and  $\alpha_{3.6-8}$ . For these two stars, we assign the classifications from  $\alpha_{3.6-8}$  because the 3.6 and 8  $\mu\text{m}$  data were measured with the same apertures and at the same time. Both stars are too close to brighter stars for useful constraints on their 24  $\mu\text{m}$  fluxes. Our final SED classifications are provided in Table 8.

Finally, we examine the SEDs of the seven known members of Chamaeleon I that are within the *Spitzer* images but have not been classified with the spectral slopes in Figure 12 because they lack photometry at 8 and 24  $\mu\text{m}$ . These measurements are unavailable because the stars are outside of the images, below the detection limits, saturated, or extended, as indicated in Table 7 for T6, T27, T41, CHXR 54, 2MASS J11112249–7745427, and 2MASS J11080609–7739406. The seventh member, 2MASS J11155827–7729046, is outside of the IRAC images and is not detected by MIPS, and thus is not present in Table 7. The absence of a detection at 24  $\mu\text{m}$  is sufficient to demonstrate that this star is class III. To classify the other six objects, we measured spectral slopes from  $K_s$  and the available IRAC data and applied thresholds similar to those developed in Figure 12. We find that T6, T27, and 2MASS J11112249–7745427 are class II and T41, CHXR 54, and 2MASS J11080609–7739406 are class III.

Table 9 summarizes the SED classifications for the known members of Chamaeleon I that are within the *Spitzer* images, with the exception of the protostar Cha-MMS1.

### 4.3. Disk Fraction

We can use our SED classifications to measure the fraction of stars and brown dwarfs in Chamaeleon I that harbor circumstellar disks. For the disk fraction to be meaningful, it must be measured from a sample of cluster members that is unbiased in terms of disks. Although some of the early studies of Chamaeleon I identified members by signatures related to disks, recent surveys at X-ray, optical, and near-IR wavelengths have been sensitive to both class II and class III sources (Feigelson & Lawson

2004; Stelzer et al. 2004; Luhman 2007). The resulting census is unbiased in terms of SED class for most of the cloud (Luhman 2007). The major exception is at high extinctions, where class I and II stars are readily found through mid-IR excesses (such as three of the new members in this work) while their class III counterparts are much more difficult to identify. However, in a cloud like Chamaeleon I that has relatively low extinction ( $A_V < 4$ ), any members that are highly embedded ( $A_V > 10$ ) are probably very young stars in their parent cores, and thus are likely to have disks. In other words, it is unlikely that Chamaeleon I contains a significant number of heavily obscured class III stars. This conclusion is supported by the X-ray surveys of Feigelson & Lawson (2004) and Stelzer et al. (2004), which were capable of detecting sources of this kind. Therefore, we include all known members of Chamaeleon I in our disk fraction measurement with the exception of the new substellar member Cha 1107–7626 and the protostar Cha-MMS1. The former is excluded because it was found through its disk emission, but it is not within the detection limits of previous unbiased surveys. As for Cha-MMS1, sources that are less evolved than class I are generally not included in disk fraction measurements.

We have computed the fraction of members that are class I or class II as a function of spectral type, which is a good proxy for stellar mass. We selected the boundaries of the spectral type bins to correspond approximately to intervals of 0.5 in the logarithm of mass based on the temperature scale of Luhman et al. (2003) and the evolutionary models of Baraffe et al. (1998) and Chabrier et al. (2000). For members that lack spectral classifications, we estimate masses and spectral types by combining their photometry, the evolutionary models, and an assumed age of 2 Myr, which should be sufficiently accurate for identifying the bins in which they belong. To compare the disk fractions of Chamaeleon I and the young cluster IC 348, we have applied our SED classification criteria to the IRAC data for IC 348 from Lada et al. (2006). The resulting disk fractions as a function of mass for Chamaeleon I and IC 348 are listed in Table 10 and are plotted in Figure 13.

Through an earlier analysis of a subset of the *Spitzer* images, Luhman et al. (2005b) found that low-mass stars and brown dwarfs in Chamaeleon I exhibit similar disk fractions. We arrive at the same result with our expanded set of images. Other young clusters like IC 348 and  $\sigma$  Ori also have disk fractions that are roughly unchanged from low-mass stars to brown dwarfs (Luhman et al. 2005b; Hernández et al. 2007; Caballero et al. 2007). As shown in Figure 13, the disk fractions at low masses in Chamaeleon I and IC 348 have similar values. However, the disk fractions of the two clusters diverge significantly above  $\sim 0.3 M_\odot$ . This difference is particularly striking since similar ages have been reported for the two clusters (Luhman et al. 2003; Luhman 2007). To compare their ages in detail, we have estimated the ages of members of Chamaeleon I and IC 348 between 0.1 and  $1 M_\odot$  by combining the temperatures and luminosities from Luhman et al. (2003) and Luhman (2007) with the evolutionary models of Baraffe et al. (1998). The resulting distributions of isochronal ages are indistinguishable, as shown in Figure 14. Thus, the relative disk fractions indicate that

the typical lifetime of disks around solar-mass stars is shorter in IC 348 than in Chamaeleon I. The higher stellar density of IC 348 relative to Chamaeleon I is the only obvious potential source of this difference in disk lifetimes. The low-mass stars in IC 348 are segregated toward the outer regions of the cluster where the density is lower (Muench et al. 2003), which might explain why their disk fraction is similar to that of low-mass stars in Chamaeleon I. Several clusters and associations that are slightly older than IC 348 and Chamaeleon I, such as Upper Sco, NGC 2362, and  $\sigma$  Ori ( $\tau \sim 5$  Myr), exhibit disk fractions that decrease at higher stellar masses in the same manner observed for IC 348 (Carpenter et al. 2006; Dahm & Hillenbrand 2007; Hernández et al. 2007), which suggests that more massive stars have shorter disk lifetimes than low-mass stars in most clusters. The solar-mass stars in Chamaeleon I must have unusually long disk lifetimes, or their disks must be on the verge of rapidly dissipating.

#### 4.4. Spatial Distributions of SED Classes

In the previous section, we investigated the dependence of the disk fraction in Chamaeleon I on stellar mass. We now consider the spatial distribution of disk-bearing stars, which may provide additional insight into disk evolution.

As shown in Table 9, the southern subcluster exhibits a slightly higher disk fraction and contains more class I and flat-spectrum sources than the northern subcluster, which suggests that the southern population is slightly less evolved. A small age difference of this kind is also implied by the H-R diagrams of the two subclusters and the relative levels of extinction (Luhman 2007). The spatial distributions of the members of Chamaeleon I within the *Spitzer* images are compared in the maps in Figure 15 according to their SED classes. Because the protostellar population of Chamaeleon I is smaller than ones in younger and richer star-forming regions, the distribution of class I and flat-spectrum sources in Figure 15 is not particularly informative. We simply find that they are highly clustered and are concentrated near dense molecular gas, which are typical properties of class I objects in embedded clusters (Hartmann 2002; Lada et al. 2000, 2004; Teixeira et al. 2006; Muench et al. 2007; Allen et al. 2007; Gutermuth et al. 2007; Winston et al. 2007).

The large samples of class II and III members are more amenable to a detailed comparison than the class I and flat-spectrum objects. In Figure 15, we find that the distributions of these two classes are indistinguishable in the southern subcluster, but differ significantly in the northern one. In comparison, Damjanov et al. (2007) concluded that stars with disks share the same distribution as diskless stars in both subclusters. They did not detect the difference in the distributions of classes II and III in the northern subcluster because their sample of members was three times smaller and was less complete for class III objects than the one we are considering. The wider class III distribution in the north can be explained as a combination of the segregation of northern low-mass stars to larger radii (Luhman 2007) and the lower disk fraction of low-mass stars relative to solar-type stars (Figure 13).

#### 4.5. Transitional Disks

As mentioned in § 4.2, transitional disks are characterized by the presence of large inner holes and gaps. These disks are noteworthy because their holes may represent evidence of forming giant planets. A transitional disk is identified through the shape of its SED, which exhibits photospheric colors at shorter IR wavelengths followed by a sudden onset of excess emission from the disk at longer wavelengths. In § 4.2, we classified T11, CHXR 22E, CHXR 71, and possibly CHXR 76 as transitional disks because their spectral slopes showed excess emission at  $24 \mu\text{m}$  but not at  $\leq 8 \mu\text{m}$ . The distinctive SEDs of these stars are also illustrated in the color-color diagram in Figure 8, where they have colors of  $[3.6] - [8.0] \sim 0.2$  and  $[3.6] - [24] > 1$ . The transitional disk for T11 (also known as CS Cha) has already been studied in detail through mid-IR spectroscopy with *Spitzer* (Espaillat et al. 2007a). Meanwhile, a few other cluster members, such as C7-1 and T35, exhibit excess emission at both 8 and  $24 \mu\text{m}$ , but the excess is smaller at  $8 \mu\text{m}$ . In other words, the spectral slopes ending at  $8 \mu\text{m}$  are bluer than the ones ending at  $24 \mu\text{m}$ . These stars may possess transitional disks, as previously noted by Damjanov et al. (2007). Edge-on disks also produce redder slopes at longer wavelengths, as in Cha J11081938–7731522 and ESO H $\alpha$  569 (§ 4.2). However, unlike a transitional disk, an edge-on disk makes the star appear much fainter at optical and near-IR wavelengths than unocculted stars at the same spectral type, which is not the case for stars discussed in this section.

#### 4.6. Disk Variability

Our *Spitzer* survey has produced high-precision mid-IR photometry at multiple epochs for a large fraction of a young stellar population. As a result, we have a rare opportunity to characterize the variability of young stars and brown dwarfs at mid-IR wavelengths.

We have measured photometry at multiple epochs for 27, 30, 70, and 61 members at 3.6, 4.5, 5.8, and  $8.0 \mu\text{m}$ , respectively. The errors are less than 0.06 mag for 26, 29, 64, and 54 members, respectively. Fewer members have multiple measurements at shorter wavelengths because the saturation limit is fainter at 3.6 and  $4.5 \mu\text{m}$ . To quantify the variability of these data, we have computed the difference between each magnitude and the average magnitude for a given object and wavelength. We then constructed histograms of these magnitude differences, which are weighted by the inverse of the number of measurements so that all members contribute equally to the distribution. In Figure 16, the resulting histograms are shown separately for each IRAC band and for stars with and without disks. In all four bands, nearly all sources with  $\Delta m > 0.05$  mag have disks, which indicates that disks are responsible for these large photometric variations, either directly through fluctuations in the disk emission or indirectly through the effect of the disk on the emergent flux from the stellar photosphere. Based on Figure 16, the frequency of large photometric variations appears to be similar among the four IRAC bands. A comparison of this kind between diskless and disk-bearing stars at  $24 \mu\text{m}$  is problematic because of the larger photometric errors, particularly for the fainter class III sources.

## 5. CONCLUSIONS

We have performed a thorough census of the circumstellar disk population of the Chamaeleon I star-forming region using mid-IR images obtained with the *Spitzer Space Telescope*. After analyzing most of the images that have been collected in Chamaeleon I with IRAC ( $3.6\text{--}8 \mu\text{m}$ ) and MIPS ( $24 \mu\text{m}$ ) onboard *Spitzer*, we have searched for new disk-bearing members of the cluster by identifying sources with red colors in these data. Through spectroscopy of a small sample of the resulting candidates, we have confirmed the membership of four objects, which we classify as M4, M6, M7.5, and L0. The first three sources are located in highly embedded areas ( $A_J \sim 5$ ) near known protostars, indicating that they may be among the youngest low-mass members of the cluster. The L0 source is the coolest known member of Chamaeleon I and has a mass of  $0.004\text{--}0.01 M_\odot$  according to the luminosities predicted by theoretical evolutionary models (Burrows et al. 1997; Chabrier et al. 2000), making it the least massive brown dwarf for which a disk has been reliably detected. With the exception of stars with edge-on disks, our survey demonstrates that the current census of disk-bearing members of Chamaeleon I is complete at stellar masses for areas covered by all four bands of IRAC, which encompass most of the cloud. At faint magnitudes that correspond to substellar cluster members, the *Spitzer* images detect hundreds of red sources. Most of these objects are probably galaxies, but we have identified a sample of the most promising candidate members, which include possible low-mass companions and protostellar sources.

We have presented a tabulation of IRAC and MIPS photometry for 191 and 144 known members of Chamaeleon I, respectively. We have used these data to classify the SEDs of the 203 members that are encompassed by the IRAC and MIPS images and that are detected by IRAC (i.e., excluding the protostar ChAMMS1), arriving at 4, 10, 94, and 95 members that are class I, flat spectrum, class II, and class III, respectively. The disk fraction (I+flat+II/I+flat+II+III) is roughly constant at  $\sim 50\%$  from  $0.01$  to  $0.3 M_\odot$ , which closely resembles measurements in IC 348. The disk fraction in Chamaeleon I increases with higher stellar masses to a value of  $\sim 65\%$  at  $1\text{--}2 M_\odot$ , whereas disks in IC 348 are much less common in this mass range ( $\sim 20\%$ ). Because the two clusters have the same age, this comparison indicates that solar-type stars in Chamaeleon I have longer disk lifetimes than their counterparts in IC 348. The high stellar density of the more massive stars in IC 348 may have contributed to their shorter disk lifetimes. We have also examined the spatial distribution of disk-bearing members of Chamaeleon I. The distributions of classes II and III are similar in the southern subcluster, while the class III sources have a wider distribution in the northern one. We interpret the relative distributions in the north as a reflection of the segregation of low-mass stars to larger radii in the northern subcluster (Luhman 2007) combined with the lower disk fraction of low-mass stars relative to members at higher masses. Finally, we have identified possible transitional disks around several cluster members, and have used our multi-epoch measurements to demonstrate that stars with disks exhibit greater mid-IR variability than diskless stars.

We thank Eric Feigelson for comments on the manuscript and Gus Muench for helpful discussions. K. L. and P. A. were supported by grant AST-0544588 from the National Science Foundation. This publication

makes use of data products from 2MASS, which is a joint project of the University of Massachusetts and the Infrared Processing and Analysis Center/California Institute of Technology, funded by NASA and the NSF.

## APPENDIX

## MEMBERSHIP OF YOUNG STARS SURROUNDING THE CHAMAELEON I CLOUD

Frink et al. (1998) demonstrated that the stars in the vicinity of Chamaeleon I consist of two kinematic subgroups: a rich group of young stars associated with the Chamaeleon I cloud, and a more dispersed, older group with larger motion. The latter has been referred to as the  $\epsilon$  Cha group (Mamajek et al. 2000) because it is centered on  $\epsilon$  Cha and the Herbig Ae star HD 104237. The group appears to have an age of  $\sim 6$  Myr and a distance of  $d \simeq 114$  pc (Feigelson et al. 2003; Luhman 2004b). Proper motions with accuracies of  $\sim 5$  mas/yr (e.g., UCAC2) are sufficient for distinguishing between the two populations. Therefore, to clarify the membership status of the young stars at distances of  $\sim 1$ - $3^\circ$  from the center of the Chamaeleon I cloud (Covino et al. 1997; Luhman 2007), we compare their proper motions to those of Chamaeleon I and the  $\epsilon$  Cha group.

The median proper motion for the 61 of the 226 sources in the census of Chamaeleon I from Luhman (2007) that have UCAC2 proper motions (Zacharias et al. 2004) is  $\mu_\alpha, \mu_\delta = -21, +2$  mas/yr. The median proper motion of the members of the  $\epsilon$  Cha group proposed by Mamajek et al. (2000) and Zuckerman & Song (2004) is  $\mu_\alpha, \mu_\delta = -40, -7$  mas/yr. The uncertainties in these median proper motions are at the level of  $\sim 1$  mas/yr. We first consider the eight young stars from Covino et al. (1997) that are within  $3^\circ$  from Chamaeleon I. The UCAC2 proper motions of RX J1108.8–7519A and B and RX J1129.2–7546 are consistent with membership in Chamaeleon I. Mamajek et al. (2000) classified RX J1158.5–7754A (= DW Cha) as a member of the  $\epsilon$  Cha group, and we assume that its companion (for which a reliable proper motion is not available) is a member of that group as well. RX J1150.4–7704 was classified as a “Cha-Near” member by Zuckerman & Song (2004, “Cha-Near” is ostensibly the same as the  $\epsilon$  Cha group), and the UCAC2 proper motion corroborates membership in the  $\epsilon$  Cha group. The UCAC2 proper motion for RX J1149.8–7850 (= DZ Cha) also indicates membership in  $\epsilon$  Cha rather than Chamaeleon I. For the final star from Covino et al. (1997), RX J1123.2–7924, the proper motion from Ducourant et al. (2006) is inconsistent with both Chamaeleon I and  $\epsilon$  Cha. However, RX J1123.2–7924 was incorrectly matched to 2MASS J11231052–7924434 in Ducourant et al. (2006). By examining the finder chart from Alcalá et al. (1995), we find that RX J1123.2–7924 is instead 2MASS J11225562–7924438. The UCAC2 proper motion for this star is  $\mu_\alpha, \mu_\delta = -32, -12$  mas/yr (errors of 6 mas/yr in each component). Thus, we classify it as a likely member of  $\epsilon$  Cha. We also have examined the proper motions of young stars from Luhman (2007) that are between  $\epsilon$  Cha and the Chamaeleon I cloud. Using proper motions from UCAC2 and from available optical and IR sky surveys, we find that 2MASS J11183572–7935548, 2MASS J11432669–7804454, 2MASS J11404967–7459394, and 2MASS J11334926–7618399 are more likely to be members of  $\epsilon$  Cha than Chamaeleon I. Other young stars from Luhman (2007) that are between these two populations have the proper motions that indicate membership, are inconclusive, or are unavailable.

We present the IRAC and MIPS data, spectral slopes, and SED classifications for the probable members of the  $\epsilon$  Cha association in Tables 11 and 12. We note that one of the  $\epsilon$  Cha stars has a flat-spectrum SED, which is surprising for a population as old as  $\epsilon$  Cha ( $\tau \sim 6$  Myr, Luhman 2004b).

## REFERENCES

- Adams, F. C., Lada, C. J., & Shu, F. H. 1987, *ApJ*, 213, 788  
 Alcalá, J. M., Krautter, J., Schmitt, J. H. M. M., Covino, E., Wichmann, R., & Mundt, R. 1995, *A&AS*, 114, 109  
 Allen, L. E., et al. 2004, *ApJS*, 154, 363  
 Allen, L. E., et al. 2007, *Protostars and Planets V*, B. Reipurth, D. Jewitt, and K. Keil (eds.), University of Arizona Press, Tucson, 361  
 Allen, P. R., Luhman, K. L., Myers, P. C., Megeath, S. T., Allen, L. E., Hartmann, L., & Fazio, G. G. 2007, *ApJ*, 655, 1095  
 Allers, K. N., Kessler-Silacci, J. E., Cieza, L. A., & Jaffe, D. T. 2006, *ApJ*, 644, 364  
 Apai, D., Pascucci, I., Henning, Th., Sterzik, M. F., Klein, R., Semenov, D., Günther, E., & Stecklum, B. 2002, *ApJ*, 573, L115  
 Assendorp, R., Wesselius, P. R., Prusti, T., & Whittet, D. C. B. 1990, *MNRAS*, 247, 624  
 Bally, J., Walawender, J., Luhman, K. L., & Fazio, G. 2006, *AJ*, 132, 1923  
 Baraffe, I., Chabrier, G., Allard, F., & Hauschildt, P. H. 1998, *A&A*, 337, 403  
 Baraffe, I., Chabrier, G., Allard, F., & Hauschildt, P. H. 2002, *A&A*, 382, 563  
 Barrado y Navascués, D., et al. 2007, *ApJ*, 664, 481  
 Baud, B., et al. 1984, *ApJ*, 278, L53  
 Belloche, A., Parise, B., van der Tak, F. F. S., Schilke, P., Leurini, S., et al. 2006, *A&A*, 454, L51  
 Bertout, C., Robichon, N., & Arenou, F. 1999, *A&A*, 352, 574  
 Briceño, C., Luhman, K. L., Hartmann, L., Stauffer, J. R., & Kirkpatrick, J. D. 2002, *ApJ*, 580, 317  
 Burgasser, A. J., Kirkpatrick, J. D., Reid, I. N., Brown, M. E., Miskey, C. L., & Gizis, J. E. 2003, *ApJ*, 586, 512  
 Burrows, A., et al. 1997, *ApJ*, 491, 856  
 Caballero, J. A., et al. 2007, *A&A*, 470, 903  
 Calvet, N., D’Alessio, P., Hartmann, L., Wilner, D., Walsh, A., & Sitko, M. 2002, *ApJ*, 568, 1008  
 Calvet, N., et al. 2005, *ApJ*, 630, L185  
 Cambrésy, L., Epchtein, N., Copet, E., de Batz, B., Kimeswenger, S., Le Bertre, T., Rouan, D., & Tiphene, D. 1997, *A&A*, 324, L5  
 Carpenter, J. M., Mamajek, E. E., Hillenbrand, L. A., & Meyer, M. R. 2006, *ApJ*, 651, L49  
 Chabrier, G., Baraffe, I., Allard, F., & Hauschildt, P. 2000, *ApJ*, 542, L119  
 Comerón, F., Reipurth, B., Henry, A., & Fernández, M. 2004, *A&A*, 417, 583  
 Covino, E., Alcalá, J. M., Allain, S., Bouvier, J., Terranegra, L., & Krautter, J. 1997, *A&A*, 328, 187  
 Dahm, S. E., & Hillenbrand, L. A. 2007, *AJ*, 133, 2072  
 Dahn, C. C., et al. 2002, *AJ*, 124, 1170  
 D’Alessio, P., et al. 2005, *ApJ*, 621, 461  
 Damjanov, I., Jayawardhana, R., Scholz, A., Ahmic, M., Nguyen, D. C., Brandeker, A., & van Kerkwijk, M. H. 2007, *ApJ*, in press  
 Ducourant, C., et al. 2006, *A&A*, 448, 1235

- Engelbracht, C. W., et al. 2007, *PASP*, 119, 994
- Espaillet, C., et al. 2007a, *ApJ*, 664, L111
- Espaillet, C., et al. 2007b, *ApJ*, 670, L135
- Fazio, G. G., et al. 2004a, *ApJS*, 154, 10
- Fazio, G. G., et al. 2004b, *ApJS*, 154, 39
- Feigelson, E. D., & Lawson, W. A. 2004, *ApJ*, 614, 267
- Feigelson, E. D., Lawson, W. A., & Garmire, G. P. 2003, *ApJ*, 599, 1207
- Flaherty, K. M., Pipher, J. L., Megeath, S. T., Winston, E. M., Gutermuth, R. A., Muzerolle, J., Allen, L. E., & Fazio, G. G. 2007, *ApJ*, 663, 1069
- Frink, S., Roeser, S., Alcalá, J. M., Covino, E., & Brandner, W. 1998, *A&A*, 338, 442
- Furlan, E., et al. 2007, *ApJ*, 644, 1176
- Gizis, J. E., Reid, I. N., & Hawley, S. L. 2002, *AJ*, 123, 3356
- Glass, I. S. 1979, *MNRAS*, 187, 305
- Gómez, M., & Kenyon, S. J. 2001, *AJ*, 121, 974
- Greene, T. P., Wilking, B. A., André, P., Young, E. T., & Lada, C. J. 1994, *ApJ*, 434, 614
- Guieu, S., et al. 2007, *A&A*, 465, 855
- Gutermuth, R. A., Megeath, S. T., Muzerolle, J., Allen, L. E., Pipher, J. L., Myers, P. C., & Fazio, G. G. 2004, *ApJS*, 154, 374
- Gutermuth, R. A., et al. 2007, *ApJ*, in press
- Hartmann, L. 2002, *ApJ*, 578, 914
- Hartmann, L., Ballesteros-Paredes, J., & Bergin, E. 2001, *ApJ*, 562, 852
- Hartmann, L., Megeath, S. T., Allen, L., Luhman, K., Calvet, N., D'Alessio, P., Franco-Hernandez, R., & Fazio, G. 2005, *ApJ*, 629, 881
- Harvey, P. M., et al. 2006, *ApJ*, 644, 307
- Harvey, P. M., et al. 2007, *ApJ*, 663, 1139
- Hernández, J., Briceño, C., Calvet, N., Hartmann, L., Muzerolle, J., & Quintero, A. 2006, *ApJ*, 652, 472
- Hernández, J., et al. 2007, *ApJ*, 662, 1067
- Hora, J. L., et al. 2004, *Proc. SPIE*, 5487, 77
- Jayawardhana, R., Ardila, D. R., Stelzer, B., & Haisch, K. E. 2003, *AJ*, 126, 1515
- Jørgensen, J. K., et al. 2006, *ApJ*, 645, 1246
- Kenyon, S. J., & Gómez, M. 2001, *AJ*, 121, 2673
- Kirkpatrick, J. D. 2005, *ARA&A*, 43, 195
- Kirkpatrick, J. D., Barman, T. S., Burgasser, A. J., McGovern, M. R., McLean, I. S., Tinney, C. G., & Lowrance, P. J. 2006, *ApJ*, 639, 1120
- Kirkpatrick, J. D., et al. 1999, *ApJ*, 519, 802
- Lada, C. J. 1987, in *IAU Symp.* 115, *Star Forming Regions*, ed. M. Peimbert & J. Jugaku (Dordrecht: Reidel), 1
- Lada, C. J., Muench, A. A., Haisch, K. E., Lada, E. A., Alves, J. F., Tollestrup, E. V., & Willner, S. P. 2000, *ApJ*, 120, 3162
- Lada, C. J., Muench, A. A., Lada, E. A., & Alves, J. F. 2004, *AJ*, 128, 1254
- Lada, C. J., & Wilking, B. A. 1984, *ApJ*, 287, 610
- Lada, C. J., et al. 2006, *AJ*, 131, 1574
- Landsman, W.B. 1993, *ASP Conf. Ser.* 52: *Astronomical Data Analysis Software and Systems II*, 52, 246
- Lehtinen, K., Haikala, L. K., Mattila, K., & Lemke, D. 2001, *A&A*, 367, 311
- Lucas, P. W., Roche, P. F., Allard, F., & Hauschildt, P. H. 2001, *MNRAS*, 326, 695
- Luhman, K. L. 1999, *ApJ*, 525, 466
- Luhman, K. L. 2004a, *ApJ*, 602, 816
- Luhman, K. L. 2004b, *ApJ*, 616, 1033
- Luhman, K. L. 2004c, *ApJ*, 617, 1216
- Luhman, K. L. 2007, *ApJS*, 173, 104
- Luhman, K. L. 2008, *Handbook of Star Forming Regions*, ASP Conference Series, submitted
- Luhman, K. L., Adame, L., D'Alessio, P., Calvet, N., Hartmann, L., Megeath, S. T., & Fazio, G. G. 2005c, *ApJ*, 635, L93
- Luhman, K. L., D'Alessio, P., Calvet, N., Allen, L. E., Hartmann, L., Megeath, S. T., Myers, P. C., & Fazio, G. G. 2005a, *ApJ*, 620, L51
- Luhman, K. L., Peterson, D. E., & Megeath, S. T. 2004, *ApJ*, 617, 565
- Luhman, K. L., Stauffer, J. R., Muench, A. A., Rieke, G. H., Lada, E. A., Bouvier, J., & Lada, C. J. 2003, *ApJ*, 593, 1093
- Luhman, K. L., Whitney, B. A., Meade, M. R., Babler, B. L., Indebetouw, R., Bracker, S., & Churchwell, E. B. 2006, *ApJ*, 647, 1180
- Luhman, K. L., et al. 2005b, *ApJ*, 631, L69
- Mamajek, E., Lawson, W. A., & Feigelson, E. D. 2000, *ApJ*, 544, 356
- Megeath, S. T., Hartmann, L., Luhman, K. L., & Fazio, G. G. 2005, *ApJ*, 634, L113
- Megeath, S. T., et al. 2004, *ApJS*, 154, 367
- Mohanty, S., Jayawardhana, R., & Basri, G. 2005, *ApJ*, 626, 498
- Muench, A. A., Lada, C. J., Luhman, K. L., Muzerolle, J., & Young, E. 2007, *AJ*, 134, 411
- Muench, A. A., et al. 2003, *AJ*, 125, 2029
- Muzerolle, J., Luhman, K. L., Briceño, C., Hartmann, L., & Calvet, N. 2005, *ApJ*, 625, 906
- Muzerolle, J., et al. 2004, *ApJS*, 154, 379
- Natta, A., & Testi, L. 2001, *A&A*, 376, L22
- Nordh, L., et al. 1996, *A&A*, 315, L185
- Persi, P., Marenzi, A. R., Gómez, M., & Olofsson, G. 2001, *A&A*, 376, 907
- Persi, P., et al. 2000, *A&A*, 357, 219
- Pipher, J. L., et al. 2004, *Proc. SPIE*, 5487, 234
- Porrás, A., et al. 2007, *ApJ*, 656, 493
- Prusti, T., Clark, F. O., Whittet, D. C. B., Laureijs, R. J., & Zhang, C. Y. 1991, *MNRAS*, 251, 303
- Reach, W. T., et al. 2005, *PASP*, 117, 978
- Rebull, L. M., et al. 2007, *ApJS*, 171, 447
- Reipurth, B., Nyman, L.-Å., & Chini, R. 1996, *A&A*, 314, 258
- Rieke, G. H. et al. 2004, *ApJS*, 154, 25
- Scholz, A., & Jayawardhana, R. 2007, *ApJ*, in press
- Scholz, A., Jayawardhana, R., Wood, K., Meeus, G., Stelzer, B., Walker, C., & O'Sullivan, M. 2007, *ApJ*, 660, 1517
- Sicilia-Aguilar, A., et al. 2006, *ApJ*, 638, 897
- Skrutskie, M., et al. 2006, *AJ*, 131, 1163
- Stelzer, B., Micela, G., & Neuhäuser, R. 2004, *A&A*, 423, 1029
- Teixeira, P. S., et al. 2006, *ApJ*, 636, L45
- Werner, M. W., et al. 2004, *ApJS*, 154, 1
- Whittet, D. C. B., Prusti, T., Franco, G. A. P., Gerakines, P. A., Kilkenny, D., Larson, K. A., & Wesselius, P. R. 1997, *A&A*, 327, 1194
- Wichmann, R., Bastian, U., Krautter, J., Jankovics, I., & Ruciński, S. M. 1998, *MNRAS*, 301, L39
- Winston, E., et al. 2007, *ApJ*, 669, 493
- Young, K. E., et al. 2005, *ApJ*, 628, 283
- Zacharias, N., Urban, S. E., Zacharias, M. I., Wycoff, G. L., Hall, D. M., Monet, D. G., & Rafferty, T. J., 2004, *AJ*, 127, 3043
- Zapatero Osorio, M. R., et al. 2007, *A&A*, 472, L9
- Zuckerman, B., & Song, I. 2004, *ARA&A*, 42, 685

TABLE 1  
 IRAC OBSERVING LOG

AOR	PID	3.6/5.8 Center (J2000)		4.5/8.0 Center (J2000)		Dimensions (arcmin)	Angle <sup>a</sup> (deg)	Exp Time <sup>b</sup> (s)	Date (UT)
6526208	36	11 08 46	-77 37 19	11 06 45	-77 39 37	20 × 15	72	968	2004 Feb 19
5662720	173	11 02 59	-77 36 25	11 01 38	-77 31 09	13 × 7	142	20.8 HDR	2004 May 1
5663232	173	11 24 06	-79 27 30	11 22 21	-79 22 40	13 × 6	135	20.8 HDR	2004 May 1
		11 17 50	-80 31 00	11 15 56	-80 26 09	13 × 6	135	20.8 HDR	
5663744	173	11 50 46	-77 07 50	11 49 55	-77 01 33	12 × 6	148	20.8 HDR	2004 May 26
		12 05 00	-77 34 30	12 04 04	-77 28 30	12 × 6	148	20.8 HDR	
		12 17 30	-77 56 30	12 16 28	-77 50 40	12 × 6	148	20.8 HDR	
3960320	37	11 07 44	-77 34 46	11 07 48	-77 28 03	33 × 29	3	20.8 HDR	2004 Jun 6
5663488	173	11 58 52	-77 58 00	11 58 28	-77 51 15	13 × 6	170	20.8 HDR	2004 Jun 6
		11 49 48	-78 54 10	11 49 25	-78 47 23	13 × 6	170	20.8 HDR	
3651328	6	11 09 26	-76 36 26	11 10 16	-76 30 20	33 × 29	28	20.8 HDR	2004 Jul 4
5105920	139	11 02 02	-77 42 47	11 03 01	-77 36 43	19 × 10	120	41.6	2004 Jul 4
5662976	173	11 08 15	-75 21 43	11 09 25	-75 16 38	12 × 6	43	20.8 HDR	2004 Jul 21
		11 28 41	-75 49 00	11 29 49	-75 43 35	12 × 6	43	20.8 HDR	
		11 10 16	-76 47 22	11 11 35	-76 42 16	12 × 6	43	20.8 HDR	
3955968	36	11 06 41	-77 39 09	11 08 47	-77 37 55	20 × 15	80	968	2004 Sep 2
12620032	36	11 10 38	-76 34 35	11 09 23	-76 29 21	25 × 15	131	968	2005 May 9
12620544	36	11 02 00	-77 35 17	11 00 43	-77 29 58	12 × 5	144	52	2005 May 9
18373888	30540	11 18 24	-79 39 16	11 18 50	-79 32 34	13 × 6	12	52	2006 Jul 6
18373376	30540	11 02 12	-75 06 00	11 02 41	-74 59 26	12 × 5	18	10.4	2006 Jul 7
18366720	30540	11 12 07	-77 18 08	11 12 41	-77 11 37	13 × 6	18	134	2006 Jul 10
18366976	30540	11 01 14	-77 21 38	11 01 54	-77 15 10	13 × 6	18	134	2006 Jul 10
18367232	30540	11 12 16	-76 56 50	11 12 50	-76 50 19	13 × 6	19	134	2006 Jul 10
18367488	30540	11 19 44	-75 08 11	11 20 12	-75 01 37	13 × 6	20	134	2006 Jul 10
18367744	30540	11 03 53	-76 16 03	11 04 30	-76 09 35	13 × 6	20	52	2006 Jul 10
18368000	30540	11 06 17	-76 28 37	11 06 52	-76 22 08	13 × 6	19	134	2006 Jul 10
18368256	30540	11 06 47	-76 14 12	11 07 22	-76 07 43	13 × 6	19	134	2006 Jul 10
18368512	30540	11 07 30	-76 18 33	11 08 05	-76 12 04	13 × 6	19	134	2006 Jul 10
18368768	30540	11 14 11	-77 36 20	11 14 45	-77 29 50	13 × 6	20	52	2006 Jul 10
18369024	30540	11 17 23	-76 49 37	11 17 54	-76 43 04	13 × 6	19	134	2006 Jul 10
18369280	30540	11 00 55	-77 25 52	11 01 35	-77 19 27	13 × 6	20	52	2006 Jul 10
18369536	30540	10 57 46	-77 15 04	10 58 28	-77 08 38	13 × 6	20	52	2006 Jul 10
18369792	30540	11 09 13	-77 02 34	11 09 48	-76 56 04	13 × 6	20	52	2006 Jul 10
18370048	30540	11 18 20	-76 46 20	11 18 50	-76 39 48	13 × 6	20	52	2006 Jul 10
18370304	30540	11 19 29	-76 26 52	11 19 59	-76 20 16	13 × 6	20	52	2006 Jul 10
18370816	30540	11 24 00	-76 34 02	11 24 27	-76 27 27	13 × 6	20	52	2006 Jul 10
18371072	30540	11 43 19	-78 08 08	11 43 39	-78 01 24	13 × 6	9	52	2006 Jul 10
18371328	30540	11 40 42	-75 03 00	11 41 00	-74 56 19	13 × 6	12	52	2006 Jul 10
18371584	30540	11 07 23	-75 56 08	11 07 57	-75 49 40	13 × 6	20	52	2006 Jul 10
18371840	30540	11 24 18	-75 57 42	11 24 45	-75 51 07	13 × 6	20	52	2006 Jul 10
18372096	30540	11 33 39	-76 22 00	11 34 03	-76 15 20	13 × 6	20	52	2006 Jul 10
18372352	30540	11 33 13	-76 25 33	11 33 37	-76 18 50	13 × 6	20	52	2006 Jul 10
18372608	30540	11 06 44	-75 34 11	11 07 18	-75 27 44	13 × 6	19	134	2006 Jul 10
18372864	30540	11 02 03	-75 40 11	11 02 39	-75 33 44	13 × 6	20	52	2006 Jul 10
18373120	30540	10 52 19	-74 43 39	10 52 58	-74 37 20	13 × 6	23	52	2006 Jul 10
18373632	30540	11 05 45	-75 10 39	11 06 19	-75 04 10	13 × 6	20	52	2006 Jul 10
18374400	30540	11 02 24	-77 27 40	11 03 03	-77 21 12	13 × 6	20	52	2006 Jul 10

<sup>a</sup> Position angle of the long axis of the maps.<sup>b</sup> Total exposure time for each position and filter. "HDR" indicates that 0.4 s exposures were also obtained.
 TABLE 2  
 MIPS 24  $\mu$ M OBSERVING LOG

AOR	PID	Center (J2000)		Dimensions (arcmin)	Angle <sup>a</sup> (deg)	Exp Time (s)	Date (UT)
5706752	173	11 09 13	-77 29 10	8 × 7	55	220	2004 Feb 3
		11 12 09	-77 21 22	8 × 5	55	480	
		11 07 00	-77 32 30	7 × 6	55	160	
4549376	72	11 58 29	-77 54 29	8 × 7	61	280	2004 Feb 22
		12 01 46	-77 47 39	8 × 5	61	600	
5707008	173	11 10 52	-76 44 20	8 × 7	115	140	2004 Apr 8
		11 14 15	-76 48 39	8 × 5	115	360	
9410304	139	11 02 31	-77 39 46	17 × 8	28	37	2004 Apr 8
		11 06 09	-77 44 34	13 × 10	118	500	
3661312	6	11 10 31	-76 35 30	56 × 32	119	80	2004 Apr 11
5686784	173	11 02 24	-77 33 33	8 × 7	15	37	2004 Jun 22
		11 01 41	-77 45 45	8 × 5	15	31	
5687296	173	11 12 24	-76 37 07	8 × 7	29	37	2004 Jul 8
		11 10 53	-76 48 22	8 × 5	29	120	
5200128	148	11 11 45	-76 20 10	8 × 7	53	73	2004 Aug 3

TABLE 2 — *Continued*

AOR	PID	Center (J2000)	Dimensions (arcmin)	Angle <sup>a</sup> (deg)	Exp Time (s)	Date (UT)
		11 09 07 -76 28 24	8 × 5	53	240	
5687808	173	11 23 09 -79 25 00	8 × 7	50	73	2004 Aug 3
		11 19 55 -79 33 40	8 × 5	50	360	
3962112	37	11 08 29 -77 30 36	56 × 32	73	80	2005 Feb 27
5687040	173	11 08 54 -75 19 37	8 × 7	72	110	2005 Feb 27
		11 11 54 -75 14 46	8 × 5	72	360	
5688576	173	11 50 30 -77 04 36	8 × 7	62	73	2005 Feb 27
		11 53 35 -76 57 50	8 × 5	62	360	
5688064	173	11 29 14 -75 46 25	8 × 7	73	140	2005 Mar 6
		11 32 22 -75 41 53	8 × 5	73	360	
5688320	173	11 49 46 -78 50 51	8 × 7	67	110	2005 Mar 6
		11 53 36 -78 45 19	8 × 5	67	360	
12663040	37	11 10 10 -76 32 20	8 × 7	110	37	2005 Apr 9
		11 13 37 -76 35 27	8 × 5	110	120	
13468416	248	11 06 39 -77 43 14	8 × 7	143	420	2005 May 11
13472000	248	11 07 38 -77 35 34	8 × 7	150	420	2005 May 17
21916928	40302	11 04 11 -76 12 50	8 × 7	155	120	2007 Jun 6
		11 05 55 -76 23 40	8 × 5	155	120	
21917184	40302	11 09 29 -76 59 20	8 × 7	153	120	2007 Jun 6
		11 11 25 -77 09 57	8 × 5	153	120	
21917440	40302	11 18 34 -76 43 07	8 × 7	151	120	2007 Jun 6
		11 20 34 -76 53 28	8 × 5	151	120	
21917696	40302	11 19 43 -76 23 36	8 × 7	151	120	2007 Jun 6
		11 21 40 -76 33 56	8 × 5	151	120	
21918208	40302	11 07 38 -75 52 56	8 × 7	154	120	2007 Jun 6
		11 09 23 -76 03 39	8 × 5	154	120	
21918464	40302	11 24 30 -75 54 27	8 × 7	150	120	2007 Jun 6
		11 26 27 -76 04 38	8 × 5	150	120	
21918720	40302	11 33 50 -76 18 43	8 × 7	147	120	2007 Jun 6
		11 35 57 -76 28 36	8 × 5	147	120	
21918976	40302	11 33 24 -76 22 12	8 × 7	147	120	2007 Jun 6
		11 35 31 -76 32 07	8 × 5	147	120	
21919488	40302	11 19 57 -75 04 57	8 × 7	152	120	2007 Jun 6
		11 21 43 -75 15 20	8 × 5	152	120	
21917952	40302	11 40 49 -74 59 40	8 × 7	9	120	2007 Jul 16
		11 40 35 -75 12 09	8 × 5	9	120	
21919232	40302	11 02 19 -75 37 00	8 × 7	18	120	2007 Jul 16
		11 01 32 -75 49 07	8 × 5	18	120	
21919744	40302	10 52 37 -74 40 32	8 × 7	21	120	2007 Jul 16
		10 51 44 -74 52 29	8 × 5	21	120	
21920000	40302	11 02 25 -75 02 44	8 × 7	18	120	2007 Jul 16
		11 01 40 -75 14 49	8 × 5	18	120	
21920256	40302	11 06 00 -75 07 27	8 × 7	17	120	2007 Jul 16
		11 05 17 -75 19 37	8 × 5	17	120	

<sup>a</sup> Position angle of the long axis of the maps.TABLE 3  
SPECTROSCOPY OBSERVING LOG

Night	Date	Telescope + Instrument	Disperser	$\lambda$ ( $\mu\text{m}$ )	$\lambda/\Delta\lambda$
1	2005 Mar 23	Gemini + GNIRS	31.7 cross-dispersed	1-2.5	2000
2	2005 Mar 24	Gemini + GNIRS	31.7 cross-dispersed	1-2.5	2000
3	2006 Feb 9	Magellan II + LDSS-3	VPH red grism	0.68-1.1	1300
4	2006 Feb 10	Magellan II + LDSS-3	VPH red grism	0.58-1	1300
5	2006 Feb 11	Magellan II + LDSS-3	VPH red grism	0.58-1	1300

TABLE 4  
 NEW MEMBERS OF CHAMAELEON I

Name	Spectral Type	$T_{\text{eff}}^{\text{a}}$ (K)	$A_J$	$L_{\text{bol}}$ ( $L_{\odot}$ )	Membership Evidence <sup>b</sup>	$J^{\text{c}}$	$H^{\text{c}}$	$K_s^{\text{c}}$	Night
2M J11062942–7724586	M6±1	2990	5.6	0.035	$A_V, \text{H}_2\text{O}, \text{ex}$	...	15.20±0.10	13.81±0.06	1
2M J11070369–7724307	M7.5±1	2795	4.7	0.020	$A_V, \text{H}_2\text{O}, \text{ex}$	...	15.26±0.12	13.95±0.07	1
Cha J11070768–7626326	L0±1	2200	0	0.00033	e,ex	17.61±0.03	16.80±0.03	15.91±0.02	4,5
2M J11084296–7743500	M4±1	3270	5.6	0.053	$A_V, \text{e}, \text{ex}$	...	14.87±0.10	13.48±0.05	2

<sup>a</sup> Temperature scale from Luhman et al. (2003). For Cha J11070768–7626326, that scale has been extrapolated to L0.

<sup>b</sup> Membership in Chamaeleon is indicated by  $A_V \gtrsim 1$  and a position above the main sequence for the distance of Chamaeleon (“ $A_V$ ”), strong emission lines (“e”), IR excess emission (“ex”), or the shape of the gravity-sensitive  $\text{H}_2\text{O}$  bands (“ $\text{H}_2\text{O}$ ”).

<sup>c</sup> From the 2MASS Point Source Catalog for 2M J11062942–7724586 and 2M J11070369–7724307 and from the ISPI images of Luhman (2007) for Cha J11070768–7626326.

 TABLE 5  
*Spitzer* PHOTOMETRY FOR NONMEMBERS

Name	[3.6]	[4.5]	[5.8]	[8.0]	[24]
Cha J11055362–7638533	14.59±0.03	13.82±0.03	12.90±0.05	12.19±0.06	8.89±0.06
2M J11081204–7622124	14.16±0.03	13.73±0.03	13.48±0.05	11.29±0.04	8.31±0.05
Cha J11081724–7631107	15.04±0.03	14.78±0.04	14.76±0.04	13.55±0.04	...
Cha J11083029–7733067	14.49±0.03	14.28±0.03	14.33±0.04	13.59±0.06	...
Cha J11084006–7627085	15.81±0.02	15.51±0.02	15.58±0.06	14.97±0.08	...
2M J11085651–7645154	12.47±0.02	12.48±0.02	12.46±0.05	12.34±0.08	...
Cha J11090876–7626234	16.22±0.02	15.89±0.02	15.64±0.06	14.55±0.08	10.75±0.17
2M J11105185–7642259	13.79±0.02	13.77±0.03	13.70±0.07	13.43±0.11	...
2M J11105353–7726389	12.44±0.02	12.38±0.02	12.33±0.05	12.29±0.05	...
Cha J11112420–7637434	14.97±0.03	14.20±0.03	13.34±0.04	12.58±0.05	9.58±0.10
Cha J11114773–7642167	14.02±0.02	13.19±0.02	12.42±0.04	11.60±0.05	7.90±0.05
Cha J11120546–7631376	15.00±0.02	13.89±0.02	12.92±0.04	11.82±0.04	8.28±0.05
Cha J11130714–7638575	15.04±0.03	14.20±0.04	13.56±0.07	12.62±0.06	8.79±0.06

 TABLE 6  
*Spitzer* PHOTOMETRY FOR CANDIDATE MEMBERS OF CHAMAELEON I

Name	[3.6]	[4.5]	[5.8]	[8.0]	Date	[24]	Date
2M J11020610–7718079	13.42±0.02	13.10±0.02	12.84±0.03	12.34±0.03	2006 Jul 10	out	...
2M J11025374–7722561 <sup>a</sup>	13.93±0.02	13.63±0.02	13.43±0.03	13.07±0.05	2006 Jul 10	9.80±0.07	2005 Feb 27
Cha J11062788–7724543 <sup>b,c</sup>	15.57±0.05	14.45±0.05	13.37±0.07	12.41±0.07	2004 Jun 10	8.89±0.20	2005 Feb 27
Cha J11062854–7618039	14.21±0.02	13.89±0.02	13.62±0.03	13.15±0.05	2006 Jul 10	10.27±0.15	2004 Apr 11
Cha J11080397–7730382 <sup>c</sup>	15.31±0.02	14.50±0.02	13.80±0.03	12.72±0.03	2004 Feb 19	7.82±0.03	2005 Feb 27
	15.28±0.03	14.48±0.02	14.03±0.08	12.80±0.07	2004 Jun 10		
2M J11085367–7521359 <sup>d</sup>	8.70±0.02	8.48±0.02	8.32±0.03	7.96±0.03	2004 Jul 21	4.98±0.03	2005 Feb 27
2M J11100336–7633111 <sup>c,e</sup>	12.74±0.02	11.98±0.02	11.51±0.04	10.94±0.08	2004 Jul 4	5.28±0.10	2004 Apr 11
	12.67±0.02	11.91±0.02	11.28±0.03	10.67±0.03	2005 May 9	5.33±0.10	2005 Apr 9
2M J11291470–7546256 <sup>f</sup>	12.91±0.02	12.29±0.02	11.56±0.03	10.60±0.03	2004 Jul 21	7.34±0.10	2005 Mar 6

<sup>a</sup> [LES2004] 424.

<sup>b</sup> 7'' from 2M J11062942–7724586.

<sup>c</sup> Possible class I source.

<sup>d</sup> 2' from RX J1108.8–7519A and B.

<sup>e</sup> OTS 32. 18'' from Hn 11.

<sup>f</sup> 8'' from RX J1129.2–7546.

 TABLE 7  
*Spitzer* PHOTOMETRY FOR KNOWN MEMBERS OF CHAMAELEON I

2MASS <sup>a</sup>	Name	[3.6]	[4.5]	[5.8]	[8.0]	Date	[24]	Date
J10523694–7440287	...	10.19±0.02	10.11±0.02	10.08±0.03	10.14±0.04	2006 Jul 10	9.44±0.15	2007 Jul 16
J10580597–7711501	...	11.70±0.02	11.45±0.02	11.26±0.03	10.75±0.04	2006 Jul 10	out	...
J10581677–7717170	T6	sat	out	6.41±0.03	out	2006 Jul 10	out	...
J11011370–7722387	...	11.69±0.02	11.61±0.02	11.60±0.03	11.56±0.04	2006 Jul 10	...	2005 Feb 27
J11011926–7732383	...	out	10.87±0.02	out	10.77±0.04	2004 Jul 4	...	2004 Jun 22
		11.00±0.02	10.86±0.02	10.81±0.03	10.76±0.04	2005 May 9		

TABLE 7 — *Continued*

2MASS <sup>a</sup>	Name	[3.6]	[4.5]	[5.8]	[8.0]	Date	[24]	Date
J11013205–7718249	ESO H $\alpha$ 554	11.00±0.02	out	10.78±0.03	out	2006 Jul 10		
J11021927–7536576	...	13.05±0.02	12.97±0.02	12.89±0.03	12.88±0.05	2006 Jul 10	out	...
J11022491–7733357	T11	10.89±0.02	10.79±0.02	10.78±0.03	10.80±0.04	2006 Jul 10	10.30±0.30	2007 Jul 16
		8.15±0.02	8.14±0.02	8.03±0.03	7.87±0.03	2004 May 1	2.56±0.04	2004 Apr 8
		out	sat	out	7.88±0.03	2004 Jul 4	2.59±0.04	2004 Jun 22
		sat	out	7.97±0.03	out	2006 Jul 10	2.56±0.04	2005 Feb 27
J11022610–7502407	...	10.55±0.02	10.48±0.02	10.41±0.05	10.38±0.05	2006 Jul 7	9.79±0.19	2007 Jul 16
J11023265–7729129	CHXR 71	9.78±0.02	out	9.53±0.03	out	2004 May 1	7.50±0.04	2005 Feb 27
		9.78±0.02	out	9.50±0.03	out	2006 Jul 10		
J11024183–7724245	[LES2004] 423	11.20±0.02	11.10±0.02	11.05±0.03	11.10±0.04	2006 Jul 10	...	2005 Feb 27
J11025504–7721508	T12	9.78±0.02	bad	9.20±0.03	8.65±0.03	2006 Jul 10	5.90±0.04	2005 Feb 27
J11034186–7726520	ISO 28	11.23±0.02	11.20±0.02	11.06±0.03	11.03±0.04	2004 Jun 10	...	2005 Feb 27
J11034764–7719563	Hn 2	9.69±0.02	9.61±0.02	9.55±0.03	9.62±0.04	2004 Jun 10	9.38±0.13	2005 Feb 27
		out	9.64±0.02	out	9.63±0.03	2006 Jul 10		
J11035682–7721329	CHXR 12	9.63±0.02	9.46±0.02	9.37±0.03	9.43±0.04	2004 Jun 10	9.19±0.08	2005 Feb 27
J11040425–7639328	CHSM 1715	out	out	out	out	...	4.89±0.04	2004 Apr 11
J11040909–7627193	T14	out	out	out	out	...	2.44±0.04	2004 Apr 11
J11041060–7612490	CHSM 1982	11.69±0.02	11.59±0.02	11.56±0.03	11.53±0.03	2006 Jul 10	...	2007 Jun 6
J11042275–7718080	T14A	10.06±0.02	9.23±0.02	8.25±0.03	6.97±0.04	2004 Jun 10	3.47±0.04	2005 Feb 27
J11044258–7741571	ISO 52	out	sat	out	8.84±0.04	2004 Feb 19	5.28±0.04	2004 Apr 8
		9.92±0.02	9.71±0.02	9.48±0.03	8.93±0.03	2004 Jun 10	5.40±0.04	2005 Feb 27
		9.82±0.02	9.49±0.02	9.29±0.03	8.79±0.04	2004 Jul 4		
		sat	out	9.60±0.03	out	2004 Sep 2		
J11045100–7625240	CHXR 14N	out	out	out	out	...	9.26±0.07	2004 Apr 11
J11045285–7625514	CHXR 14S	out	out	out	out	...	8.66±0.08	2004 Apr 11
J11045701–7715569	T16	out	9.57±0.02	out	8.72±0.04	2004 Jun 10	out	...
J11051467–7711290	Hn 4	out	9.14±0.02	out	9.11±0.03	2004 Jun 10	out	...
J11052472–7626209	...	out	out	out	out	...	9.98±0.21	2004 Apr 11
							10.49±0.11	2007 Jun 6
J11054300–7726517	CHXR 15	9.86±0.02	9.70±0.02	9.66±0.03	9.69±0.04	2004 Jun 10	9.41±0.08	2005 Feb 27
J11055261–7618255	T20	sat	out	9.02±0.03	out	2006 Jul 10	8.77±0.05	2004 Apr 11
J11055780–7607488	HD 96675	out	out	out	out	...	7.05±0.11	2004 Apr 11
J11060010–7507252	...	11.14±0.02	11.05±0.02	11.01±0.03	10.98±0.03	2006 Jul 10	...	2007 Jul 16
J11061540–7721567	Ced 110-IRS2/T21	6.26±0.02	6.16±0.02	6.09±0.03	6.10±0.04	2004 Jun 10	5.55±0.07	2005 Feb 27
J11061545–7737501	Cam 2-19	sat	sat	9.53±0.03	9.55±0.04	2004 Feb 19	9.50±0.09	2005 Feb 27
		9.76±0.02	9.71±0.02	9.58±0.03	9.60±0.04	2004 Jun 10		
		sat	sat	9.58±0.03	9.53±0.03	2004 Sep 2		
J11062554–7633418	ESO H $\alpha$ 559	10.83±0.02	10.42±0.02	10.07±0.03	9.38±0.04	2004 Jul 4	5.34±0.04	2004 Apr 11
		10.64±0.02	out	9.90±0.03	out	2006 Jul 10		
J11062877–7737331	CHXR 73A	sat	sat	10.10±0.03	10.10±0.03	2004 Feb 19	9.58±0.14	2005 Feb 27
		10.29±0.02	10.23±0.02	10.18±0.03	10.10±0.03	2004 Jun 10		
		sat	sat	10.15±0.03	10.13±0.04	2004 Sep 2		
J11062942–7724586	...	12.18±0.02	11.63±0.02	11.14±0.03	10.59±0.04	2004 Jun 10	8.73±0.20	2005 Feb 27
J11063276–7625210	CHSM 7869	out	12.22±0.02	out	11.29±0.03	2005 May 9	8.57±0.06	2004 Apr 11
		12.52±0.02	12.21±0.02	11.94±0.03	11.30±0.04	2006 Jul 10	8.42±0.06	2007 Jun 6
...	Cha-MMS1	...	...	...	...	2004 Jun 10	8.86±0.09	2005 Feb 27
J11063799–7743090	Cha H $\alpha$ 12	sat	sat	11.18±0.03	11.12±0.04	2004 Feb 19	11.17±0.16	2004 Apr 8
		11.34±0.02	11.25±0.02	bad	11.20±0.04	2004 Jun 10	10.61±0.22	2005 Feb 27
		sat	sat	11.17±0.03	11.13±0.03	2004 Sep 2	10.77±0.10	2005 May 11
J11063945–7736052	ISO 79	sat	sat	10.41±0.03	9.78±0.04	2004 Feb 19	6.21±0.04	2004 Feb 3
		11.44±0.02	10.76±0.02	10.34±0.03	9.71±0.03	2004 Jun 10	6.37±0.04	2005 Feb 27
		sat	sat	10.36±0.03	9.71±0.04	2004 Sep 2	6.35±0.04	2005 May 17
J11064180–7635489	Hn 5	9.15±0.02	8.58±0.02	8.03±0.03	7.06±0.04	2004 Jul 4	4.71±0.04	2004 Apr 11
J11064346–7726343	T22	9.10±0.02	9.05±0.02	9.00±0.03	9.01±0.03	2004 Jun 10	8.59±0.06	2005 Feb 27
J11064510–7727023	CHXR 20	8.51±0.02	8.36±0.02	7.93±0.03	6.94±0.04	2004 Jun 10	4.45±0.04	2005 Feb 27
J11064658–7722325	Ced 110-IRS4	11.12±0.06	10.00±0.04	9.34±0.03	8.46±0.03	2004 Jun 10	2.10±0.04	2005 Feb 27
J11065733–7742106	CHXR 74	sat	sat	9.75±0.03	9.79±0.04	2004 Feb 19	9.60±0.07	2004 Apr 8
		9.90±0.02	9.81±0.02	9.80±0.03	9.74±0.03	2004 Jun 10	9.57±0.11	2005 Feb 27
		sat	sat	9.74±0.03	9.76±0.04	2004 Sep 2	9.75±0.07	2005 May 11
J11065803–7722488	ISO 86	10.21±0.02	8.93±0.02	8.27±0.03	7.54±0.04	2004 Jun 10	3.58±0.04	2005 Feb 27
J11065906–7718535	T23	9.84±0.02	9.55±0.02	9.19±0.03	8.25±0.04	2004 Jun 10	5.25±0.04	2005 Feb 27
J11065939–7530559	...	12.16±0.02	11.88±0.02	11.64±0.03	11.06±0.04	2006 Jul 10	out	...
J11070324–7610565	...	12.27±0.02	12.15±0.02	12.10±0.03	12.13±0.03	2006 Jul 10	...	2004 Apr 11
...	ESO H $\alpha$ 281	...	...	...	...	2004 Jul 4	6.93±0.04	2004 Apr 11
J11070369–7724307	...	12.86±0.02	12.35±0.02	11.84±0.04	10.99±0.04	2004 Jun 10	7.26±0.04	2005 Feb 27
...	Cha J11070768–7626326	14.98±0.03	14.56±0.03	14.22±0.11	13.30±0.11	2004 Jul 4	10.43±0.18	2004 Apr 11
		out	14.54±0.02	out	13.46±0.04	2005 May 9		
		14.93±0.02	14.54±0.02	14.02±0.06	13.47±0.06	2006 Jul 10		
J11070919–7723049	Ced 110-IRS6	7.95±0.02	6.92±0.02	6.36±0.03	5.50±0.03	2004 Jun 10	1.63±0.04	2005 Feb 27
J11070925–7718471	ISO 91	10.08±0.02	9.54±0.02	9.23±0.03	8.44±0.03	2004 Jun 10	5.27±0.04	2005 Feb 27
J11071148–7746394	CHXR 21	sat	sat	9.19±0.03	9.21±0.04	2004 Feb 19	9.04±0.06	2004 Apr 8
		9.34±0.02	out	9.23±0.03	out	2004 Jun 10	8.50±0.07	2005 Feb 27
							9.08±0.05	2005 May 11
J11071181–7625501	CHSM 9484	11.98±0.02	11.78±0.02	11.60±0.03	11.05±0.04	2004 Jul 4	9.34±0.08	2004 Apr 11
		out	11.69±0.02	out	11.06±0.04	2005 May 9		
		12.00±0.02	11.76±0.02	11.56±0.03	11.09±0.03	2006 Jul 10		
J11071206–7632232	T24	8.65±0.02	8.38±0.02	8.02±0.03	7.42±0.04	2004 Jul 4	4.48±0.04	2004 Apr 11

TABLE 7 — *Continued*

2MASS <sup>a</sup>	Name	[3.6]	[4.5]	[5.8]	[8.0]	Date	[24]	Date
J11071330–7743498	CHXR 22E	sat 9.60±0.02	sat 9.46±0.02	9.36±0.03 9.40±0.03	9.37±0.03 9.38±0.03	2004 Feb 19 2004 Jun 10	6.80±0.04 6.85±0.05	2004 Apr 8 2005 Feb 27
J11071622–7723068	ISO 97	sat 9.57±0.02	sat 8.84±0.02	9.32±0.03 8.23±0.03	9.38±0.04 7.47±0.04	2004 Sep 2 2004 Jun 10	6.91±0.04 3.83±0.04	2005 May 11 2005 Feb 27
J11071668–7735532	Cha H $\alpha$ 1	sat 11.54±0.02	sat 11.18±0.02	10.66±0.03 10.74±0.03	9.61±0.04 9.83±0.04	2004 Feb 19 2004 Jun 10	6.01±0.04 6.01±0.04	2005 Feb 27 2005 May 17
J11071860–7732516	Cha H $\alpha$ 9	sat 10.96±0.02	sat 10.54±0.02	10.74±0.03 10.11±0.03	9.78±0.03 9.59±0.04	2004 Sep 2 2004 Feb 19	7.01±0.04 7.10±0.04	2004 Feb 3 2005 Feb 27
J11071915–7603048	T25	out 9.97±0.02	9.60±0.02	out 9.93±0.03	9.48±0.03	2006 Jul 10	out	...
J11072040–7729403	ISO 99	9.97±0.02	9.90±0.02	9.93±0.03	9.88±0.04	2004 Jun 10	10.04±0.10 9.94±0.10	2004 Feb 3 2005 Feb 27
J11072074–7738073	T26	sat	sat	4.69±0.03	4.16±0.04	2004 Jun 10	1.09±0.04 0.99±0.04	2005 Feb 27 2005 May 17
J11072142–7722117	B35	9.50±0.02	8.86±0.02	8.21±0.03	7.26±0.04	2004 Jun 10	3.61±0.04	2005 Feb 27
J11072443–7743489	[LES2004] 429	sat 11.35±0.02	sat 11.19±0.02	11.07±0.03 11.11±0.03	11.08±0.03 11.11±0.04	2004 Feb 19 2004 Jun 10	11.06±0.24 11.06±0.37	2004 Apr 8 2005 May 11
...	Cha J11072647–7742408	14.78±0.02 14.81±0.02	14.63±0.03 14.62±0.02	14.47±0.04 14.42±0.06	14.40±0.05 14.34±0.05	2004 Feb 19 2004 Sep 2	...	2005 Feb 27
J11072825–7652118	T27	9.02±0.02	out	8.37±0.03	out	2004 Jul 4	out	...
J11073519–7734493	CHXR 76	sat 10.54±0.02	sat 10.43±0.02	10.38±0.03 10.37±0.03	10.37±0.04 10.46±0.04	2004 Feb 19 2004 Jun 10	9.22±0.07 9.11±0.08	2004 Feb 3 2005 Feb 27
J11073686–7733335	CHXR 26	sat 8.77±0.02	sat 8.66±0.02	8.58±0.03 8.60±0.03	8.60±0.04 8.54±0.03	2004 Sep 2 2004 Jun 10	9.13±0.08 8.21±0.05	2005 May 17 2004 Feb 3
J11073775–7735308	Cha H $\alpha$ 7	sat 11.88±0.02	sat 11.75±0.02	8.64±0.03 11.68±0.03	8.61±0.04 11.66±0.04	2004 Sep 2 2004 Feb 19	8.34±0.05 ...	2005 May 17 2005 Feb 27
J11073832–7747168	ESO H $\alpha$ 560	sat 10.68±0.02	sat out	11.68±0.03 10.57±0.03	11.58±0.03 out	2004 Sep 2 2004 Jun 10	9.63±0.09 9.60±0.22	2004 Apr 8 2005 Feb 27
J11073840–7552519	...	11.48±0.02	11.37±0.02	11.36±0.03	11.36±0.04	2006 Jul 10	...	2007 Jun 6
J11074245–7733593	Cha H $\alpha$ 2	sat 9.96±0.02	sat 9.58±0.02	9.20±0.03 9.22±0.03	8.60±0.04 8.61±0.04	2004 Feb 19 2004 Jun 10	5.98±0.05 6.10±0.04	2004 Feb 3 2005 Feb 27
J11074366–7739411	T28	sat 7.34±0.02	sat 7.01±0.02	9.17±0.03 6.82±0.03	8.58±0.04 6.20±0.04	2004 Sep 2 2004 Jun 10	6.17±0.04 3.32±0.05	2005 May 17 2005 Feb 27
J11074610–7740089	Cha H $\alpha$ 8	sat 11.03±0.02	sat 10.90±0.02	10.90±0.03 10.90±0.03	10.82±0.03 10.81±0.04	2004 Feb 19 2004 Jun 10	...	2005 Feb 27
J11074656–7615174	CHSM 10862	11.47±0.02	11.10±0.02	10.75±0.03	10.21±0.04	2006 Jul 10	7.00±0.04	2004 Apr 11
J11075225–7736569	Cha H $\alpha$ 3	sat 10.70±0.02	sat 10.57±0.02	10.47±0.03 10.47±0.03	10.48±0.03 10.49±0.03	2004 Feb 19 2004 Jun 10	10.01±0.26	2005 May 17
J11075588–7727257	CHXR 28	sat 7.47±0.02	sat 7.49±0.02	10.57±0.03 7.47±0.03	10.50±0.04 7.43±0.03	2004 Sep 2 2004 Jun 10	7.22±0.04	2005 Feb 27
J11075730–7717262	CHXR 30B	out	7.88±0.02	out	6.96±0.03	2004 Jun 10	3.88±0.04	2005 Feb 27
J11075792–7738449	T29	6.03±0.02	5.21±0.02	4.49±0.03	3.62±0.04	2004 Jun 10	sat	2005 May 17
J11075809–7742413	T30	8.58±0.02	8.16±0.02	7.93±0.03	7.29±0.04	2004 Jun 10	4.53±0.11 4.41±0.11	2004 Apr 8 2005 Feb 27
J11075993–7715317	ESO H $\alpha$ 561	out	10.60±0.02	out	10.58±0.04	2004 Jun 10	...	2005 Feb 27
J11080002–7717304	CHXR 30A	out	8.38±0.02	out	7.63±0.04	2004 Jun 10	5.22±0.11	2005 Feb 27
J11080148–7742288	T31	6.20±0.02	5.83±0.02	5.66±0.03	5.09±0.04	2004 Jun 10	1.89±0.04 1.83±0.11	2004 Apr 8 2005 Feb 27
J11080234–7640343	[LES2004] 717	11.51±0.02	11.39±0.02	11.41±0.03	11.31±0.04	2004 Jul 4	...	2004 Apr 11
J11080297–7738425	ISO 126	6.79±0.02	6.12±0.02	5.47±0.03	4.72±0.04	2004 Jun 10	sat	2005 Feb 27
J11080329–7739174	T32	sat	sat	3.87±0.03	2.72±0.04	2004 Jun 10	sat	2005 May 17
J11080609–7739406	...	14.37±0.18 13.77±0.06	14.15±0.20 13.81±0.07	...	...	2004 Feb 19 2004 Jun 10	...	2005 Feb 27
J11081509–7733531	T33A	sat	sat	4.17±0.03	3.19±0.03	2004 Jun 10	sat	2005 May 17
J11081648–7744371	T34	sat 9.78±0.02	sat 9.75±0.02	9.73±0.03 9.68±0.03	9.71±0.03 9.78±0.04	2004 Feb 19 2004 Jun 10	...	2004 Apr 8
J11081703–7744118	Cha H $\alpha$ 13	sat 10.25±0.02	sat 10.18±0.02	9.76±0.03 10.12±0.03	9.73±0.04 10.10±0.03	2004 Sep 2 2004 Feb 19	...	2005 Feb 27
J11081850–7730408	ISO 138	sat 12.51±0.02	sat 12.22±0.02	10.10±0.03 12.06±0.03	10.08±0.03 11.39±0.03	2004 Sep 2 2004 Feb 19	7.94±0.05	2004 Feb 3
J11081896–7739170	Cha H $\alpha$ 4	sat 10.67±0.02	sat 10.59±0.02	11.92±0.04 12.15±0.02	11.51±0.11 11.26±0.04	2004 Jun 10 2004 Sep 2	8.11±0.06	2005 Feb 27
...	Cha J11081938–7731522	16.18±0.02 16.11±0.07	15.87±0.02 15.76±0.11	15.65±0.05 ...	14.76±0.07 ...	2004 Feb 19 2004 Jun 10	6.79±0.04 6.78±0.04	2004 Feb 3 2005 Feb 27
		16.13±0.02	15.79±0.03	15.80±0.10	14.69±0.09	2004 Sep 2		

TABLE 7 — *Continued*

2MASS <sup>a</sup>	Name	[3.6]	[4.5]	[5.8]	[8.0]	Date	[24]	Date
J11082238–7730277	ISO 143	sat 10.31±0.02	sat 9.85±0.02	9.50±0.03	8.78±0.04	2004 Feb 19	6.17±0.04	2004 Feb 3
J11082404–7739299	Cha H $\alpha$ 10	12.75±0.02 12.79±0.02 12.76±0.02	12.62±0.02 12.63±0.02 12.60±0.02	12.59±0.04 12.43±0.06 12.54±0.04	12.59±0.08 12.56±0.11 12.62±0.07	2004 Jun 10 2004 Feb 19 2004 Sep 2	6.21±0.04 ...	2005 Feb 27 2005 Feb 27
J11082410–7741473	Cha H $\alpha$ 5	sat 10.30±0.02	sat 10.14±0.02	10.08±0.03 10.10±0.03	10.10±0.03 10.13±0.04	2004 Feb 19 2004 Jun 10	...	2005 Feb 27
J11082570–7716396	...	out 13.01±0.02	sat 14.95±0.02	out 14.95±0.04	11.98±0.04 14.71±0.07	2004 Jun 10 2004 Sep 2	9.72±0.10	2005 Feb 27
J11082650–7715550	ISO 147	out 12.94±0.02	out 11.27±0.02	out 6.31±0.02	10.33±0.04 3.66±0.04	2004 Jun 10	7.60±0.05	2005 Feb 27
J11082927–7739198	Cha H $\alpha$ 11	12.91±0.02 12.98±0.02	12.76±0.02 12.73±0.02	12.45±0.04 12.49±0.04	11.97±0.04 12.29±0.07	2004 Feb 19 2004 Sep 2	...	2005 Feb 27
...	Cha J11083040–7731387	15.11±0.02 15.14±0.03 15.14±0.02	14.94±0.02 14.85±0.04 14.95±0.02	14.68±0.04 ...	14.59±0.05 ...	2004 Feb 19 2004 Jun 10 2004 Sep 2	...	2004 Feb 3
J11083896–7743513	IRN	7.37±0.04	6.31±0.02	5.22±0.03	3.66±0.04	2004 Jun 10	sat	2005 Feb 27
J11083905–7716042	T35	out 8.11±0.02	sat 8.11±0.02	out 9.86±0.03	7.89±0.04 9.32±0.04	2004 Jun 10 2004 Feb 19	4.45±0.04 6.69±0.04	2005 Feb 27 2005 Feb 27
J11083952–7734166	Cha H $\alpha$ 6	sat 10.41±0.02	sat 10.09±0.02	9.93±0.03 9.77±0.03	9.36±0.04 9.35±0.03	2004 Jun 10 2004 Sep 2	6.77±0.04	2005 May 17
J11084069–7636078	CHXR 33	9.05±0.02	8.98±0.02	8.94±0.03	8.96±0.04	2004 Jul 4	8.82±0.07	2004 Apr 11
J11084296–7743500	...	sat 12.34±0.15 12.39±0.14	sat 11.68±0.13 11.65±0.15	8.89±0.03 10.98±0.11 11.01±0.10	8.94±0.04 9.54±0.10 9.43±0.10	2005 May 9 2004 Feb 19 2004 Jun 10	...	2004 Apr 8
J11084952–7638443	...	13.61±0.02 13.70±0.02	13.22±0.02 13.21±0.02	12.86±0.05 12.88±0.03	12.12±0.04 12.29±0.04	2004 Jul 4 2005 May 9	9.79±0.08	2004 Apr 11
J11085090–7625135	T37	10.68±0.02	10.34±0.02	9.96±0.03	9.41±0.03	2004 Jul 4	7.06±0.04	2004 Apr 11
J11085176–7632502	[LES2004] 737	sat 12.43±0.02 12.42±0.02	sat 12.29±0.02 12.31±0.02	9.98±0.03 12.27±0.05 12.19±0.03	9.39±0.03 12.32±0.06 12.26±0.04	2005 May 9 2004 Jul 4 2005 May 9	...	2005 Apr 9
J11085242–7519027	RX J1108.8–7519B	8.96±0.02	8.70±0.02	8.54±0.03	7.93±0.03	2004 Jul 21	5.27±0.04	2005 Feb 27
J11085326–7519374	RX J1108.8–7519A	8.62±0.02	8.56±0.02	8.51±0.03	8.50±0.03	2004 Jul 21	8.46±0.06	2005 Feb 27
J11085421–7732115	CHXR 78C	sat 10.80±0.02	sat 10.65±0.02	10.63±0.03 10.59±0.03	10.65±0.04 10.63±0.04	2004 Feb 19 2004 Jun 10	10.17±0.19 10.98±0.52	2004 Feb 3 2005 Feb 27
J11085464–7702129	T38	sat out 10.66±0.02	sat out 10.34±0.02	10.61±0.03 out 9.96±0.03	10.60±0.03 out 9.50±0.03	2004 Sep 2 ...	4.09±0.04 7.07±0.05	2007 Jun 6 2004 Apr 11
J11085497–7632410	ISO 165	sat 11.07±0.02	sat 10.95±0.02	9.96±0.03 10.85±0.03	9.50±0.03 10.89±0.04	2005 May 9 2004 Jun 10	10.29±0.16	2004 Feb 3
J11085596–7727132	ISO 167	sat 8.64±0.02	sat 8.60±0.02	8.50±0.03 8.59±0.03	8.50±0.03 8.54±0.04	2004 Feb 19 2004 Jun 10	8.08±0.05 8.18±0.06	2004 Feb 3 2005 Feb 27
J11091172–7729124	T39A	14.61±0.03 14.62±0.02	14.33±0.04 14.28±0.02	13.96±0.08 14.05±0.03	13.42±0.09 13.57±0.05	2004 Jun 10 2004 Sep 2	...	2005 Feb 27
J11091380–7628396	CHXR 35	10.55±0.02	10.44±0.02	10.40±0.03	10.40±0.04	2004 Jul 4	10.09±0.20	2004 Apr 11
J11091769–7627578	CHXR 37	sat 8.44±0.02	sat 8.45±0.02	10.37±0.03 8.33±0.03	10.37±0.03 8.32±0.03	2005 May 9 2004 Jul 4	10.23±0.10 8.19±0.06	2004 Aug 3 2004 Apr 11
J11091812–7630292	CHXR 79	sat 7.92±0.02	sat 7.43±0.02	8.34±0.03 7.15±0.03	8.38±0.04 6.50±0.04	2005 May 9 2004 Jul 4	8.22±0.05 3.57±0.04 3.55±0.04 3.57±0.04	2004 Aug 3 2004 Apr 11 2004 Aug 3 2005 Apr 9
J11092266–7634320	C1-6	7.22±0.02	6.51±0.02	6.03±0.03	5.17±0.04	2004 Jul 4	1.46±0.04 1.80±0.04	2004 Apr 11 2005 Apr 9
J11092379–7623207	T40	7.11±0.02	6.56±0.02	6.22±0.03	5.56±0.03	2004 Jul 4	3.33±0.04	2004 Apr 11
J11092855–7633281	ISO 192	8.47±0.02	6.97±0.02	5.86±0.03	4.58±0.03	2004 Jul 4	0.39±0.04	2004 Apr 11
J11092913–7659180	[LES2004] 602	11.73±0.02	11.62±0.02	11.59±0.03	11.59±0.04	2006 Jul 10	...	2007 Jun 6
J11093543–7731390	...	13.80±0.02 13.82±0.02	out 13.63±0.03	13.55±0.03 13.52±0.07	out 13.39±0.09	2004 Feb 19 2004 Jun 10	...	2004 Feb 3
J11094006–7628391	CHXR 40	out 8.76±0.02	out 8.76±0.02	13.68±0.02 8.70±0.03	13.57±0.04 8.67±0.03	2004 Sep 2 2004 Jul 4	8.43±0.05	2004 Apr 11
J11094192–7634584	C1-25	sat 8.53±0.02	sat 7.95±0.02	8.75±0.03 7.38±0.03	8.72±0.04 6.66±0.04	2005 May 9 2004 Jul 4	8.33±0.05 3.26±0.04 3.13±0.04	2004 Aug 3 2004 Apr 11 2005 Apr 9
J11094260–7725578	C7-1	9.60±0.02	9.18±0.02	9.08±0.03	8.90±0.04	2004 Jun 10	6.66±0.04 6.57±0.04	2004 Feb 3 2005 Feb 27
J11094525–7740332	ESO H $\alpha$ 566	sat 10.55±0.02	sat 10.40±0.02	10.36±0.03 10.39±0.03	10.35±0.04 10.39±0.04	2004 Feb 19 2004 Jun 10	9.82±0.18	2005 Feb 27
J11094621–7634463	Hn 10E	sat 9.49±0.02	sat 8.92±0.02	10.42±0.03 8.46±0.03	10.37±0.04 7.59±0.04	2004 Sep 2 2004 Jul 4	3.70±0.06	2004 Apr 11
J11094742–7726290	B43	sat 9.04±0.02	sat 8.50±0.02	8.41±0.03 8.37±0.03	sat 7.82±0.03	2005 May 9 2004 Jun 10	3.58±0.07 4.65±0.04 4.21±0.04	2005 Apr 9 2004 Feb 3 2005 Feb 27
J11094866–7714383	ISO 209	out 11.22±0.02	10.89±0.02	out 11.09±0.03	9.86±0.04	2004 Jun 10	7.08±0.04	2005 Feb 27
J11094918–7731197	KG 102	sat out	out 11.06±0.02	out 11.09±0.03	out 11.05±0.04	2004 Feb 19 2004 Jun 10	10.70±0.38 10.13±0.14	2004 Feb 3 2005 Feb 27

TABLE 7 — *Continued*

2MASS <sup>a</sup>	Name	[3.6]	[4.5]	[5.8]	[8.0]	Date	[24]	Date
J11095003–7636476	T41	out	11.08±0.02	out	11.00±0.03	2004 Sep 2		
J11095215–7639128	ISO 217	7.08±0.02	7.05±0.02	6.72±0.08	extended	2004 Jul 4	extended	2004 Apr 11
		10.80±0.02	10.29±0.02	9.83±0.03	9.16±0.03	2004 Jul 4	6.71±0.04	2004 Apr 11
		sat	sat	8.95±0.03	8.30±0.04	2005 May 9		
J11095262–7740348	CHSM 15991	12.67±0.02	11.97±0.02	11.13±0.03	10.06±0.04	2004 Feb 19	7.21±0.05	2005 Feb 27
		11.98±0.02	11.37±0.02	10.71±0.03	9.87±0.03	2004 Jun 10		
		12.64±0.02	11.88±0.02	11.10±0.03	10.10±0.04	2004 Sep 2		
J11095336–7728365	ISO 220	sat	out	10.75±0.03	out	2004 Feb 19	7.25±0.04	2004 Feb 3
		11.39±0.02	10.98±0.02	10.64±0.03	10.01±0.03	2004 Jun 10	7.25±0.04	2005 Feb 27
J11095340–7634255	T42	sat	sat	3.72±0.03	3.04±0.03	2004 Jul 4	sat	2004 Apr 11
J11095407–7629253	T43	8.55±0.02	8.14±0.02	7.62±0.03	6.83±0.04	2004 Jul 4	3.76±0.04	2004 Apr 11
							3.58±0.04	2004 Aug 3
							3.74±0.04	2005 Apr 9
J11095437–7631113	ISO 225	11.22±0.02	10.35±0.02	9.61±0.03	8.70±0.04	2004 Jul 4	4.85±0.04	2004 Apr 11
		sat	sat	9.60±0.03	8.58±0.03	2005 May 9	5.02±0.04	2005 Apr 9
J11095505–7632409	C1-2	7.90±0.02	7.15±0.02	6.75±0.03	5.96±0.03	2004 Jul 4	2.19±0.04	2004 Apr 11
							2.14±0.04	2005 Apr 9
J11095873–7737088	T45	6.99±0.02	6.50±0.02	6.16±0.03	5.52±0.04	2004 Jun 10	3.17±0.04	2005 Feb 27
J11100010–7634578	T44	sat	sat	3.70±0.03	3.15±0.04	2004 Jul 4	sat	2004 Apr 11
J11100192–7725451	[LES2004] 419	11.46±0.02	11.24±0.02	11.24±0.03	11.22±0.04	2004 Jun 10	...	2005 Feb 27
J11100369–7633291	Hn 11	8.18±0.02	7.52±0.02	6.84±0.03	6.04±0.04	2004 Jul 4	3.23±0.04	2004 Apr 11
							3.20±0.04	2005 Apr 9
J11100469–7635452	T45A	8.70±0.02	8.41±0.02	8.10±0.03	7.55±0.03	2004 Jul 4	4.58±0.04	2004 Apr 11
		sat	sat	8.37±0.03	sat	2005 May 9	4.38±0.05	2005 Apr 9
J11100658–7642486	...	14.47±0.03	14.27±0.03	14.29±0.11	...	2004 Jul 4	...	2004 Apr 8
		14.41±0.02	14.29±0.02	14.08±0.03	14.15±0.06	2005 May 9		
J11100704–7629376	T46	7.69±0.02	7.29±0.02	6.82±0.03	5.97±0.03	2004 Jul 4	3.54±0.04	2004 Apr 11
							3.64±0.04	2005 Apr 9
J11100785–7727480	ISO 235	10.48±0.02	10.05±0.02	9.60±0.03	8.86±0.03	2004 Jun 10	6.38±0.04	2004 Feb 3
							6.38±0.04	2005 Feb 27
J11100934–7632178	OTS 44	13.69±0.02	13.22±0.02	12.68±0.05	12.10±0.05	2004 Jul 4	8.81±0.11	2004 Apr 11
		13.67±0.02	13.17±0.02	12.65±0.03	12.03±0.03	2005 May 9	9.65±0.20	2005 Apr 9
J11101141–7635292	ISO 237	8.07±0.02	7.55±0.02	7.04±0.03	6.18±0.03	2004 Jul 4	2.33±0.04	2004 Apr 11
							2.27±0.04	2005 Apr 9
J11101153–7733521	...	sat	out	10.37±0.03	out	2004 Feb 19	10.27±0.20	2005 Feb 27
		10.47±0.02	10.47±0.02	10.36±0.03	10.39±0.04	2004 Jun 10		
		out	sat	out	10.37±0.04	2004 Sep 2		
J11102226–7625138	CHSM 17173	11.97±0.02	11.87±0.02	11.78±0.04	11.82±0.05	2004 Jul 4	...	2004 Apr 11
		11.95±0.02	11.84±0.02	11.73±0.03	11.79±0.04	2005 May 9		
J11102852–7716596	Hn 12W	out	10.23±0.02	out	10.26±0.04	2004 Jun 10	10.00±0.09	2005 Feb 27
J11103481–7722053	[LES2004] 405	9.60±0.02	9.43±0.02	9.42±0.03	9.42±0.04	2004 Jun 10	9.19±0.10	2005 Feb 27
J11103644–7722131	ISO 250	10.15±0.02	9.94±0.02	9.88±0.03	9.94±0.04	2004 Jun 10	...	2005 Feb 27
J11103801–7732399	CHXR 47	7.66±0.02	7.39±0.02	6.95±0.03	6.26±0.04	2004 Jun 10	3.52±0.04	2005 Feb 27
J11104006–7630547	...	12.84±0.02	12.72±0.02	12.64±0.05	12.63±0.07	2004 Jul 4	...	2005 Apr 9
		12.83±0.02	12.65±0.02	12.60±0.03	12.66±0.04	2005 May 9		
J11104141–7720480	ISO 252	11.45±0.02	11.02±0.02	10.57±0.03	9.75±0.03	2004 Jun 10	7.05±0.04	2005 Feb 27
J11104959–7717517	T47	out	8.13±0.02	out	6.37±0.04	2004 Jun 10	2.96±0.04	2005 Feb 27
J11105076–7718031	ESO H $\alpha$ 568	out	10.26±0.02	out	10.22±0.05	2004 Jun 10	...	2005 Feb 27
J11105333–7634319	T48	9.14±0.02	8.56±0.02	8.25±0.03	7.33±0.03	2004 Jul 4	4.52±0.04	2004 Apr 11
		sat	sat	8.30±0.03	sat	2005 May 9	4.66±0.05	2005 Apr 9
J11105359–7725004	ISO 256	9.50±0.02	8.93±0.02	8.61±0.03	7.74±0.04	2004 Jun 10	4.89±0.11	2005 Feb 27
J11105597–7645325	Hn 13	9.26±0.02	8.84±0.02	8.45±0.03	7.86±0.03	2004 Jul 4	5.02±0.04	2004 Apr 8
		9.29±0.02	8.90±0.02	8.53±0.03	7.93±0.04	2004 Jul 21	5.06±0.04	2004 Apr 11
		sat	out	8.52±0.03	out	2005 May 9		
J11111083–7641574	ESO H $\alpha$ 569	14.21±0.03	13.76±0.03	13.23±0.06	12.50±0.05	2004 Jul 4	7.12±0.04	2004 Apr 8
		13.92±0.02	13.48±0.03	13.08±0.08	12.19±0.05	2004 Jul 21	7.30±0.05	2004 Apr 11
		14.16±0.02	out	13.17±0.03	out	2005 May 9		
J11112249–7745427	[LES2004] 436	13.57±0.02	out	12.80±0.05	out	2004 Jun 10	out	...
J11112260–7705538	ISO 274	out	out	out	out	...	10.34±0.29	2007 Jun 6
J11113474–7636211	CHXR 48	9.50±0.02	9.47±0.02	9.41±0.03	9.41±0.03	2004 Jul 4	9.15±0.06	2004 Apr 11
		sat	sat	9.47±0.03	9.43±0.03	2005 May 9	9.74±0.20	2004 Jul 8
J11113965–7620152	T49	out	7.92±0.02	out	6.86±0.03	2004 Jul 4	3.75±0.04	2004 Apr 11
							3.72±0.04	2004 Aug 3
J11114533–7636505	[LES2004] 743	13.31±0.02	12.92±0.02	12.70±0.05	12.15±0.05	2004 Jul 4	9.71±0.10	2004 Apr 11
		13.32±0.02	12.98±0.02	12.65±0.03	12.20±0.03	2005 May 9	9.01±0.13	2004 Jul 8
J11114632–7620092	CHX 18N	out	6.74±0.02	out	6.26±0.03	2004 Jul 4	3.88±0.04	2004 Apr 11
							3.72±0.04	2004 Aug 3
J11115400–7619311	CHXR 49NE	out	8.90±0.02	out	8.85±0.03	2004 Jul 4	8.54±0.06	2004 Aug 3
J11120288–7722483	...	12.05±0.02	11.93±0.02	11.91±0.04	11.80±0.05	2004 Jun 10	...	2004 Feb 3
		12.07±0.02	out	11.89±0.03	out	2006 Jul 10		
J11120327–7637034	CHXR 84	10.39±0.02	10.27±0.02	10.23±0.03	10.29±0.04	2004 Jul 4	9.81±0.15	2004 Apr 11
		out	10.28±0.02	out	10.29±0.04	2004 Jul 21	9.81±0.14	2004 Jul 8
		sat	sat	10.22±0.03	10.29±0.04	2005 May 9		
J11120351–7726009	ISO 282	10.74±0.02	10.44±0.02	10.19±0.03	9.63±0.04	2004 Jun 10	7.02±0.04	2005 Feb 27
J11120984–7634366	T50	9.35±0.02	9.03±0.02	8.74±0.03	8.09±0.04	2004 Jul 4	5.17±0.04	2004 Apr 11
		sat	sat	8.80±0.03	8.13±0.04	2005 May 9	5.10±0.04	2004 Jul 8
J11122250–7714512	...	13.86±0.02	13.71±0.02	13.53±0.04	12.93±0.04	2006 Jul 10	10.13±0.15	2005 Feb 27

TABLE 7 — *Continued*

2MASS <sup>a</sup>	Name	[3.6]	[4.5]	[5.8]	[8.0]	Date	[24]	Date
J11122441–7637064	T51	7.28±0.02	6.72±0.02	6.29±0.03	5.30±0.04	2004 Jul 4	3.40±0.04	2004 Apr 11
		out	6.75±0.02	out	5.32±0.04	2004 Jul 21	3.45±0.04	2004 Jul 8
J11122772–7644223	T52	5.93±0.02	5.57±0.02	5.24±0.03	4.56±0.04	2004 Jul 4	1.19±0.04	2004 Apr 11
J11123092–7644241	T53	8.19±0.02	7.73±0.02	7.42±0.03	6.54±0.04	2004 Jul 4	...	2004 Apr 11
J11123099–7653342	[LES2004] 601	12.58±0.02	12.48±0.02	12.45±0.03	12.39±0.03	2006 Jul 10	...	2004 Apr 11
J11124210–7658400	CHXR 54	sat	out	9.35±0.03	out	2006 Jul 10	out	...
J11124268–7722230	T54	out	out	out	out	...	4.81±0.04	2004 Feb 3
							4.84±0.04	2005 Feb 27
J11124299–7637049	CHXR 55	9.20±0.02	9.19±0.02	9.17±0.03	9.14±0.04	2004 Jul 4	8.94±0.06	2004 Apr 11
		out	9.14±0.02	out	9.09±0.03	2004 Jul 21	9.12±0.13	2004 Jul 8
		sat	out	9.08±0.03	out	2005 May 9	8.98±0.07	2005 Apr 9
J11124861–7647066	Hn 17	out	10.35±0.02	out	9.30±0.04	2006 Jul 10	7.00±0.04	2004 Apr 11
J11132446–7629227	Hn 18	10.07±0.02	9.70±0.02	9.40±0.03	8.86±0.03	2004 Jul 4	5.95±0.04	2004 Apr 11
J11132737–7634165	CHXR 59	9.47±0.02	9.41±0.02	9.37±0.03	9.39±0.03	2004 Jul 4	9.24±0.07	2004 Apr 11
							9.27±0.08	2005 Apr 9
J11132970–7629012	CHXR 60	10.29±0.02	10.18±0.02	10.15±0.03	10.26±0.04	2004 Jul 4	10.14±0.17	2004 Apr 11
J11133356–7635374	T55	10.41±0.02	10.35±0.02	10.30±0.03	10.34±0.04	2004 Jul 4	10.06±0.17	2004 Apr 11
		sat	out	10.28±0.03	out	2005 May 9	9.76±0.10	2005 Apr 9
J11141565–7627364	CHXR 62	9.81±0.02	9.77±0.02	9.76±0.03	9.72±0.03	2004 Jul 4	9.03±0.10	2004 Apr 11
J11142454–7733062	Hn 21W	10.06±0.04	9.84±0.04	9.54±0.04	8.96±0.04	2006 Jul 10	6.42±0.04	2005 Feb 27
J11142611–7733042	Hn 21E	11.01±0.04	10.89±0.04	10.79±0.06	10.57±0.08	2006 Jul 10	...	2005 Feb 27
J11142906–7625399	ESO H $\alpha$ 571	out	11.20±0.02	out	11.22±0.04	2004 Jul 4	...	2004 Apr 11
J11145031–7733390	B53	9.35±0.02	9.28±0.02	9.26±0.03	9.24±0.03	2006 Jul 10	9.06±0.05	2005 Feb 27
J11152180–7724042	ESO H $\alpha$ 572	out	10.39±0.02	out	10.37±0.04	2006 Jul 10	10.37±0.16	2005 Feb 27
J11173792–7646193	...	12.21±0.02	12.09±0.02	12.07±0.03	12.03±0.03	2006 Jul 10	...	2004 Apr 11
J11182024–7621576	CHXR 68A	out	out	out	out	...	8.38±0.11	2007 Jun 6
J11183379–7643041	...	10.01±0.02	9.90±0.02	9.90±0.03	9.86±0.03	2006 Jul 10	9.87±0.15	2007 Jun 6
J11194214–7623326	...	11.42±0.02	11.31±0.02	11.30±0.03	11.34±0.04	2006 Jul 10	...	2007 Jun 6
J11195652–7504529	...	12.47±0.02	12.36±0.02	12.32±0.03	12.39±0.04	2006 Jul 10	...	2007 Jun 6
J11241186–7630425	...	11.56±0.02	11.40±0.02	11.33±0.03	10.88±0.04	2006 Jul 10	out	...
J11242980–7554237	...	9.61±0.02	9.54±0.02	9.54±0.03	9.50±0.03	2006 Jul 10	9.36±0.11	2007 Jun 6
J11291261–7546263	RX J1129.2–7546	8.78±0.02	8.76±0.02	8.79±0.03	8.72±0.04	2004 Jul 21	8.27±0.20	2005 Mar 6
J11332327–7622092	...	9.44±0.02	9.36±0.02	9.33±0.03	9.31±0.03	2006 Jul 10	9.15±0.10	2007 Jun 6

NOTE. — Entries of “...”, “sat”, “out”, and “bad” indicate measurements that are absent because of non-detection, saturation, a position outside the field of view of the filter, and contamination by a cosmic ray or a ghost from a bright star, respectively.

<sup>a</sup> 2MASS Point Source Catalog.

TABLE 8  
SPECTRAL SLOPES FOR KNOWN MEMBERS OF CHAMAELEON I

Name	$\alpha(2-8 \mu\text{m})$	$\alpha(2-24 \mu\text{m})$	$\alpha(3.6-8 \mu\text{m})$	$\alpha(3.6-24 \mu\text{m})$	SED Class
2M J10523694–7440287	–2.60	–2.51	–2.81	–2.58	III
2M J10580597–7711501	–1.76	...	–1.78	...	II
2M J11011370–7722387	–2.45	...	–2.73	...	III
2M J11011926–7732383	–2.24	...	–2.62	...	III
2M J11013205–7718249	–2.31	...	–2.65	...	III
2M J11021927–7536576	–2.55	–2.56	–2.77	–2.66	III
2M J11022491–7733357	–2.57	–0.72	–2.54	–0.24	II
2M J11022610–7502407	–2.51	–2.50	–2.67	–2.57	III
2M J11023265–7729129	...	–1.91	...	–1.84	II
2M J11024183–7724245	–2.53	...	–2.79	...	III
2M J11025504–7721508	–1.50	–1.13	–1.55	–1.05	II
2M J11034186–7726520	–2.41	...	–2.66	...	III
2M J11034764–7719563	–2.63	–2.70	–2.82	–2.80	III
2M J11035682–7721329	–2.62	–2.70	–2.64	–2.73	III
2M J11040425–7639328	...	–0.62	...	...	II
2M J11040909–7627193	...	–0.51	...	...	II
2M J11041060–7612490	–2.38	...	–2.67	...	III
2M J11042275–7718080	0.96	0.49	0.69	0.25	I
2M J11044258–7741571	–1.56	–0.84	–1.70	–0.72	II
2M J11045100–7625240	...	–2.77	...	...	III
2M J11045285–7625514	...	–2.48	...	...	III
2M J11045701–7715569	–1.81	...	...	...	II
2M J11051467–7711290	–2.55	...	...	...	III
2M J11052472–7626209	...	–2.89	...	...	III
2M J11054300–7726517	–2.41	–2.58	–2.66	–2.72	III
2M J11055261–7618255	...	–2.67	...	...	III
2M J11055780–7607488	...	–2.92	...	...	III
2M J11060010–7507252	–2.50	...	–2.69	...	III
2M J11061540–7721567	–2.70	–2.62	–2.73	–2.62	III
2M J11061545–7737501	–2.71	–2.82	–2.82	–2.89	III
2M J11062554–7633418	–1.43	–0.59	–1.36	–0.35	II
2M J11062877–7737331	–2.64	–2.60	–2.77	–2.64	III

TABLE 8 — *Continued*

Name	$\alpha(2-8 \mu\text{m})$	$\alpha(2-24 \mu\text{m})$	$\alpha(3.6-8 \mu\text{m})$	$\alpha(3.6-24 \mu\text{m})$	SED Class
2M J11062942–7724586	–1.31	–1.37	–1.40	–1.42	II
2M J11063276–7625210	–1.58	–1.12	–1.46	–0.96	II
2M J11063799–7743090	–2.34	–2.50	–2.64	–2.66	III
2M J11063945–7736052	–1.03	–0.63	–0.94	–0.49	II
2M J11064180–7635489	–0.64	–0.82	–0.46	–0.79	II
2M J11064346–7726343	–2.67	–2.65	–2.82	–2.72	III
2M J11064510–7727023	–1.56	–1.26	–1.12	–1.00	II
2M J11064658–7722325 <sup>a</sup>	0.90	1.56	0.22	1.44	I
2M J11065733–7742106	–2.55	–2.75	–2.73	–2.88	III
2M J11065803–7722488 <sup>a</sup>	1.44	0.92	0.24	0.28	flat
2M J11065906–7718535	–1.53	–1.05	–1.02	–0.71	II
2M J11065939–7530559	–1.64	...	–1.59	...	II
2M J11070324–7610565	–2.36	...	–2.69	...	III
Cha J11070350–7631460	...	–1.16	...	...	II
2M J11070369–7724307	–1.36	–0.67	–1.02	–0.35	II
Cha J11070768–7626326	–1.03	–0.77	–1.13	–0.74	II
2M J11070919–7723049 <sup>a</sup>	1.11	0.71	–0.03	0.13	flat
2M J11070925–7718471	–1.28	–0.85	–1.27	–0.73	II
2M J11071148–7746394	–2.62	–2.75	–2.77	–2.84	III
2M J11071181–7625501	–1.85	–1.71	–1.82	–1.66	II
2M J11071206–7632232	–1.48	–1.04	–1.48	–0.93	II
2M J11071330–7743498	–2.55	–1.80	–2.69	–1.67	II
2M J11071622–7723068 <sup>a</sup>	0.24	0.15	–0.43	–0.15	flat
2M J11071668–7735532	–1.04	–0.50	–0.78	–0.25	II
2M J11071860–7732516	–1.44	–1.16	–1.38	–1.07	II
2M J11071915–7603048	–2.65	...	...	...	III
2M J11072040–7729403	–2.52	–2.80	–2.74	–2.97	III
2M J11072074–7738073	–1.42	–0.92	...	...	II
2M J11072142–7722117 <sup>a</sup>	–0.15	–0.05	–0.26	–0.08	flat
2M J11072443–7743489	–2.43	–2.67	–2.65	–2.83	III
Cha J11072647–7742408	–1.95	...	–2.38	...	III
2M J11073519–7734493	–2.50	–2.23	–2.75	–2.27	III
2M J11073686–7733335	–2.58	–2.68	–2.79	–2.79	III
2M J11073775–7735308	–2.26	...	–2.60	...	III
2M J11073832–7747168	...	–2.40	...	–2.45	III
2M J11073840–7552519	–2.51	...	–2.73	...	III
2M J11074245–7733593	–1.46	–1.23	–1.36	–1.13	II
2M J11074366–7739411	–1.51	–0.99	–1.63	–0.91	II
2M J11074610–7740089	–2.38	...	–2.67	...	III
2M J11074656–7615174	–1.33	–0.86	–1.43	–0.78	II
2M J11075225–7736569	–2.45	–2.52	–2.66	–2.62	III
2M J11075588–7727257	–2.83	–2.83	–2.92	–2.86	III
2M J11075730–7717262	–1.11	–0.79	...	...	II
2M J11075792–7738449	–0.66	...	–0.15	...	flat
2M J11075809–7742413	–1.11	–0.91	–1.44	–1.00	II
2M J11075993–7715317	–2.47	...	...	...	III
2M J11080002–7717304	–2.18	–1.63	...	...	II
2M J11080148–7742288	–1.56	–0.98	–1.63	–0.86	II
2M J11080234–7640343	–2.35	...	–2.63	...	III
2M J11080297–7738425	–0.41	...	–0.56	...	II
2M J11080329–7739174	–0.58	...	...	...	II
2M J11081509–7733531	–0.23	...	...	...	flat
2M J11081648–7744371	–2.63	...	–2.83	...	III
2M J11081703–7744118	–2.44	...	–2.72	...	III
2M J11081850–7730408	–1.56	–0.91	–1.50	–0.72	II
2M J11081896–7739170	–2.45	...	–2.67	...	III
Cha J11081938–7731522	–1.76	0.75	–1.26	1.60	II
2M J11082238–7730277	–1.29	–1.07	–1.16	–0.96	II
2M J11082404–7739299	–2.37	...	–2.70	...	III
2M J11082410–7741473	–2.44	...	–2.67	...	III
2M J11082570–7716396	–1.16	–1.13	...	...	II
2M J11082650–7715550	–1.44	–1.10	...	...	II
2M J11082927–7739198	–1.73	...	–1.84	...	II
Cha J11083040–7731387	–1.84	...	–2.24	...	III
2M J11083896–7743513 <sup>a</sup>	0.84	...	1.44	...	I
2M J11083905–7716042	–2.11	–1.19	...	...	II
2M J11083952–7734166	–1.63	–1.26	–1.65	–1.18	II
2M J11084069–7636078	–2.75	–2.81	–2.83	–2.86	III
2M J11084296–7743500	–0.79	...	0.06	...	flat
2M J11084952–7638443	–1.11	–1.05	–1.17	–1.06	II
2M J11085090–7625135	–1.44	–1.25	–1.38	–1.18	II
2M J11085176–7632502	–2.37	...	–2.70	...	III
2M J11085242–7519027	–1.77	–1.31	–1.66	–1.14	II
2M J11085326–7519374	–2.58	–2.75	–2.71	–2.86	III
2M J11085421–7732115	–2.45	–2.52	–2.70	–2.65	III
2M J11085464–7702129	...	–0.88	...	...	II
2M J11085497–7632410	–1.50	–1.25	–1.57	–1.21	II

TABLE 8 — *Continued*

Name	$\alpha(2-8 \mu\text{m})$	$\alpha(2-24 \mu\text{m})$	$\alpha(3.6-8 \mu\text{m})$	$\alpha(3.6-24 \mu\text{m})$	SED Class
2M J11085596-7727132	-2.52	-2.51	-2.76	-2.61	III
2M J11091172-7729124	-2.54	-2.57	-2.76	-2.67	III
Cha J11091363-7734446	-1.37	...	-1.69	...	II
2M J11091380-7628396	-2.47	-2.65	-2.68	-2.79	III
2M J11091769-7627578	-2.68	-2.77	-2.81	-2.85	III
2M J11091812-7630292	-1.23	-0.91	-1.34	-0.88	II
2M J11092266-7634320	-0.75	-0.49	-0.70	-0.40	II
2M J11092379-7623207	-0.95	-1.03	-1.10	-1.12	II
2M J11092855-7633281 <sup>a</sup>	1.86	1.23	1.65	0.99	I
2M J11092913-7659180	-2.48	...	-2.73	...	III
2M J11093543-7731390	-2.22	...	-2.58	...	III
2M J11094006-7628391	-2.68	-2.69	-2.82	-2.74	III
2M J11094192-7634584 <sup>a</sup>	-0.39	-0.23	-0.69	-0.31	II
2M J11094260-7725578	-1.89	-1.53	-2.18	-1.57	II
2M J11094525-7740332	-2.39	-2.46	-2.68	-2.60	III
2M J11094621-7634463	-1.17	-0.46	-0.72	-0.09	II
2M J11094742-7726290	-1.39	-0.91	-1.60	-0.87	II
2M J11094866-7714383 <sup>a</sup>	-1.02	-0.86	...	...	II
2M J11094918-7731197	-2.34	-2.51	-2.68	-2.70	III
2M J11095215-7639128	-0.67	-0.96	-0.51	-0.97	II
2M J11095262-7740348	-0.01	-0.31	-0.11	-0.42	flat
2M J11095336-7728365	-1.44	-1.09	-1.37	-0.97	II
2M J11095340-7634255	-0.55	...	...	...	II
2M J11095407-7629253	-1.27	-0.87	-0.96	-0.64	II
2M J11095437-7631113	0.26	0.16	0.04	0.04	flat
2M J11095505-7632409 <sup>a</sup>	-0.12	0.03	-0.61	-0.14	flat
2M J11095873-7737088	-1.11	-1.07	-1.19	-1.10	II
2M J11100010-7634578	-0.88	...	...	...	II
2M J11100192-7725451	-2.52	...	-2.71	...	III
2M J11100369-7633291	-0.66	-0.64	-0.52	-0.58	II
2M J11100469-7635452	-1.66	-1.05	-1.57	-0.86	II
2M J11100658-7642486	-2.13	...	-2.52	...	III
2M J11100704-7629376	-1.17	-1.11	-0.94	-1.00	II
2M J11100785-7727480	-1.36	-1.16	-1.14	-1.01	II
2M J11100934-7632178	-0.95	-0.96	-0.99	-0.98	II
2M J11101141-7635292	-1.32	-0.58	-0.80	-0.17	II
2M J11101153-7733521	-2.59	-2.73	-2.79	-2.86	III
2M J11102226-7625138	-2.33	...	-2.67	...	III
2M J11102852-7716596	-2.42	-2.58	...	...	III
2M J11103481-7722053	-2.64	-2.71	-2.78	-2.79	III
2M J11103644-7722131	-2.61	...	-2.77	...	III
2M J11103801-7732399	-1.55	-1.16	-1.33	-0.97	II
2M J11104006-7630547	-2.39	...	-2.69	...	III
2M J11104141-7720480	-1.12	-0.95	-0.95	-0.83	II
2M J11104959-7717517	-0.95	-0.57	...	...	II
2M J11105076-7718031	-2.54	...	...	...	III
2M J11105333-7634319	-0.86	-0.82	-0.76	-0.76	II
2M J11105359-7725004	-0.58	-0.59	-0.99	-0.77	II
2M J11105597-7645325	-1.38	-1.01	-1.28	-0.88	II
2M J11111083-7641574	-1.28	-0.05	-0.87	0.43	II
2M J11112260-7705538	...	-2.79	...	...	III
2M J11113474-7636211	-2.56	-2.88	-2.78	-3.06	III
2M J11113965-7620152	-1.39	-0.92	...	...	II
2M J11114533-7636505	-1.44	-0.93	-1.56	-0.86	II
2M J11114632-7620092	-1.74	-1.34	...	...	II
2M J11115400-7619311	-2.54	-2.63	...	...	III
2M J11120288-7722483	-2.39	...	-2.60	...	III
2M J11120327-7637034	-2.44	-2.51	-2.74	-2.65	III
2M J11120351-7726009	-1.35	-1.10	-1.64	-1.16	II
2M J11120984-7634366	-1.56	-1.06	-1.42	-0.87	II
2M J11122250-7714512	-1.71	-1.22	-1.77	-1.12	II
2M J11122441-7637064	-0.86	-1.13	-0.58	-1.08	II
2M J11122772-7644223	-1.21	-0.73	-1.30	-0.65	II
2M J11123092-7644241	-1.05	...	-1.00	...	II
2M J11123099-7653342	-2.31	...	-2.63	...	III
2M J11124268-7722230	...	-1.75	...	...	II
2M J11124299-7637049	-2.71	-2.79	-2.78	-2.84	III
2M J11124861-7647066	-1.44	-1.27	...	...	II
2M J11132446-7629227	-1.42	-1.02	-1.47	-0.94	II
2M J11132737-7634165	-2.64	-2.75	-2.77	-2.84	III
2M J11132970-7629012	-2.57	-2.72	-2.82	-2.87	III
2M J11133356-7635374	-2.52	-2.51	-2.77	-2.62	III
2M J11141565-7627364	-2.56	-2.49	-2.78	-2.57	III
2M J11142454-7733062	-1.69	-1.31	-1.63	-1.19	II
2M J11142611-7733042	-2.21	...	-2.38	...	II
2M J11142906-7625399	-2.54	...	...	...	III
2M J11145031-7733390	-2.57	-2.70	-2.72	-2.79	III

TABLE 8 — *Continued*

Name	$\alpha(2-8 \mu\text{m})$	$\alpha(2-24 \mu\text{m})$	$\alpha(3.6-8 \mu\text{m})$	$\alpha(3.6-24 \mu\text{m})$	SED Class
2M J11152180–7724042	–2.53	–2.74	...	...	III
2M J11173792–7646193	–2.37	...	–2.65	...	III
2M J11182024–7621576	...	–2.71	...	...	III
2M J11183379–7643041	–2.39	–2.67	–2.69	–2.87	III
2M J11194214–7623326	–2.55	...	–2.77	...	III
2M J11195652–7504529	–2.37	...	–2.77	...	III
2M J11241186–7630425	–2.10	...	–2.12	...	II
2M J11242980–7554237	–2.55	–2.70	–2.75	–2.82	III
2M J11291261–7546263	–2.68	–2.65	–2.79	–2.69	III
2M J11332327–7622092	–2.51	–2.67	–2.71	–2.79	III

<sup>a</sup> Spectral slopes are the observed values without a correction for extinction.

TABLE 9  
SED CLASSES IN CHAMAELEON I

Class	North <sup>a</sup>	South <sup>b</sup>	Total
I	1	3	4
flat	2	8	10
II	43	51	94
III	44	51	95

<sup>a</sup>  $\delta > -77^\circ$ .

<sup>b</sup>  $\delta < -77^\circ$ .

TABLE 10  
DISK FRACTIONS

Spectral Type	Chamaeleon I	IC 348
<K6	14/19 = $0.74^{+0.08}_{-0.12}$	7/35 = $0.20^{+0.08}_{-0.05}$
>K6 and ≤M3.5	42/66 = $0.64 \pm 0.06$	41/94 = $0.44 \pm 0.05$
>M3.5 and <M6	36/83 = $0.43 \pm 0.05$	62/130 = $0.48 \pm 0.04$
≥M6 and ≤M8	10/24 = $0.42^{+0.1}_{-0.09}$	13/23 = $0.57 \pm 0.1$
>M8	5/10 = $0.50^{+0.14}_{-0.15}$	5/12 = $0.42^{+0.14}_{-0.12}$

NOTE. — The statistical errors in the disk fractions are computed in the manner described by Burgasser et al. (2003).

TABLE 11  
*Spitzer* PHOTOMETRY FOR PROBABLE MEMBERS OF  $\epsilon$  CHA

ID <sup>a</sup>	2MASS <sup>b</sup>	Name	[3.6]	[4.5]	[5.8]	[8.0]	Date	[24]	Date
13	J11183572–7935548	...	9.31±0.02	9.15±0.02	9.06±0.03	8.50±0.04	2006 Jul 6	out	...
14	J11225562–7924438	RX J1123.2–7924	9.45±0.02	9.46±0.02	9.42±0.03	9.40±0.03	2004 May 1	9.53±0.10	2004 Aug 3
15	J11334926–7618399	...	10.92±0.02	10.84±0.02	10.82±0.03	10.79±0.03	2006 Jul 10	9.95±0.27	2007 Jun 6
16	J11404967–7459394	...	11.38±0.02	11.28±0.02	11.24±0.03	11.17±0.03	2006 Jul 10	...	2007 Jul 16
17	J11432669–7804454	...	10.08±0.02	9.87±0.02	9.67±0.03	9.26±0.03	2006 Jul 10	out	...
18	J11493184–7851011	RX J1149.8–7850	7.96±0.02	7.53±0.02	7.01±0.03	5.81±0.03	2004 Jun 10	1.75±0.04	2005 Mar 6
19	J11502829–7704380	RX J1150.4–7704	8.86±0.02	8.86±0.02	8.85±0.03	8.82±0.04	2004 May 26	8.76±0.06	2005 Feb 27
20	J11582681–7754450	RX J1158.5–7754B	9.25±0.02	9.20±0.02	9.16±0.03	9.15±0.04	2004 Jun 10	8.61±0.06	2004 Feb 22
21	J11582816–7754294	RX J1158.5–7754A	7.31±0.02	7.27±0.02	7.28±0.03	7.22±0.03	2004 Jun 10	7.14±0.04	2004 Feb 22

<sup>a</sup> Identifications assigned in this work, which conform to the ones used for previously known members of  $\epsilon$  Cha (Feigelson et al. 2003; Luhman 2004b).

<sup>b</sup> 2MASS Point Source Catalog.

TABLE 12  
SPECTRAL SLOPES FOR PROBABLE MEMBERS OF  $\epsilon$  CHA

ID <sup>a</sup>	$\alpha(2-8 \mu\text{m})$	$\alpha(2-24 \mu\text{m})$	$\alpha(3.6-8 \mu\text{m})$	$\alpha(3.6-24 \mu\text{m})$	SED Class
13	–1.99	...	–1.92	...	II
14	–2.60	–2.83	–2.80	–2.97	III

TABLE 12 — *Continued*

ID <sup>a</sup>	$\alpha(2-8 \mu\text{m})$	$\alpha(2-24 \mu\text{m})$	$\alpha(3.6-8 \mu\text{m})$	$\alpha(3.6-24 \mu\text{m})$	SED Class
15	-2.54	-2.43	-2.71	-2.47	III
16	-2.37	...	-2.62	...	III
17	-1.87	...	-1.92	...	II
18	-0.86	-0.28	-0.37	0.08	flat
19	-2.68	-2.80	-2.80	-2.88	III
20	-2.59	-2.57	-2.74	-2.62	III
21	-2.66	-2.78	-2.75	-2.85	III

<sup>a</sup> Identifications from Table 11.

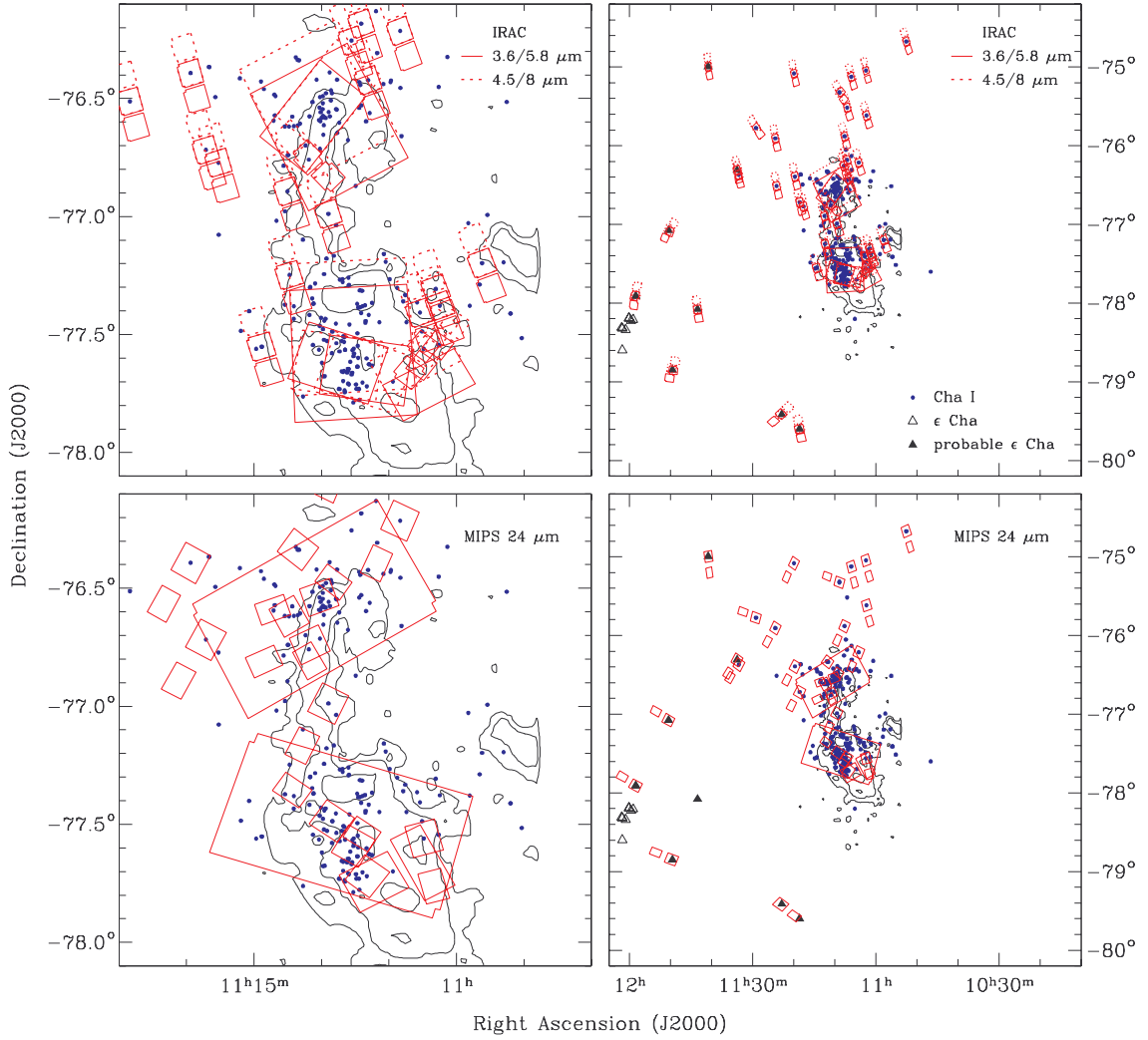


FIG. 1.— Fields in the Chamaeleon I star-forming region that have been imaged with IRAC (*top*) and MIPS (*bottom*). The known members of the cluster are indicated (*points*). We also have measured IRAC and MIPS photometry for young stars near Chamaeleon I that we have identified as probable members of the  $\epsilon$  Cha young association (§ A, *filled triangles*). The original members of  $\epsilon$  Cha are located 3° southeast of the Chamaeleon I clouds (*open triangles*, Feigelson et al. 2003; Luhman 2004b). The contours represent the extinction map of Cambr sy et al. (1997) at intervals of  $A_J = 0.5, 1,$  and  $2$ .

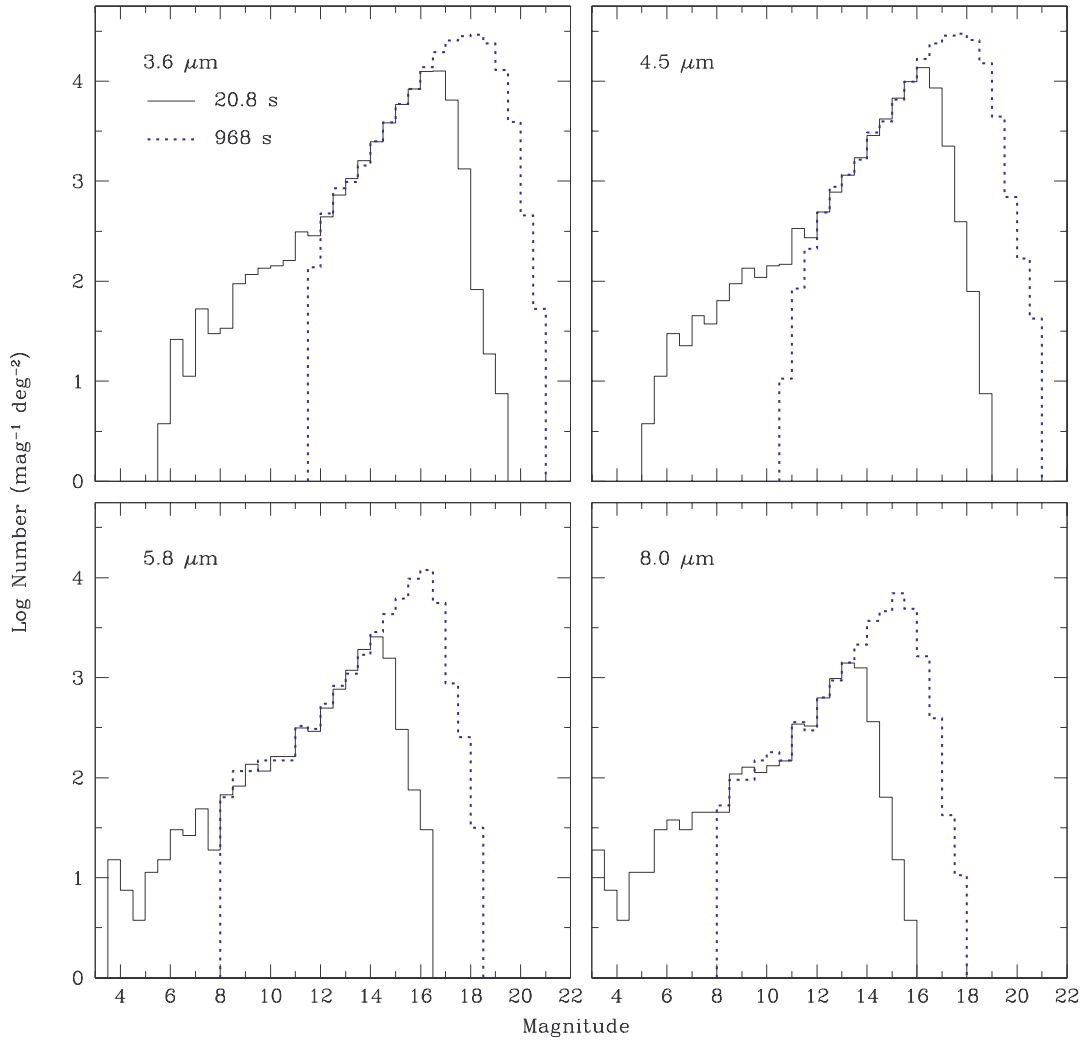


FIG. 2.— Distributions of IRAC magnitudes for images of Chamaeleon I that have short (*solid lines*) and long (*dotted lines*) total exposure times.

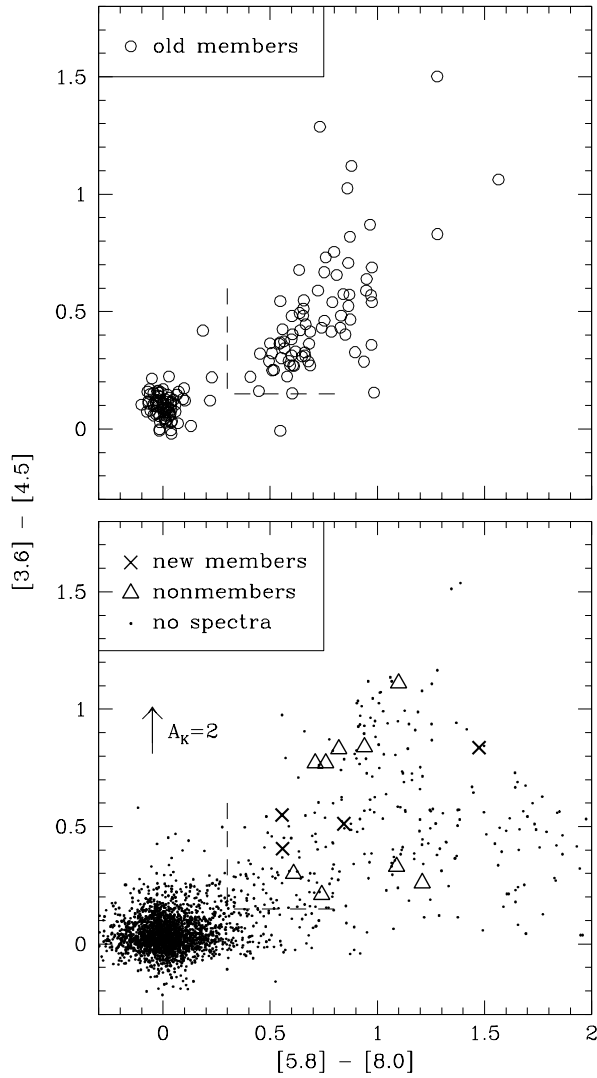


FIG. 3.— *Spitzer* IRAC color-color diagrams for the survey fields in the Chamaeleon I star-forming region that are indicated in Figure 1. *Top*: The previously known members of Chamaeleon I (*circles*) exhibit either neutral colors consistent with stellar photospheres or significantly redder colors that are indicative of circumstellar disks. *Bottom*: Among the other point sources in the IRAC data, we selected a sample of candidate disk-bearing members based on colors of  $[5.8] - [8.0] > 0.3$  and  $[3.6] - [4.5] > 0.15$  (*dashed line*) and obtained spectra of them. The candidates classified as new members (*crosses*) and nonmembers (*triangles*) are listed in Tables 4 and 5, respectively. Most of the remaining red sources are probably galaxies based on their faint magnitudes (see Fig. 8). Only objects with photometric errors less than 0.1 mag in all four bands are shown in these diagrams, with the exception of the new member 2M J1108–7743. The reddening vector is based on the extinction law from Flaherty et al. (2007).

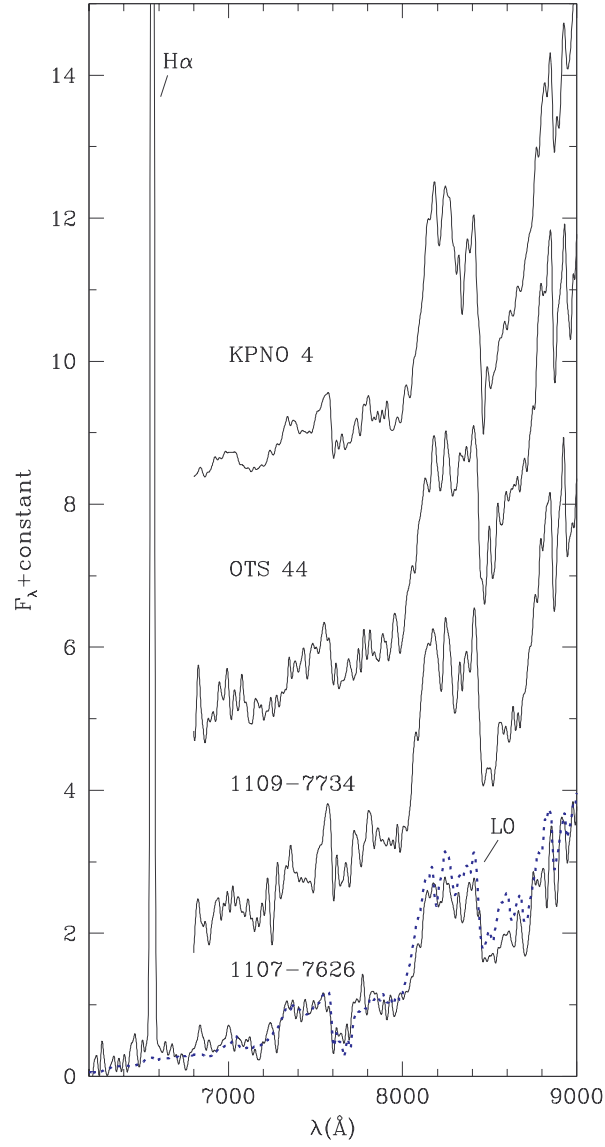


FIG. 4.— Optical spectrum of a new member of Chamaeleon I, Cha J1107-7626, compared to data for the young M9.5 objects KPNO 4, OTS 44, and Cha J11091363-7734446 (Briceño et al. 2002; Luhman 2007) and the L0 field dwarf 2MASS J03454316+2540233 (*dotted line*, Kirkpatrick et al. 1999). The spectrum of Cha J11091363-7734446 has been dereddened by  $A_J = 0.28$  (Luhman 2007). The data are displayed at a resolution of 18  $\text{\AA}$  and are normalized at 7500  $\text{\AA}$ .

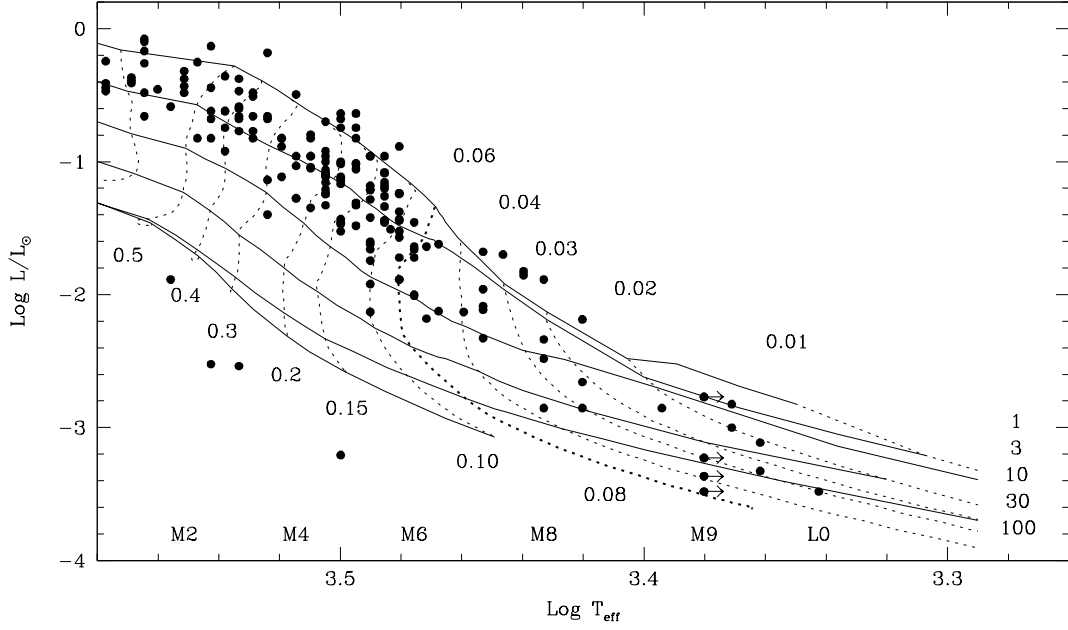


FIG. 5.— H-R diagram for all known low-mass stars and brown dwarfs in Chamaeleon I (Luhman 2007, § 3). These data are shown with the theoretical evolutionary models of Baraffe et al. (1998) ( $0.1 < M/M_{\odot} \leq 1$ ) and Chabrier et al. (2000) ( $M/M_{\odot} \leq 0.1$ ), where the mass tracks (*dotted lines*) and isochrones (*solid lines*) are labeled in units of  $M_{\odot}$  and Myr, respectively. The four stars that are below the main sequence (ISO 225, CHSM 15991, Cha J11081938–7731522, ESO H $\alpha$  569) are probably detected primarily in scattered light, which precludes the measurement of accurate luminosities.

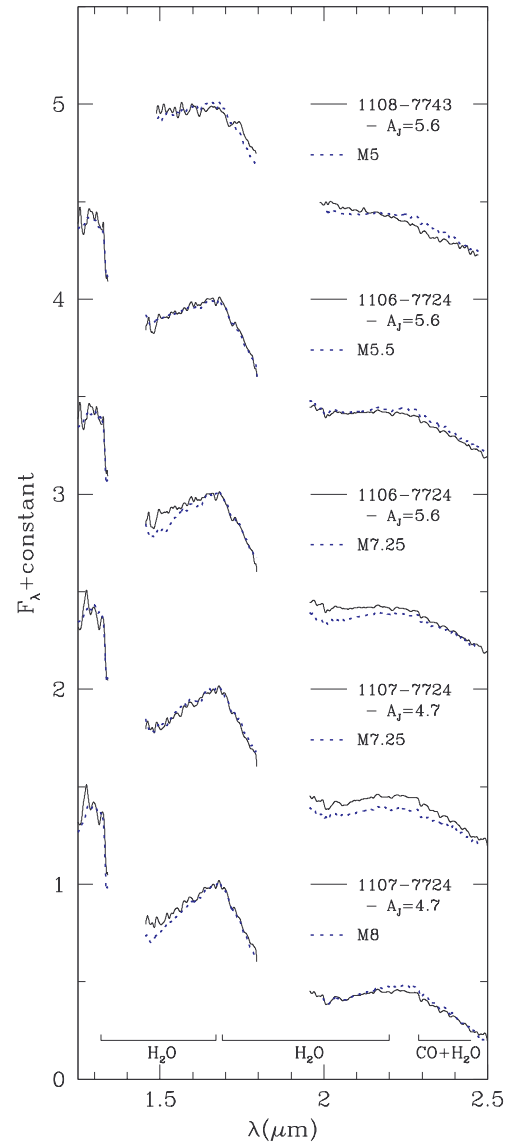


FIG. 6.— Near-IR spectra of three new members of Chamaeleon I, 2M J1108–7743, 2M J1106–7724, and 2M J1107–7724, compared to data for previously known members with optical spectral types, T50 (M5), Hn 12W (M5.5), Cha H $\alpha$  11 (M7.25), and CHSM 17173 (M8). The spectra of the new members have been dereddened to match the slopes of the young optical standards. The spectra are displayed at a resolution of  $R = 200$  and are normalized at  $1.68 \mu\text{m}$ .

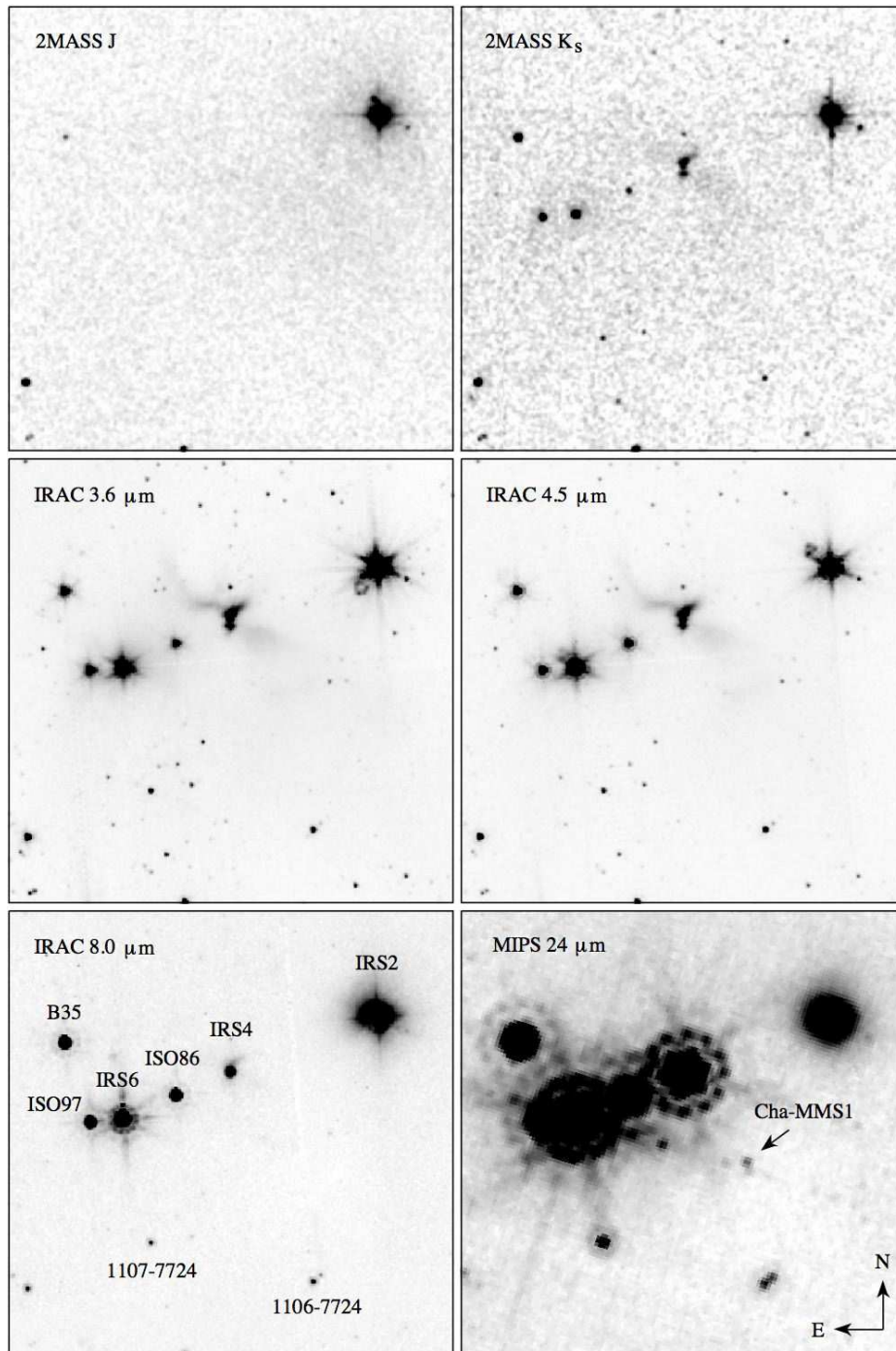


FIG. 7.— 2MASS and *Spitzer* images of the region surrounding the Cederblad 110 reflection nebula in Chamaeleon I ( $5' \times 5'$ ). 2M 1106–7724 and 2M 1107–7724 are highly reddened, low-mass disk-bearing sources discovered in this work. A redder and fainter candidate member of Chamaeleon I appears  $7''$  northwest of 2M 1106–7724 (Table 6). The protostar Cha-MMS1 is detected at  $24 \mu\text{m}$ . The faint source in the middle of the  $24 \mu\text{m}$  image (southeast of Ced 110-IRS4) is a latent image from Ced 110-IRS6.

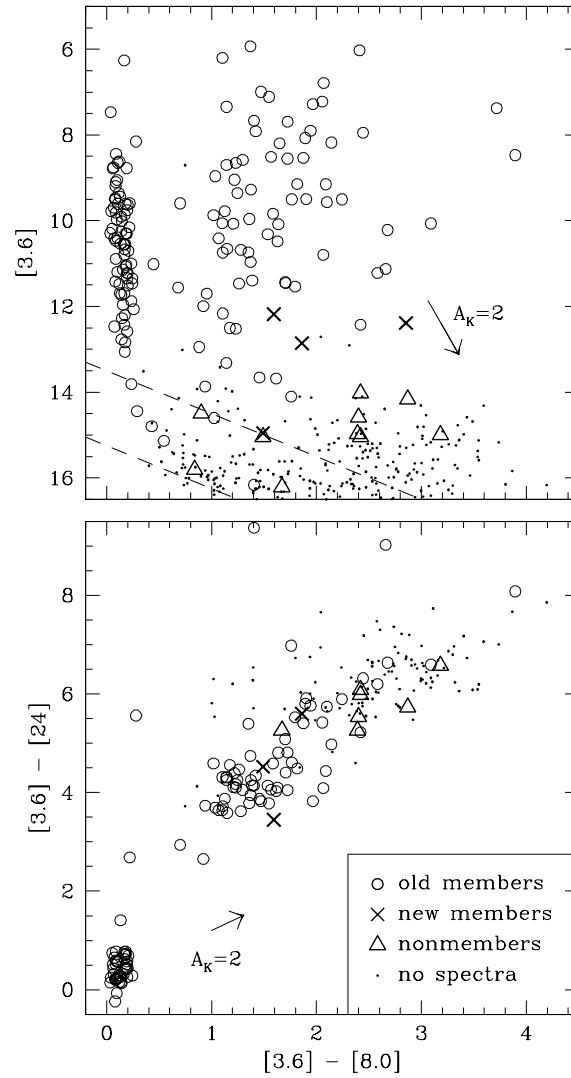


FIG. 8.— *Spitzer* color-magnitude and color-color diagrams for the survey fields in the Chamaeleon I star-forming region that are indicated in Figure 1. We show the previously known members of Chamaeleon I (*circles*) and objects that have red colors in Figure 3 and that have been spectroscopically classified as new members (*crosses*, Table 4) and nonmembers (*triangles*, Table 5). We also include the remaining sources from Figure 3 that have red colors ( $[3.6] - [4.5] > 0.15$ ,  $[5.8] - [8.0] > 0.3$ ) and lack spectroscopy (*points*), most of which are probably galaxies based on their faint magnitudes. Only objects with photometric errors less than 0.1 mag in all four bands are shown in these diagrams, with the exception of the new member 2M J1108–7743. The  $8\ \mu\text{m}$  completeness limits for the shortest and longest exposures are shown in the color-magnitude diagram (*dashed lines*, Fig. 2). The reddening vectors are based on the extinction law from Flaherty et al. (2007).

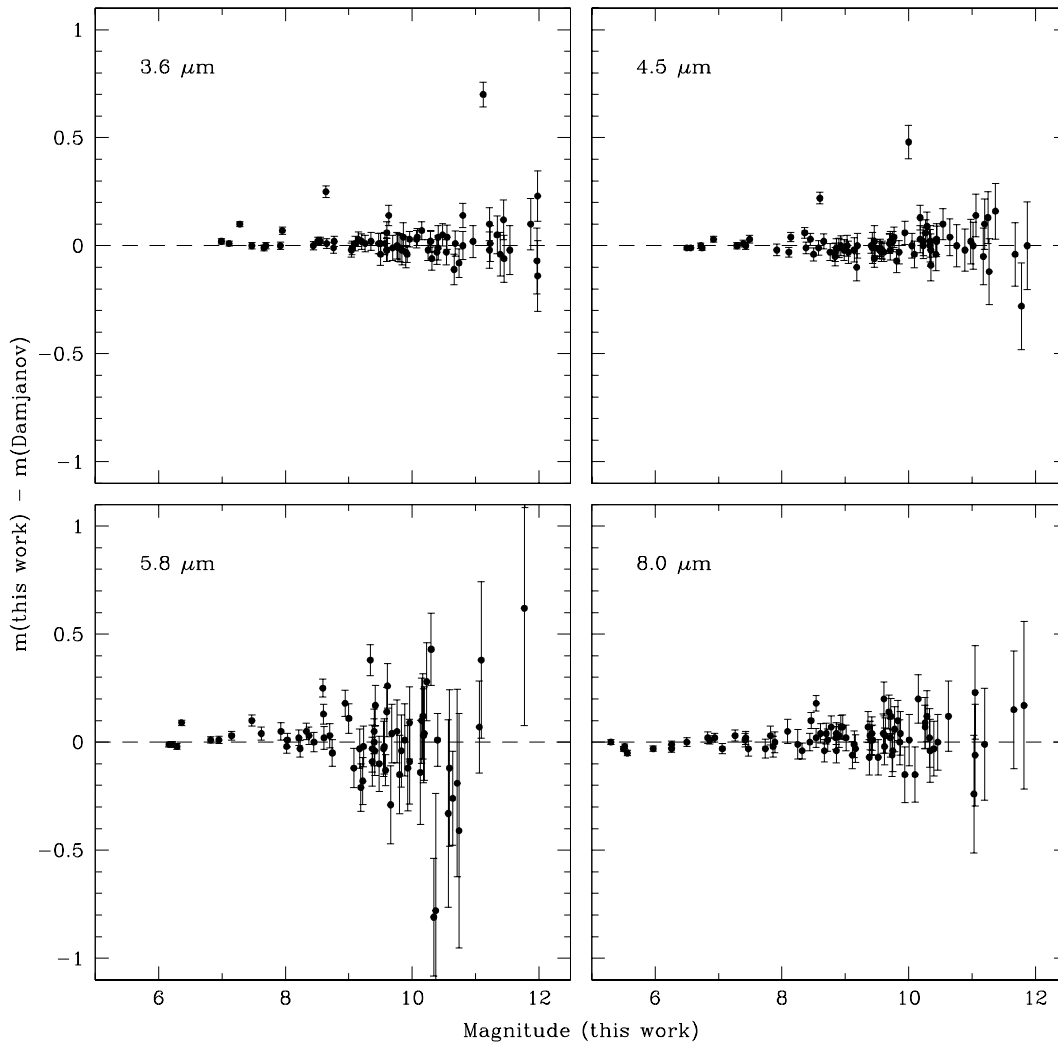


FIG. 9.— Comparison of the IRAC magnitudes from Damjanov et al. (2007) to our measurements of the same objects from the same images considered in that study. The errors reported by Damjanov et al. (2007) are indicated. Nearly all of our measurements have errors of 0.02-0.04 mag.

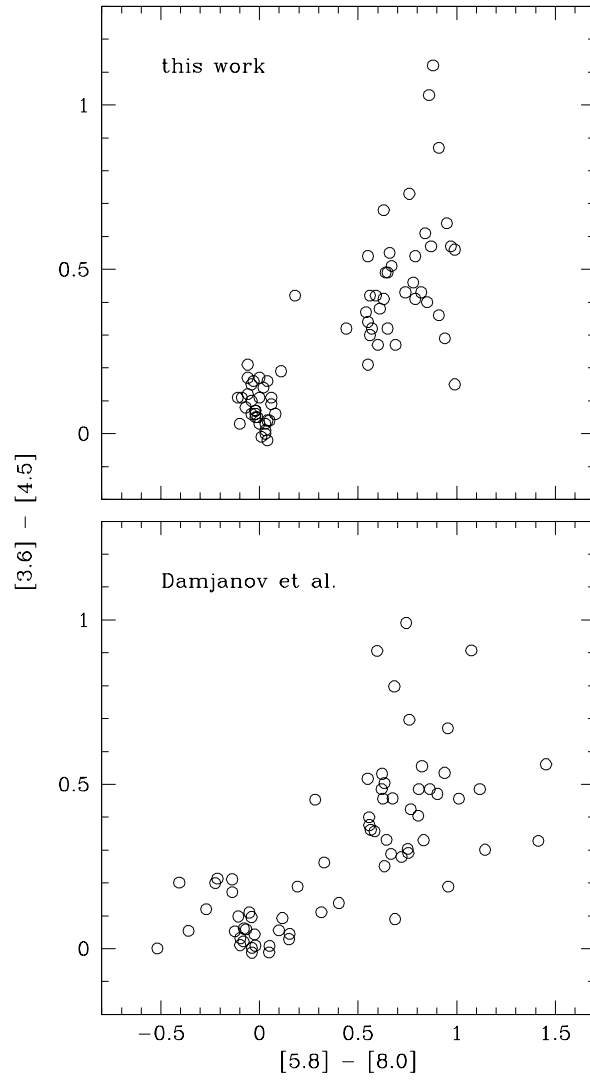


FIG. 10.— Comparison of the IRAC colors from Damjanov et al. (2007) (*bottom*) to our measurements of the same objects from the same images considered in that study (*top*).

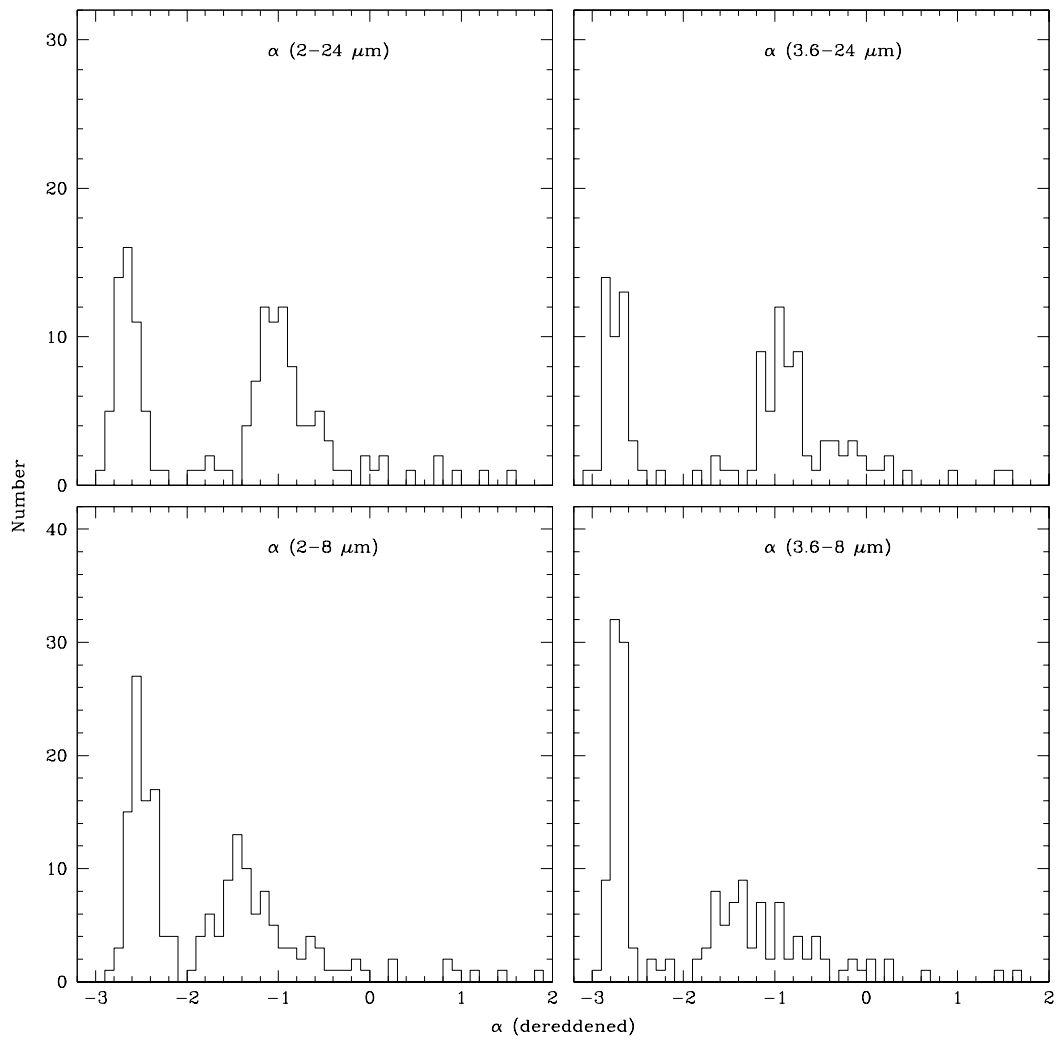


FIG. 11.— Distributions of spectral slopes for members of Chamaeleon I (Table 8).

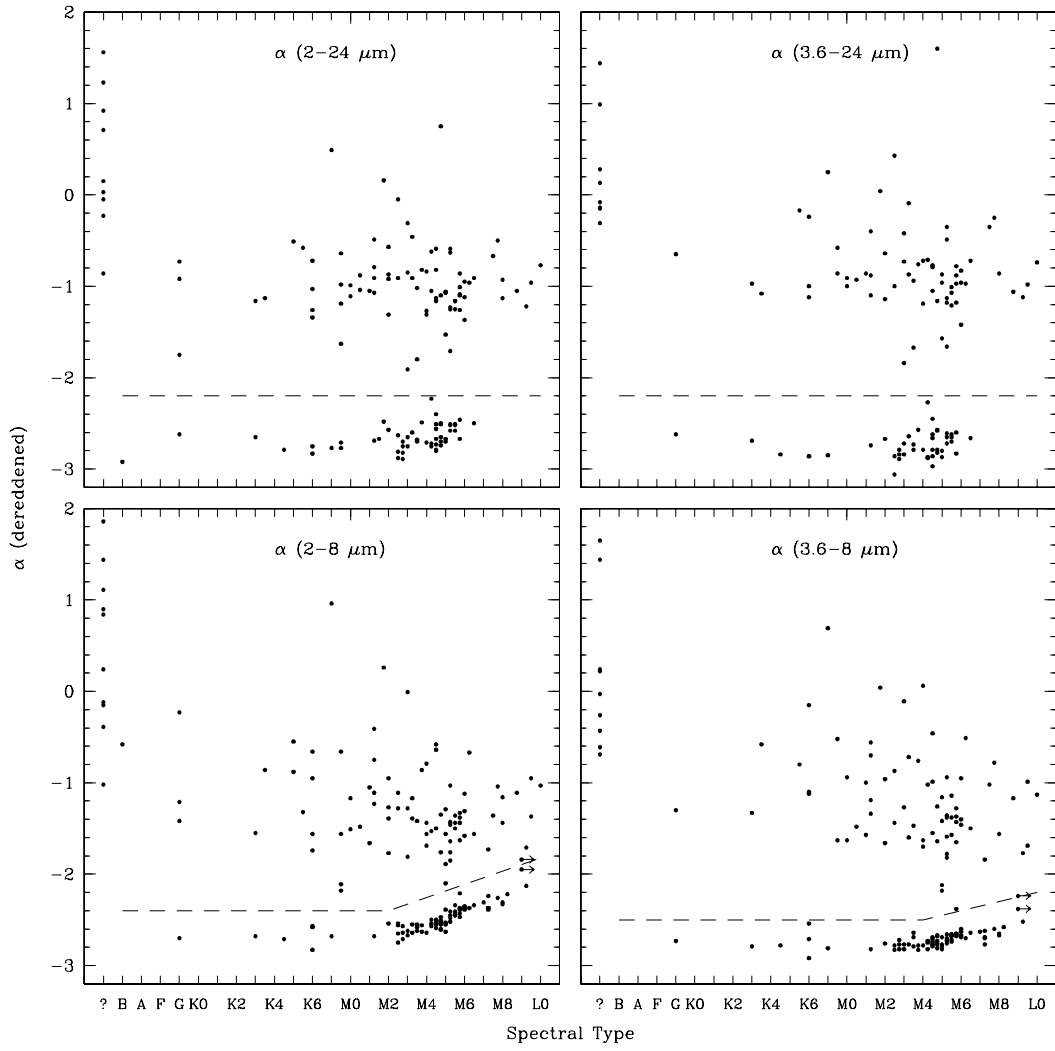


FIG. 12.— Spectral slopes as function of spectral type for members of Chamaeleon I (Table 8). Our adopted boundaries for separating SED classes II and III are indicated (*dashed lines*).

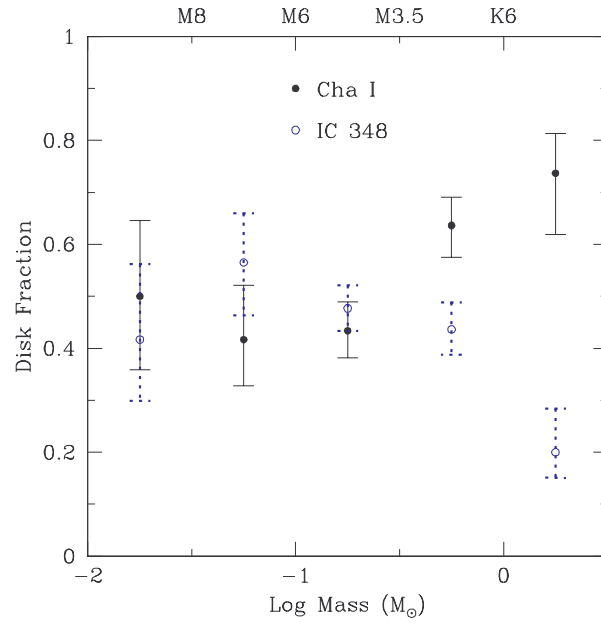


FIG. 13.— Disk fraction as a function of mass and spectral type for members of Chamaeleon I based on the SED classifications from Figure 12. For comparison, we include the disk fraction of IC 348 computed in the same manner using data from Luhman et al. (2005b) and Lada et al. (2006).

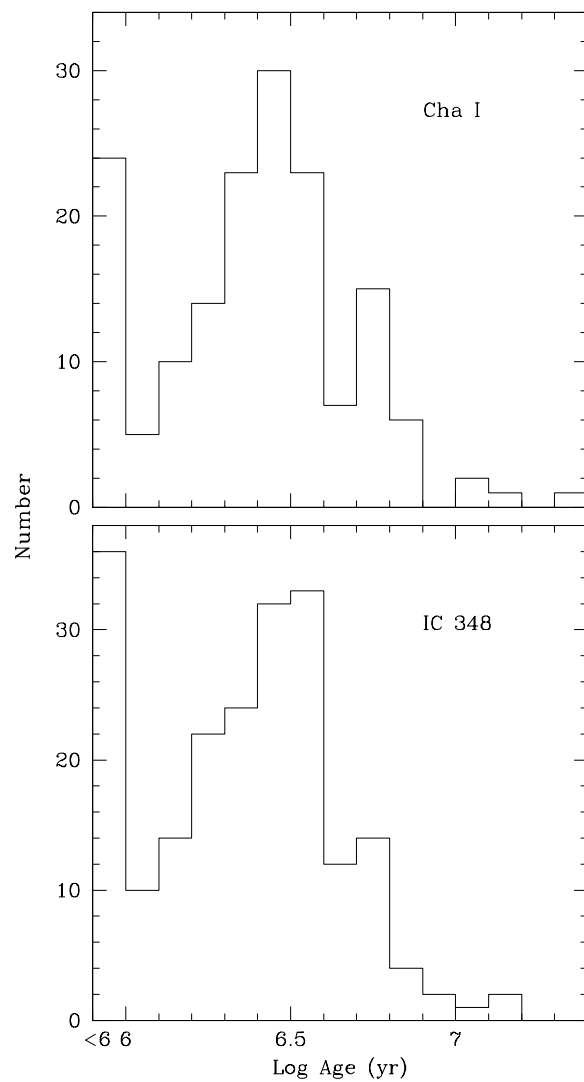


FIG. 14.— Distributions of isochronal ages for members of Chamaeleon I (*top*) and IC 348 (*bottom*) with masses between 0.1 and  $1 M_{\odot}$  (Luhman et al. 2003; Luhman 2007).

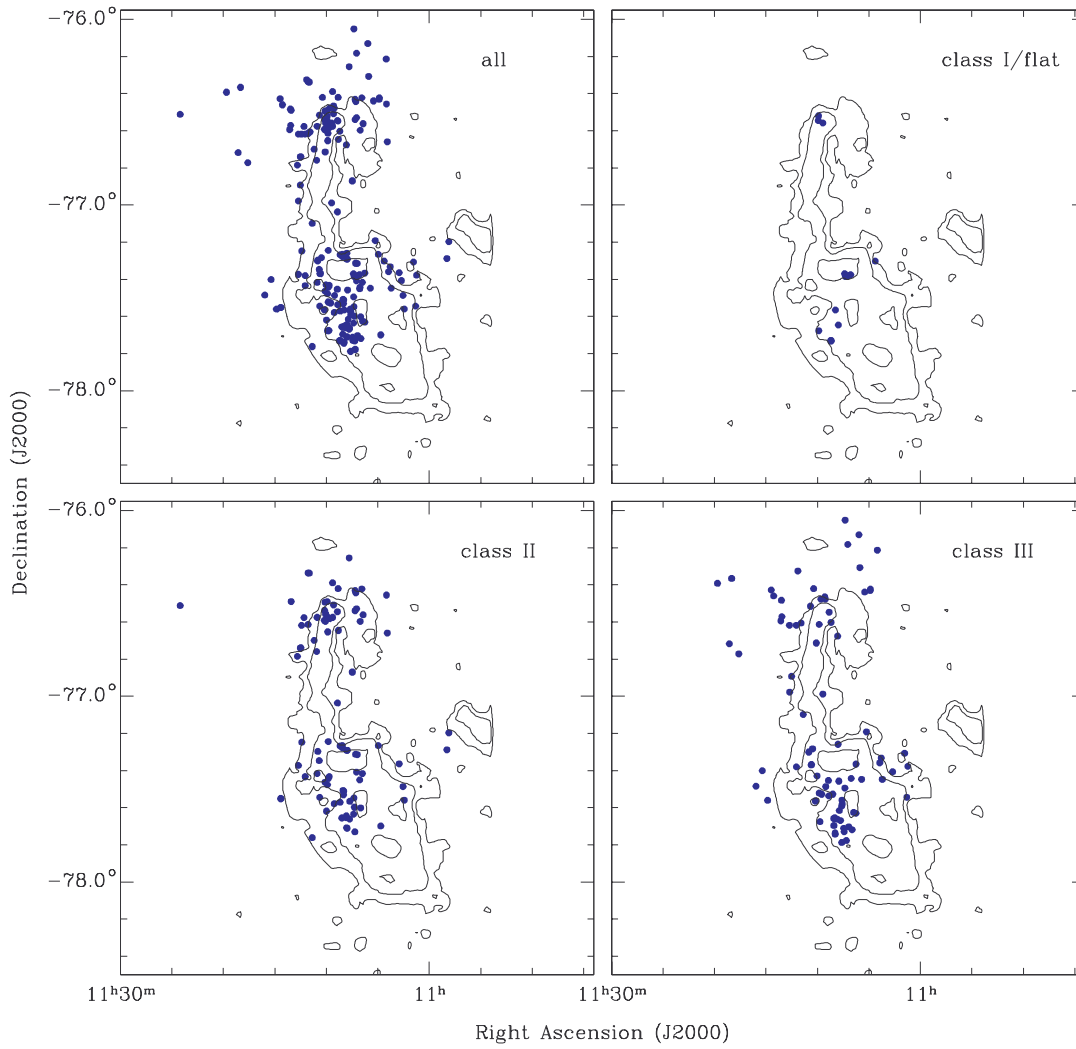


FIG. 15.— Spatial distributions of members of Chamaeleon I in the SED classes from Table 8. The contours represent the extinction map of Cambrésy et al. (1997) at intervals of  $A_J = 0.5, 1, \text{ and } 2$ .

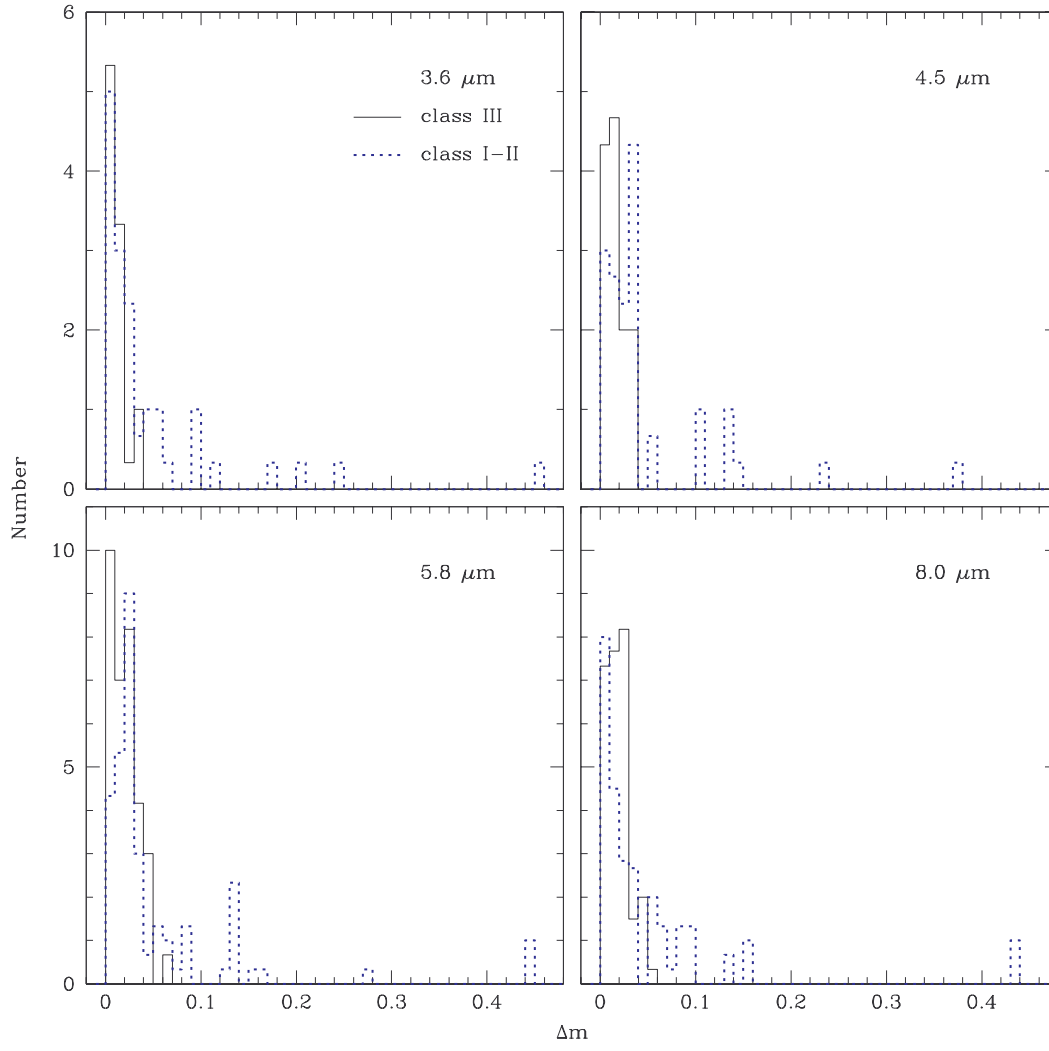


FIG. 16.— Variability of IRAC magnitudes for members of Chamaeleon I that have disks (class I through class II, *dotted histograms*) and members without disks (class III, *solid histograms*). The histograms represent distributions of differences between a magnitude and the average magnitude for a given source and band. Each magnitude difference is weighted by the inverse of the number of measurements so that all members contribute equally.